Utrecht University | Nikhef national institute for subatomic physics Theory Group
Master's thesis, 50 ECTS |
2024 |

On Power corrections of Yang-Mills Gauge Theories

Dimitrios Daskalas

Supervisor : Prof. Dr Eric Laenen
Examiner : Prof. Dr Umut Gursoy

Universiteit Utrecht

Nikhef

Utrecht University
Heidelberglaan 8, 3584 CS Utrecht
030 253 3550 , www.uu.nl

Contents

Contents **ii**
Dedication . . . 2

1 Foreword **3**
1.1 QCD, a theory of quarks and gluons . . . 3
1.2 Feynman Rules in 't Hooft-Feynman gauge [**Collins_2023**] . . . 6

I "Hard-Soft-Collinear factorization of radiative amplitudes" **8**

2 Infrared Structure **9**
2.1 Pinch Surfaces/Landau Equations . . . 9
2.2 IR Power Counting . . . 11
2.3 **Power Counting** . . . 12
2.4 Propagators . . . 13
2.5 Notes on gauge choices . . . 14
2.6 Eikonal Approximation/Wilson Lines . . . 16
2.7 The Eikonal Approximation . . . 16
2.8 Wilson Lines . . . 18
2.9 Cut Diagrams . . . 22

3 Leading Power Factorization **23**
3.1 The Soft Function . . . 24
3.2 The Jet Function . . . 25
3.3 Jet-soft Factorization . . . 26

4 Next to Leading Power Factorization. QED and extensions **28**
4.1 $e^+ + e^- \to \gamma^*$ Factorization . . . 28
4.2 Overview of Factorization . . . 30
4.3 Extension: QCD corrections . . . 34
4.4 Strategy for Power Counting . . . 40
4.5 Factorization: QCD corrections . . . 46

5 Further extensions: Higgs production **52**
5.1 Introduction . . . 52
5.2 Main Channel: Gluon-Fusion . . . 53
5.3 Higgs production via gluon fusion: Power Counting . . . 55
5.4 Reduced diagrams . . . 58
5.5 Factorization formula . . . 61

II Higher Twist Contributions **62**

6 Power Corrections in inclusive Deep Inelastic Scattering. **63**
6.1 **Framework** 63
6.2 Framework and kinematics: Corrections up to $\frac{1}{Q^2}$ 65
6.3 Towards colour gauge invariance: A first rearrangement of power corrections 68
6.4 Collinear expansion: Applied to the hadronic tensor 72
6.5 Collinear expansion of the gluon 76
6.6 Finally: Colour gauge invariance. 79
6.7 Electromagnetic Gauge Invariance 84
6.8 Decoupling of the spinor Trace 92

III "Electromagnetic Gauge Invariance revisited: QED and a special propagator's perspective" **97**

7 Ward Identities **98**
7.1 Ward Identities: QED soft radiation 98
7.2 More Ward Identities 100

8 QED **104**
8.1 Power corrections to QED form factor: An alternative approach 104
8.2 Emergence of Wilson Lines 113

9 Conclusion **117**

Bibliography **118**

Abstract

The master project investigates factorization theorems and their application on various infrared divergent scenarios in physics either caused by virtual or by real divergent momenta. Specifically it is divided in three parts:

The first part entails examining the QCD perturbation series for a number of amplitudes and cross sections, and establishing a factorization theorem in terms of jet-, soft and hard functions to next-to-leading power in the soft parton expansion. This also involves testing particular matrix element definitions of the new jet functions involved.

Part two is an analysis of the higher twist contributions in inclusive DIS, providing detailed analytical calculations of the procedure and focusing on the special propagator technique and leads to Part third's effort to apply the latter to the former QCD processes.

Dedication

To my family who never stopped fighting.
From those peculiar dark winters to today's light
everything lives inside me.

To Nujia. For everything.
Because she never moved an inch even if it was windy here.
Our warmest adventures await to be lived.

To Professor Laenen,
His lessons were invaluable, and he showed me the proper way to conduct research.

To Utrecht. I am saying goodbye as a richer man.
Surely I will keep finding my way back to the city that altered my inner rhythm forever.

1 Foreword

Quantum Chromodynamics(QCD), is catholically accepted as the fundamental theory responsible for the dynamics of partons. As partons generally we describe quarks, antiquarks, and gluons, the particles whose interactions are classified as strong. This non Abelian gauge field theory is the $\mathrm{SU}(3)$ component of the $\mathrm{SU}(3)_C \times \mathrm{SU}(2)_L \times \mathrm{U}(1)_Y$ Standard Model of Physics.
Before we dive into explicit dynamical details, such as the full form of the corresponding Lagrangian, and the properties identifying QCD, a little more light will be shed on its fundamental constituents .

1.1 QCD, a theory of quarks and gluons

Quarks are fermions, and at the moment these lines are written six types of quarks are known to exist. The mentioned quark varieties are categorized in theory as flavours, with each flavour representing fundamental distinctions in their quantum properties. . Three of them, namely up (u), charm (c), top (t) are equipped with electric charge $\frac{2}{3}$, whereas the remaining three: down (d), strange (s), bottom (b) have a negative fraction of electric charge $\left(-\frac{1}{3}\right)$. These quark types, are named *quark flavours*. Of course, there are the corresponding anti-quarks, which have the opposite electric charges, baryon number and isospin.
Quarks are described by spin $\frac{1}{2}$, Dirac fields Ψ_f, where f stands for flavour, whereas anti-quark fields are denoted as $\overline{\Psi_f}$.

Table 1.1: Baryonic number, Charge, Isospin corresponding to the six quark flavours

Flavour	**Mass** $GeVc^{-2}$	**B**	**Q**	T_3
u	0.01	$\frac{1}{3}$	$\frac{2}{3}$	$\frac{1}{2}$
d	0.01	$\frac{1}{3}$	$-\frac{1}{2}$	-$\frac{1}{2}$
c	1.5	$\frac{1}{3}$	$\frac{2}{3}$	$\frac{1}{2}$
s	0.1	$\frac{1}{3}$	$-\frac{1}{2}$	-$\frac{1}{2}$
t	172	$\frac{1}{3}$	$\frac{2}{3}$	$\frac{1}{2}$
b	5	$\frac{1}{3}$	$-\frac{1}{2}$	-$\frac{1}{2}$

A single flavour, quark field, transforms under the fundamental representation of $\mathrm{SU}(3)$ as

$$\Psi_f(x) \to \mathrm{U}(x)\Psi_f(x),$$

where $\mathrm{U}(x)$ are $\mathrm{SU}(3)$ matrices, unitary with unit determinant and matrix dimension 3×3.
For the $\mathrm{SU}(3)$ group to act on the quark field, every quark of a given flavour will appear in a threefold variety. This variety is implemented with a a second index in the quark field, i, such that a quark field is now denoted as $\Psi_{f,i}$, with i running from 1 to 3, corresponding to the three additional varieties, commonly referred to, as colours. (red, blue, green).
The $\mathrm{SU}(3)$ group, being non-Abelian, has a dimension equal to $N^2 - 1\big|_{N=3} = 8$ and therefore, we also have 8 gauge fields V_μ^a to ensure gauge invariance in the Lagrangian[40]. The V_μ^a, gauge fields correspond to the gluon bosonic fields, mediating the strong interactions, and transform under the adjoint representation of $\mathrm{SU}(3)$.

$$\mathrm{V}_\mu(x) = \mathrm{U}(x)\mathrm{V}_\mu\mathrm{U}^+(x) + \frac{i}{g_s}\mathrm{U}(x)\left(\partial_\mu \mathrm{U}^+(x)\right),$$

where g_s is the strong coupling constant, that[40] will determine the interaction strength between quarks and gluons.
The quark field, transforms under $\mathrm{SU}(3)$, in the fundamental triplet representation [18]

$$\Psi(x) \to \Psi'(x) = e^{\xi^a(x)t_a}\Psi(x),$$

$\xi^a(x)$: 8 transformation parameters of SU(3)
$(t_a)^i_j$: anti-hermitian traceless, 3×3 matrices, generators of SU(3)

$[t_a, t_b] = f^c_{abtc}, f^c_{ab}$ structure constants of SU(3)

Conveniently the SU(3) generators can be expressed via the 8 Gell-Man matrices λ_α as $t_a = \frac{i}{2}\lambda_a$.

$$\lambda^1 = \begin{pmatrix} 0 & 1 & 0 \\ 1 & 0 & 0 \\ 0 & 0 & 0 \end{pmatrix}, \lambda^2 = \begin{pmatrix} 0 & -i & 0 \\ i & 0 & 0 \\ 0 & 0 & 0 \end{pmatrix}, \lambda^3 = \begin{pmatrix} 1 & 0 & 0 \\ 0 & -1 & 0 \\ 0 & 0 & 0 \end{pmatrix}, \lambda^4 = \begin{pmatrix} 0 & 0 & 1 \\ 0 & 0 & 0 \\ 1 & 0 & 0 \end{pmatrix},$$
$$\lambda^5 = \begin{pmatrix} 0 & 0 & -i \\ & 0 & 0 \\ i & 0 & 0 \end{pmatrix}, \lambda^6 = \begin{pmatrix} 0 & 0 & 0 \\ 0 & 0 & 1 \\ 0 & 1 & 0 \end{pmatrix}, \lambda^7 = \begin{pmatrix} 0 & 0 & 0 \\ 0 & 0 & -i \\ 0 & i & 0 \end{pmatrix}, \lambda^8 = \frac{1}{\sqrt{3}}\begin{pmatrix} 1 & 0 & 0 \\ 0 & 1 & 0 \\ 0 & 0 & -2 \end{pmatrix}$$

1.1.1 Generators and Casimir Invariants

The $(t_a)^i_j$ obey the following useful relations [18]

$$\mathrm{Tr}\,(t_a t_\beta) = \mathrm{T}_F\,\delta_{a\beta}, \quad \mathrm{T}_F = -\frac{1}{2}$$

$$\sum_a (t^a_{ik})\left(t^a_{kj}\right) = -C_2(N)\delta_{ij},\ C_2(N) = \frac{N^2-1}{2N},\ C_2(N) = \frac{4}{3},\ \text{for SU(3)}$$

$$\sum_{a,\beta} f_{abc}f_{abd} = -C_2(G)\delta_{cd},\ C_2(G) = N,\ C_2(G) = 3\ \text{for SU(3)}$$

$C_2(N)$ is called the Casimir invariant for the fundamental representation, while $C_2(G)$ is the corresponding Casimir invariant for the adjoint representation.
These invariants equip us with [18] a set of useful relationships

$$f_{abc}t^b t^c = \frac{1}{2}f_{abc}f^{bcd}t_d = \frac{1}{2}C_2(G)t_a$$

$$t_b t_a t^b = \left(t_a t_b + f_{bac}t^c\right)t^b = -\left(C_2(R) - \frac{1}{2}C_2(G)\right)t_a$$

$$\mathrm{Tr}\,[t_a : [t_b, t_c]] = -C_2(R)\frac{\dim R}{\dim G}f_{abc}$$

$$\mathrm{Tr}\,[[t_a, t_b][t_c, t_d]] = -C_2(R)\frac{\dim R}{\dim G}f_{abe}f^e_{cd}$$

Using the known relation, for the adjoint representation $(t_a)_{bc} = -f_{abc}$ we also have

$$f^e_{ad}f^f_{be}f^d_{cf} = \frac{1}{2}C_2(G)f_{abc}$$

$$f^f_{ae}\left[f^g_{bf}f^h_{cg}f^e_{dh} - f^g_{bf}f^h_{dg}f^e_{ch} - f^g_{cf}f^h_{dg}f^e_{bh} + f^g_{df}f^h_{cg}f^e_{bh}\right] = -C_2(G)f_{abe}f^e_{cd}$$

1.1.2 The QCD Lagrangian

The invariant Lagrangian density[40] takes the following form

$$L_{QCD} = -\frac{1}{4}\mathrm{Tr}\,(G_{\mu v}G^{\mu v}) - \sum_{f=1}^{h_f}\overline{\Psi}_f\left(\not{D} + m_f\right)\Psi_f =$$

$$= -\frac{1}{4}\left(G^a_{\mu v}\right)^2 - \sum_{f=1}^{h_f}\overline{\Psi}_f\left(\not{D} + m_f\right)\Psi_f$$

$$D_\mu\Psi^i = \partial_\mu\Psi^i - gV^a_\mu\left(t_a\right)^i_j\Psi^j$$

$$G^a_{\mu v} = \partial_\mu V^a_v - \partial_v V^a_\mu - g f^a_{bc}V_\mu V^c_v$$

Therefore we see that the total Lagrangian depends on the QCD coupling constant and the masses of each flavour.

1.1.3 Gauge fixing and ghost terms

In the interest of avoiding unphysical propagating degrees of freedom, a gauge fixing term $L_{GF} = -\frac{1}{2\xi}\left(\partial^\mu V^a_\mu\right)\left(\partial^v V^a_v\right)$ is added to the QCD Lagrangian. The introduction of the aforementioned term, now, dictates the inclusion of ghost fields. Therefore an extra term $L_{ghost} = -\overline{C}^a\left(\partial^\mu\left(\delta_{a\beta}\partial_\mu + g f_{abc}V^c_\mu\right)\right)^b_c$ must be accounted for in L_{QCD}. C is an anticommuting, scalar field in the adjoint representation. One may observe that ghosts couple only to gluons[6], [15], [40].

1.2 Feynman Rules in 't Hooft-Feynman gauge [14]

$$g^{\mu v} = (+,-,-,-)$$

Fermion Propagator

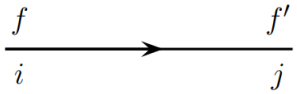

$= \frac{i(\not{p}+m)}{p^2-m^2+in}$

Gluon Propagator

$= -\frac{-i\delta^{a\beta}g^{\mu v}}{k^2+in}$

QCD fermion Vertex

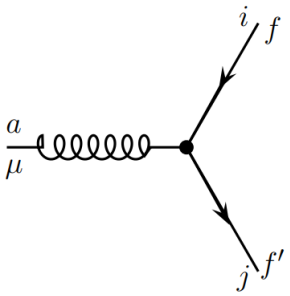

$= igt^c_{ji}\gamma^\mu$, c, i, j colour indices

2

QCD 3 gluon Vertex

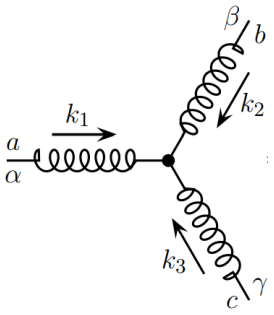

$= gf^{a\beta c}\,(g^{\mu v}(k-p)^p$
$+g^{vp}(p-q)^\mu + g^{p\mu}(q-k)^v)$

QCD
4 gluon Vertex

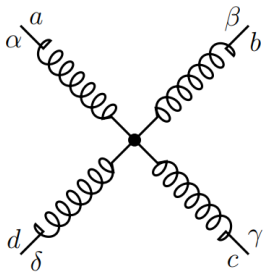

$$= -ig^2 \left(f^{abe} f^{cde} \left(g^{\mu p} g^{v\beta} - g^{\mu\beta} g^{vp} \right) + f^{ace} f^{bde} \left(g^{\mu v} g^{p\beta} - g^{\mu}{}\beta g^{vp} \right) + f^{ade} f^{bce} \left(g^{\mu v} g^{p\beta} - g^{\mu p} g^{v\beta} \right) \right)$$

Ghost
Vertex

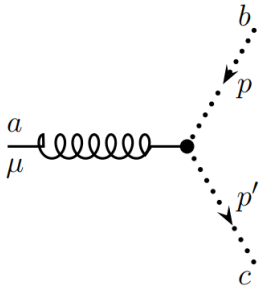

$$= -g f^{abc} p^{\mu}$$

Ghost
Propagator

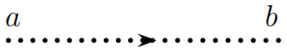

$$= \frac{i\delta^{a\beta}}{k^2 + in}$$

Part I

”Hard-Soft-Collinear factorization of radiative amplitudes”

2 Infrared Structure

2.1 Pinch Surfaces/Landau Equations

The infrared (IR) divergences that concern us in this work arise from vanishing denominators of Feynman path integrals. The denominator being zero is a necessary but not sufficient condition for the creation of these singularities, as the integrand contains a more involved structure, depending on the propagator of the theory. These divergences may be integrable. A systematic organization of the IR singularities is possible using the Landau equations [36]. To secure this set of equations, we will use a framework of a generic scattering event with arbitrary final states as follows:

- **External legs** (E): with momenta $p_1, \ldots, p_E$
- **Loops** (L): with momenta $l_1, \ldots, l_L$
- **Internal legs** (I): with momenta $k_1, \ldots, k_I$

The most generic L-loop Feynman diagram is

$$M = \prod_{i=1}^{L} \int d^d \ell_i N(k_i, p_s) \prod_{j=1}^{I} \frac{1}{k_j^2 - m_j^2 + i\varepsilon}$$

where $N(k_i, p_s)$ is the numerator, which contains possible color and spin factors of the scattering. Various combinatorics and constants have no effect on the purpose of this section and are suppressed. To highlight the singularity structure, one uses Feynman parameters a_i[31]:

$$M = (I-1)! \prod_{j=1}^{L} \int_0^1 da_j \delta(1 - a_1 - \ldots - a_I) \cdot \prod_{i=1}^{L} d^d l_i N(k_i, p_s) D^{-I}$$

with $D = \sum_{j=1}^{I} a_j (k_j^2(l_i, p_s) - m^2) + i\epsilon$.

We have now what appears to be a source of infrared divergences but denominator being zero is not an a-priori indication of a divergence. After all we have to deal with contour integrals and a suitable deformation of the contour using Cauchy's theorem[21] is enough to render the integral convergent. Locating the poles which correspond to pragmatic divergences has to be associated with

cases in which there is no possible deformation of the contour. This is possible in two cases[48]:

Coalescing singularities

If two singularities merge, the contour cannot be deformed: one singularity lies above and the other below the real axis, such that the contour is trapped between them, making any deformation of the integration contour of l_i^μ impossible. This is only possible for the l_i^μ integration as the denominator is quadratic only in the loop momenta. This case corresponds to the minimum of D that is found, requiring $\frac{\partial D}{\partial l_i^\mu} = 0$ for all l_1^μ, and combined with $D = 0$, we extract the constraint.

$$\boxed{\sum_{j=1} a_j k_j^\mu \varepsilon_{ij} = 0}$$

$\varepsilon_{ij} = 1(-1)$ when k_j flows in the same (opposite) direction as $l_i, 0$ otherwise.

Endpoint Singularities

Another scenario where the contour cannot be deformed is referred to as the **endpoint singularity**. Simply put, this means that the singularities reside at the ends of the integration path. In this context, we focus on the case where $a_i = 0$ because momentum endpoint singularities produce UV divergences, which are typically managed through standard renormalization methods, and $a_i = 1$ does not fulfill the condition $D = 0$. Nevertheless, if D is independent of a_i, this cannot be effective either. Hence, we derive the constraint from this analysis.

$$\boxed{a_i \frac{\partial D}{\partial a_i} = 0}$$

The Landau Equations

The previous discussion and the constraints that arose consist of the Landau equations. First, we have to ensure that there is a pinch singularity for all the loop momenta and also to have an endpoint singularity for every a_i or make sure that the denominator does not depend on it.

$$\boxed{k_j^2 = m^2 \text{ or } a_j = 0 \text{ and } \sum_{j \in \text{ loop } r} a_j k_j^\mu \varepsilon_{ij} = 0 \quad \forall j, r}$$

Their solutions describe surfaces in which the denominator vanishes for each integration path. They will be referred as Pinch Surfaces and for each one we shall construct a "reduced diagram" by collapsing all off-shell lines to points.[49]

2.1.1 The Norton Coleman Picture

Solutions to the Landau Equations can prove to be non-trivial in high perturbation orders as well as restrictive in the zero mass limit. A physical interpretation[12] from Norton and Coleman, simplifies the procedure. The main motivation behind their picture is that Landau equations have a different prescription for off-shell and on-shell lines. This leads to a more intuitive interpretation and definitely more practical to use. Off-shell line, Landau equation part, is just $a_i = 0$. Whereas the on-shell component is $\frac{\partial D}{\partial l_i^\mu} = 0$, $a_i \neq 0$. Then $\sum_{j=1} a_j k_j^\mu \varepsilon_{ij} = 0$ is interpreted as

$$\sum_j (\alpha_j \omega_j) U_j^\mu = 0$$

which can be read as the distance, a free classical particle covered, in time $(\alpha_j \omega_j)$ with velocity v_j^μ.

For a specific position x_1^μ to a vertex in the reduced diagram associated with the pinch surface and a line j attaches to this vertex, then $x_1^\mu + (\alpha_j \omega_j) U_j^\mu$ represents the position of the vertex at the other end of line j. By continuing this approach, we can assign space-time positions to all vertices in the reduced diagram, depicting a physical process where free particles move between these points.

As a result from this discussion, we have a very interesting interpretation of the Landau equations, and that is not all. In this picture, the pinch condition for on-shell lines is equivalent to an interpretation of every loop created from on-shell lines to be a closed classical path, as a free propagation between vertices. Vertices are now spacetime points separated by $\Delta {x_j}^\mu$. These on-shell lines make the diagram singular only if the off-shell lines do not propagate. As a result, every singular diagram can be drawn with the following prescription: Off-shell lines are shrunk into points, and on-shell lines correspond to allowed classical trajectories. The identification of solutions of Landau equations is now just a procedure of drawing all the possible reduced diagrams.

In our study, encountering collinear and soft singularities together with hard off-shell momenta will result in the generation of the following subdiagrams from this analysis.

- Jet subdiagram (on-shell collinear lines)
- Soft subdiagram (on-shell soft lines)
- Hard subdiagram (off-shell hard lines)

The subdiagrams will be connected with quark and gluon exchanges, and factorization, the main subject of this thesis focuses on disentangling those connections and approximating the amplitude as a scalar product of the separate subdiagrams.

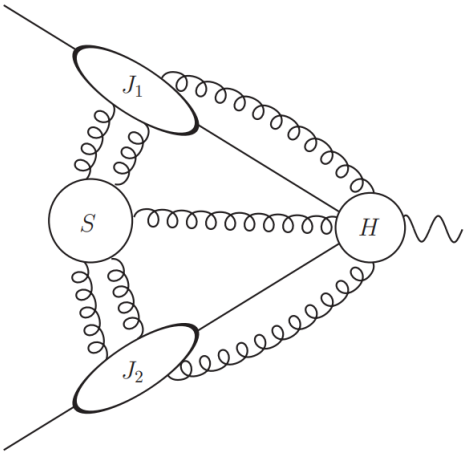

Figure 2.1: **E**xample of a reduced diagram in a 2-parton final state scattering event [10]

2.2 IR Power Counting

It is useful to devote a whole chapter to formally introduce the light-cone basis we will use in the rest of the work and to introduce the IR power counting from first principles.

2.2.1 Light Cone Coordinates

For each momentum vector p_i, we introduce two lightlike vectors n_i and $\bar{n}_i$:

$$n_i^\mu = \frac{1}{\sqrt{2}}\left(1, \frac{\vec{p_i}}{|\vec{p_i}|}\right), \quad \bar{n}_i^\mu = \frac{1}{\sqrt{2}}\left(1, -\frac{\vec{p_i}}{|\vec{p_i}|}\right),$$

$$\text{with } n_i \cdot \bar{n}_i = 1, \quad n_i^2 = \bar{n}_i^2 = 0.$$

These lightlike vectors can, of course, be used for any generic vector u^μ:

$$n_i^\mu = \frac{1}{\sqrt{2}}\left(1, \frac{\vec{u_i}}{|\vec{u_i}|}\right), \quad \bar{n}_i^\mu = \frac{1}{\sqrt{2}}\left(1, -\frac{\vec{u_i}}{|\vec{u_i}|}\right).$$

The decomposition of a vector u_i^μ in terms of these lightlike vectors is:

$$u_i^\mu = u^+ n_i^\mu + u^- \bar{n}_i^\mu + u_{1\perp}^\mu,$$

where

$$u^+ = u \cdot \bar{n}_i, \quad u^- = u \cdot n_i.$$

A scalar product between two vectors u^μ and ω_μ is now defined as:

$$u^\mu \omega_\mu = u^+ \omega^- + u^- \omega^+ + u_\perp \cdot \omega_\perp.$$

This decomposition and the associated scalar product are useful in various contexts, particularly in high-energy physics and the study of scattering amplitudes, where lightlike vectors simplify the calculations involving collinear and soft emissions.

Dirac matrices

$$\begin{aligned}
&(\gamma^+)^2 = (\gamma^\mu \bar{n}_\mu)^2 = (\gamma^\mu)^2 (\bar{n}_\mu)^2 = 0,\\
&(\gamma^-)^2 = (\gamma^\mu n_\mu)^2 = (\gamma^\mu)^2 (n_\mu)^2 = 0,\\
&\{\gamma^+, \gamma^-\} = \gamma^+\gamma^- + \gamma^-\gamma^+ = \gamma^\mu \bar{n}^\mu n_\mu \gamma_\mu + \gamma^\mu n^\mu \bar{n}_\mu \gamma_\mu = 21,\\
&\gamma^1 \gamma^\pm = -\gamma^\pm \gamma^1,\\
&\gamma^\pm = \gamma_\mp
\end{aligned}$$

2.3 Power Counting

2.3.1 Power Counting of external Momenta

It is straightforward to realise that soft and collinear modes are those which dominate cross-sections [47]. To show this I will investigate the most generic scattering event with n final state external particles, all massless and with momenta p_i. The intermediate momenta k_i are linear combinations of the external and as such $k_i^2 = \sum p_i \cdot p_j$. Therefore to acquire the dominant areas of a diagram where the propagators grow large it is necessary to have either collinear or soft external momenta.

2.3.2 Power counting of virtual momenta

Now I will present the most generic proof of the infrared scaling of virtual momenta. The IR divergences occur when virtual momenta go on shell. Technically the virtual momenta are a linear com-

bination of loop and external momenta [47][3]. Therefore they would blow up if the loop momenta would go soft or collinear. For simplicity and without loss of generality we assume the virtual momenta are in the direction of the loop momenta.

We parametrize the components of the usual lightcone decomposition

$$k^\mu = k_- \bar{n}^\mu + \ k_+ n^\mu + \vec{k}_\perp$$

$$k^\mu \to \lambda^a k_- \bar{n}^\mu + \lambda^b k_+ n^\mu + \lambda^c \vec{k}_\perp$$

$$0 < \lambda < 1 a,\ b \geq 0,\ a + b > 0,\ c > 0$$

When one expands in $\lambda \to 0$, can isolate the leading and subleading power regions of interest. We proceed analogously with [47].

Conjecture 1 (Power-Counting Finiteness Conjecture [26]) *A Feynman integral is infrared finite if and only if it scales as a positive power of k under all possible rescales in Eq. (17).*

Hard subdiagram

For the choice $a = b = c = 0$, $\lambda \to 0$ produces no singularity and therefore we can identify this region as the hard subdiagram.

2.4 Propagators

For the rest of the pinch surfaces, investigation must be more meticulous. In QCD, we will encounter propagators of the form :

$$\sim \frac{1}{k^2}$$

$$k^2 = 2k_+k_-\lambda^{a+b} + \lambda^{2c}k_1^2$$

Cases:

- $a + b > 2c$: We can drop k_+k_-.
- $a + b < 2c$: k_1^2 drops off.
- $a + b = 2c$: $k^2 = 0$, on-shell for $\lambda = 0$.

$$\sim \frac{1}{(k - p_a)^2}$$

- If p_a^μ is not lightlike:

$$\frac{1}{(k - p_a)^2} \sim \frac{1}{p_a^2} \quad \text{scales as } \lambda^0$$

- If p_a^μ is lightlike a term $\lambda^a k_- p_+$ or $\lambda^b k_+ P_-$ can appear.

$$\begin{aligned} k_+k_- &\sim \lambda^{a+b} \\ k_1^2 &\sim \lambda^{2c} \\ k_-P_+ &\sim \lambda^a \\ k_+P_- &\sim \lambda^b \end{aligned}$$

The previous statements along with the observation that if an integral is IR finite and has two comparable scale terms, then it remains IR finite if we drop one [26], constrain the discussion to scalings where at least two terms are comparable.

Synopsis

1. $a + b = 2c$: $k_+ k_- \sim k_1^2$: keeps on-shell momenta on-shell.
2. Two lines intersect four times.
   - If the integral is IR finite at all of these points, it is IR finite under any scaling.
3. Three lines intersect, $a = b = c$
   - $k_- p_+ \sim k_+ p_-$
   - $k_+ k_- \sim k_1^2$
4. All four scalings equal at four-line intersection, $a = b = c = 0$: Hard scaling.
5. The point at the origin can also not create IR singularities since $\lambda = 0$, k^μ is off-shell.

Therefore, this analysis deduces [26] the list of scalings that will be used in the present work.

Scaling Type	Momenta Configuration
Hard	$l^\mu = Q(1, 1, 1)$
Semi-Hard	$l^\mu = Q(\lambda, \lambda, \lambda)$
Collinear	$l^\mu = Q(1, \lambda, \lambda^2)$
Anti-Collinear	$l^\mu = Q(\lambda^2, \lambda, 1)$
Soft	$l^\mu = Q(\lambda^2, \lambda^2, \lambda^2)$
Ultra-Collinear	$l^\mu = Q(1, \lambda^2, \lambda^4)$
Anti-Ultra Collinear	$l^\mu = Q(\lambda^4, \lambda^2, 1)$
Ultra Soft	$l^\mu = Q(\lambda^4, \lambda^4, \lambda^4)$

Table 2.1: List of scalings used in the present work

Collinear Divergence Scaling

For a collinear divergence associated with the direction p^μ of an external momentum, we rescale:

$$d^4k \to \lambda^4 d^4k$$
$$k^2 \to \lambda^2 k^2$$
$$k \cdot p \to \lambda^2 k \cdot p$$

If q is another loop momentum, the scaling depends on whether q is collinear to p [7]:

$$k \cdot q \to k \cdot q \times \begin{cases} \lambda^2, & \text{if } q \text{ is collinear to } p \\ \lambda^0, & \text{if } q \text{ is not collinear to } p \end{cases}$$

2.5 Notes on gauge choices

2.5.1 Gluon Propagator in Axial Gauge

In Axial gauge the Lagrangian takes the form

$$L = -\frac{1}{4} G^a_{\mu v} G^{\mu v a} - \frac{1}{2}\lambda (r_\mu A^{\mu, g})^2 - \bar{r}^a r_\mu (\delta_{a\beta} + g f^{abc}\, A^{\mu, c}) r_\beta$$

With usual methods we obtain the corresponding gluon propagator:

$$\begin{aligned}\Delta^{a\beta}_{\mu v}(k,r,\lambda) &= \frac{-i\delta^{a\beta}}{k^2+i\varepsilon}\left(n_{\mu v}-\frac{r_\mu k_v + k_\mu r_v}{(r\cdot k)}+r^2\left(1+\frac{k^2}{\lambda r^2}\right)\frac{k_r k_v}{(r\cdot\mu)^2}\right)\\ &= \frac{i\delta^{a\beta}}{k^2+i\varepsilon}\pi^{\mu v}(k)\\ \pi^{\mu v}(k) &= \left(-n\mu_v+\frac{r_\mu k_v + k_\mu r_v}{(r\cdot k)}-r^2\left(1+\frac{k^2}{\lambda r^2}\right)\frac{k_r k_v}{(r\cdot k)^2}\right)\end{aligned}$$

We notice, that in the $\lambda \to \infty$ limit

$$r^\mu \Delta^{a\beta}_{\mu v}(k,r,\lambda) = r^v \Delta^{a\beta}_{\mu v}(k,r,\lambda) = 0.$$

So like in the photon propagator, in QED, there is no gluon-ghost coupling.

Furthermore $k_\mu \pi^{\mu v}(k) = \frac{k^2}{r\cdot k} r^v$, which has no pole at $k^2 = 0$ and only physical polarization are allowed. [14]

To shed further light on this physical gauge, we see that the propagator numerator is a sum over physical polarizations when the gluon goes on-shell:

$$\pi^{\mu\nu}(k) = -n^{\mu\nu} + \frac{r^\mu k^\nu + r^\nu k^\mu}{(r\cdot k)} \xrightarrow{k^2=0} \sum_{n=\pm} \varepsilon^\mu_n(k;r)\varepsilon^{\nu *}_n(k;r)$$

where r are reference vectors:

$$\begin{aligned} r_\mu \varepsilon^\mu_\pm(k;r) &= 0\\ k_\mu \varepsilon^\mu_\pm(k;r) &= 0\end{aligned}$$

At this point, we return to our power counting motivation and firstly we notice that if p^μ is some light-like direction and k_μ is collinear to p_μ, then $p_\mu \pi^{\mu\nu}(k) = 0$. Near a collinear singularity, a numerator $p\cdot\pi(k)$ has a scaling of λ.
In the present work, we will usually face numerator structures from virtual gluons of the form $p\cdot\pi(k)\cdot q$.

2.6 Eikonal Approximation/Wilson Lines

Softly emitted gauge bosons often lead to divergences in scattering processes. Propagators with $\frac{1}{k^2}$ diverge, and it becomes challenging to distinguish whether soft gauge boson radiation consists of one or multiple particles, such as gluons in the context of Quantum Chromodynamics (QCD).

Fortunately, these scattering amplitudes exhibit a universal nature that allows for a factorization between the non-radiative amplitude and a novel object in the soft limit. This factorization is encoded in the Eikonal Approximation, predominantly expressed via Wilson Lines. Wilson Lines describe the radiation emitted by a charged particle moving along a path in the semi-classical limit. The crucial aspect is that this limit holds when the particle is significantly more energetic than the soft bosons, allowing us to neglect the back-reaction of radiation on the particle. Thus, the calculations are drastically simplified and allow for exponentiation of the amplitudes, paving the way for a set of rules to compute logarithms.

2.7 The Eikonal Approximation

2.7.1 The Eikonal Identity

$$\sum_{\pi} \frac{1}{p \cdot k_{\pi_1}} \cdot \frac{1}{p \cdot (k_{\pi_1} + k_{\pi_2})} \cdots \frac{1}{p \cdot (k_{\pi_1} + \cdots + k_{\pi_n})} = \prod_{i=1}^{n} \frac{1}{p \cdot k_i} \tag{2.1}$$

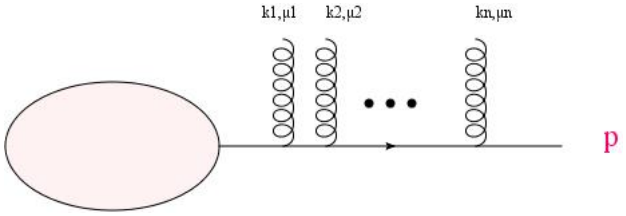

Figure 2.2: n-soft gluon emissions from a hard outgoing particle. Most of the diagrams of this thesis are done in Jaxodraw [9]

The sum over all permutations of the gauge boson momenta radiated in an n-radiation scattering in the soft limit yields the simple equation (2.1). Before practically examining its consequences, we note the decorrelation of emissions in the amplitudes as a direct result of the eikonal approximation.

For a generic graph, using the eikonal identity, the radiating amplitude can be expressed as:

$$M^{\mu_1\mu_2\cdots\mu_n}(p,k_1,\ldots,k_n) = M_0 \prod_{i=1}^{n} \frac{-ep^{\mu_i}}{p\cdot k_i}$$

Consider the simple QED M^{n+1} amplitude of the following Feynman diagram:

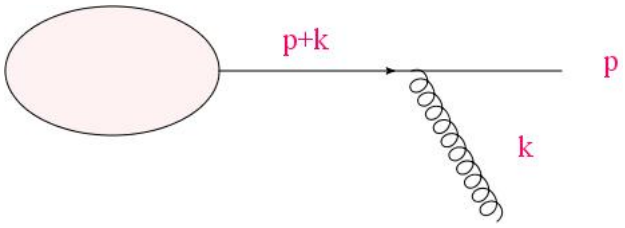

Figure 2.3: A simple QED M^{n+1} amplitude.

$$M_0 \cdot \frac{i(\not{p}+\not{k})}{(p+k)^2}(-ie\gamma^{\mu})\, u(p) = M^{\mu}(p,k)$$

After expanding in soft photon momentum k and retaining the lowest order terms, as well as using $\not{p}\, u(p) = 0$,

$$M^{\mu}\varepsilon_{\mu} \simeq M_0 \left(\frac{ep^{\mu}}{p\cdot k}u(p)\right)\varepsilon_{\mu}(k)$$

we can make two crucial observations:

1. There is no spin dependence.
2. The effective coupling is proportional to the emitting particle momentum, as in the general formula.

Each eikonal emission is expressed by the effective Feynman Rule:

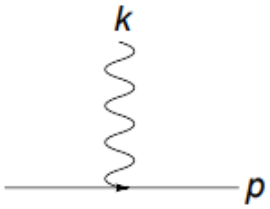

Figure 2.4: Effective Feynman Rule for eikonal emission

$$= \frac{p^{\mu}}{p\cdot k}$$

2.8 Wilson Lines

Since our goal is to work with QCD amplitudes, we immediately introduce the Wilson Line framework[22], [15] in non-Abelian gauge theories. Wilson Lines appear in the soft limit of Yang-Mills (YM) theory and also play a role in collinear limits, as we will see later.

Outgoing Wilson line, n^μ direction, particle:

$$Y_n^+(x) = P\, e^{ig\int_0^\infty ds\; n\cdot A(x^v+sn^v)e^{-\varepsilon s}}$$

Outgoing Wilson line, n^μ direction, antiparticle:

$$Y_n(x) = \overline{P}\, e^{-ig\int_0^\infty ds\; n\cdot A(x^v+sn^v)e^{-\varepsilon s}}$$

$P, (\overline{P})$: (anti) path ordering.
A: $A^a t_a$, gauge field in the fundamental representation.

2.8.1 Incoming Wilson Lines

Particles:

$$\overline{Y}_n(x) = P\, e^{ig\int_{-\infty}^0 ds\; n\cdot A(x^v+sn^v)e^{\varepsilon s}}$$

Anti-particles:

$$\overline{Y}_n^+(x) = \overline{P}\, e^{-ig\int_{-\infty}^0 ds\; n\cdot A(x^v+sn^v)e^{\varepsilon s}}$$

One can see the pattern: the path now extends from $-\infty$ to x, indicating incoming (anti) particles, in contrast to the outgoing (anti) particles path from x to ∞.

To make the discussion clearer, and to extract Feynman rules for Wilson Lines while maintaining contact with physics, we examine these objects more fundamentally. Setting $x^v = 0$ and considering a general path from s to s_2, the Wilson line $Y_n^+(0)$ after a usual Taylor expansion is of the form:

$$Y_n^+(0, s_1', s_2') = \sum_{n=0}^{\infty} \frac{1}{n!}(ig)^n P\left(\int_{s_1'}^{s_2'} ds_1 \dots ds_n\; n\cdot A(s_1 n)\cdots A(s_n n)\right)$$

- Every soft gluon is emitted at $s_i n^\mu$.
- Since all s_i are integrated over the full path, path ordering P ensures that the color generators are ordered correctly. Fields closer to s_2' are placed to the left.

To extract Feynman rules, we Fourier transform the gluon field as:

$$A_\mu^a(x) = \int \frac{d^4k}{(2\pi)^4} A_\mu^a(k) e^{-ikx}$$

As in covariant quantization, the description of the gluon field involves the creation operator accompanied by $e^{ik\psi}$; we have to shift $k^\mu \to k^\mu$ as the creation operator is contracted with a finite state gluon. Changing the path from 0 to ∞ for the outgoing particles:

$$Y_n^+(0) = 1 + igT^a \int \frac{d^4k}{(2\pi)^4} n\cdot A^a(-k) \int_0^\infty ds e^{is(k\cdot n+i\varepsilon)} = 1 - gT^a \int \frac{d^4k}{(2\pi)^4} A_\mu^a(-k)\frac{n^\mu}{nk+i\varepsilon}$$

In a similar manner, we derive the Wilson line for incoming particles:

$$\overline{Y}_n(0) = 1 + igT^a \int \frac{d^4k}{(2\pi)^4} n\cdot A^a(-k) \times \int_0^{-\infty} ds e^{is(k\cdot n-i\varepsilon)} = 1 - gT^a \int \frac{d^4k}{(2\pi)^4} A_\mu^a(-k)\frac{n^\mu}{n\cdot k-i\varepsilon}$$

Feynman Rules

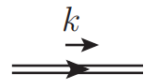

$= \frac{i}{nk+i\varepsilon}$

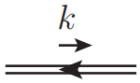

$= \frac{-i}{nk-i\varepsilon}$

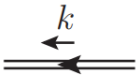

$= \frac{i}{nk+i\varepsilon}$

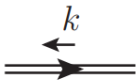

$= \frac{-i}{nk-i\varepsilon}$

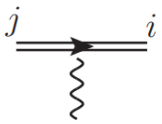

$= ign^{\mu}(t^a)ij$

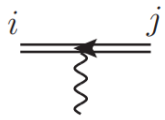

$= -ign^{\mu}(t^a)ij$

- n^{μ} direction, pointing to higher values of s, corresponds to the arrow.
- Color indices are attached against the direction of the arrow, due to path ordering.
- In the Feynman rules, outgoing and incoming antiparticles are included; one can use $Y_n(0)$ and $\overline{Y}^{+}_{n}(0)$ to extract them or simply set $k \to -k$.
- A single Wilson line can be set to 1.

2.8.2 Wilson Lines and Eikonal Approximation

Equipped with a Wilson-Line framework and a set of Feynman rules, we now examine whether we can successfully describe eikonal emissions of gluons from a hard particle.

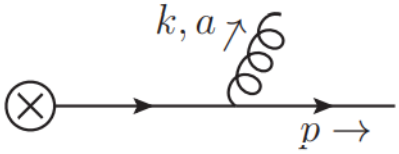

Figure 2.5: Eikonal vertex, in the soft limit of a QCD interaction

Via the Eikonal approximation, and exploiting the invariance in rescaling of p^{μ}[33], we set $p^{\mu} = n^{\mu}$ and find the result[33]:

$$\frac{-g(t^a)_{ij}n^{\mu}\varepsilon_{\mu}(k)}{n \cdot k + i\varepsilon}$$

For a quark with final state color label i, emitting eikonically a soft gluon, the contributions are encoded in $Y^{+}_{n}(0,\infty)_{ij}$, where j is the initial color index. Using the Feynman rules, we can immediately

check that we obtain the same result $\frac{-gt^a_{ij}n^\mu\varepsilon_\mu}{n\cdot k+i\varepsilon}$. To illustrate this more explicitly a state with a gluon of $\varepsilon^\mu(k)$ radiated:

$$\begin{aligned}\langle\varepsilon(k)|Y_n^+(0)|0\rangle &= ig(t^a)_{ij}\int_0^\infty ds\langle\varepsilon(k)|n\cdot A^a(s\cdot n^\mu)|0\rangle e^{-\varepsilon s} = \\ &= ig(t^a)_{ij}(n\cdot\varepsilon^*(k))\int_0^\infty ds e^{is(nk+i\varepsilon)} = \\ &= -g(t^a)_{ij}\frac{n\cdot\varepsilon^*(k)}{nk+i\varepsilon}\end{aligned}$$

Similarly, for an incoming hard particle, the correct use of Feynman rules for $\overline{Y}_n(0)$ recreates the eikonal approximation:

$g(t^a)_{ij}\frac{n\cdot\varepsilon(k)}{n\cdot k-i\varepsilon}$

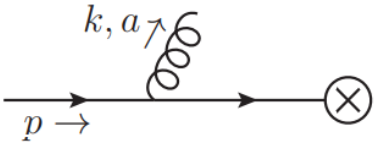

2.8.3 Collinear Wilson Lines

Apart from the soft Wilson Lines examined earlier, similar mathematical entities are used for the collinear limit[47]. The only difference with soft Wilson lines is that the path is different. Soft Wilson lines point in the direction of the particle they represent, whereas collinear Wilson lines point in some other direction ℓ^μ, which is not collinear to n^μ.

$$W_j^+(x) = P\, e^{ij\int_0^\infty ds\ell\cdot A(x^v+s\ell^v)e^{\varepsilon s}}$$

Soft Wilson lines account for the soft radiation of a particle, whereas collinear Wilson lines account for the collinear radiation from all other particles.

2.8.4 Wilson Line Properties

Wilson lines possess a set of very interesting properties[6], [15], some of which play a major role in here and in similar works:

- Under gauge transformations, a generic Wilson line $Y_n(s_1, s_2)$ transforms as:

$$Y_n(s_1, s_2) \to U(s_2) Y_n(s_1, s_2) U^{-1}(s_1)$$

where $U(\lambda) = e^{i\xi^a(\lambda) t_a}$ are the $\mathrm{SU}(3)$ transformations.

- When a trajectory can be written as the sum of two smaller ones, the corresponding Wilson lines are equal to the Wilson line of the combined trajectory:

$$Y_n(s_1, s_2) Y_n(s_2, s_3) = Y_n(s_1, s_3)$$

- The covariant derivatives acting on an endpoint of the Wilson line projected along the path vanish:

$$\frac{dx^\mu}{ds} D_\mu(x) Y_n(x, \psi) = 0$$

- Wilson lines can be expressed in any representation. For example, the adjoint Wilson Line:

$$\mathcal{Y}_n^+(x) = P\, e^{ig \int_0^\infty ds n \cdot A_\mu^a(x+sn)(t^a)_{adj} e^{-\varepsilon s}}$$

We know that $(t^a)^{bc}_{adj} = i f^{bac}$ and $[t^a, t^c] = i f^{acb} t^b$:

$$(t^c_{adj})^{a\beta} t^b = [t^a, t^c]$$

Therefore,

$$Y_n^+ A_b^\mu t^b Y_n = A_a^\mu \cdot Y_n^{a\beta} t^b$$

-

$$\begin{aligned} Y_n^+(-\infty, x) &= Y_{-n}(x, \infty) \\ Y_n^+(x, \infty) &= Y_{-n}(-\infty, \lambda) \\ \overline{Y}_n(s_1, s_2) &= Y_n^+(s_2, s_1) \end{aligned}$$

- $e^{\pm\varepsilon s}$ factors are required as they generate the pole displacements in the propagators in perturbation theory. A small discomfort occurs as these factors interfere with gauge transformations, but only in an ε-order term:

$$Y_n(x) \to e^{i\xi^a t_a} Y_n(x) e^{-i\xi^a(x) t_a} + O(\varepsilon)$$

- A very useful property of Wilson Lines is that they ensure gauge invariance for otherwise non-invariant field products. The insertion of a Wilson line $Y_n(x, \psi)$ secures invariance by transporting the gauge information from ψ to x, creating an invariant correlation function:

$$\begin{aligned} \langle 0 | T \overline{\Phi}(\psi) Y_n(x, \psi) \Phi(x) | 0 \rangle \to \langle 0 | T \overline{\Phi}(\psi) U^+(\psi) U(\psi) Y_n(x, \psi) U(x)^+ U(x) \Phi(x) | 0 \rangle = \\ = \langle 0 | T \overline{\Phi}(\psi) Y_n(x, \psi) \Phi(x) \rangle \end{aligned}$$

2.9 Cut Diagrams

A technique which will be handy for the rest, is based on a fundamental fact which originates in unitarity[41]: the sum of all conceivable cut diagrams which can be created from a scattering amplitude is equal to the imaginary part of this amplitude[2]. (Figure 2.6). A useful result of unitarity allows for construction of the squared amplitude and, consequently of the cross-section only with the method of cut diagrams. These are diagrams constructed by intersecting the original diagram into two separate parts with an on-shell ”cut line”. This is shown in Figure 2.6.

- Left Part: Consists of initial states.
- Right Part: Consists of final states.
- Cut propagators are replaced with on-shell condition.

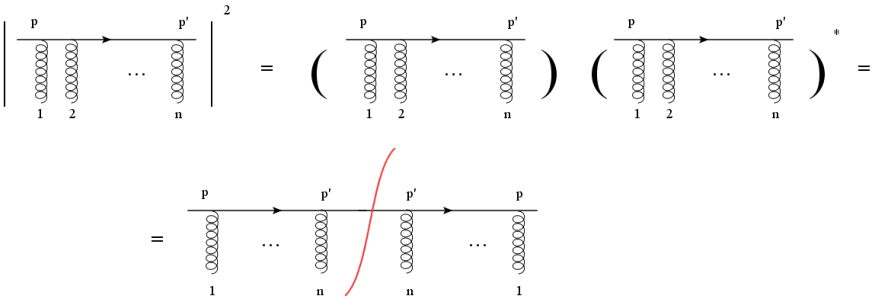

Figure 2.6: Cut diagrams

In Figure 2.6, the continuous line can represent any charged particle, allowing us to interpret the scenario as a gluon radiating quark. In such a QCD scenario, the figure equality is proven using the identity

$$\bar{u}_{s'}(p')\,\gamma_{\mu_n}\ldots\gamma_{\mu_1}u_s(p)^* = \bar{u}_s(p)\gamma_{\mu_1}\ldots\gamma_{\mu_n}u_{s'}(p') \text{ and } T^{a\,*}_{ij} = T^a_{ji}$$

Put simply, these identities suggest that by reversing both the charge flow and the i factors, we can derive the complex conjugate of a charged line. Thus, for given final momenta, we can redesign the diagram so that the final momenta converge at the midpoint of the line. These identities stem from the Hamiltonian’s hermiticity and the concept of unitarity. We can interpret the cut in Figure 2.6 as imposing the on-shell condition and the constraint of energy positivity. Summing over final spins, we derive a cut line Feynman rule equivalent to replacing a propagator with its imaginary part and the numerator arising from the spin sum.

Feynman rule for ”Cut line”

$$\mathrm{i}\frac{\not{p}+m}{p^2-m^2+\mathrm{i}\eta} \to (2\pi)\delta\left(p^2-m^2\right)\theta\left(p_0\right)\sum_s u_s(p)\bar{u}_s(p) \equiv (2\pi)\delta_+\left(p^2-m^2\right)(\not{p}+m).$$

2.9.1 Conclusion

Equipped with a new set of useful entities, such as the Wilson lines, their Feynman rules, and their identities, which are linked to the eikonal approximation, we are ready to define the soft and jet functions.

3 Leading Power Factorization

Having set the table thanks to the previous discussion, it is now time to finally show how can we factorize a QCD process or in other words decouple Hard Jet and Soft functions. Very concretely so far we identified regions of real or virtual phase space as candidates to create IR singularities only in order to interpret them later as subdiagrams in Coleman Norton picture[34] and power count them in an infrared framework[50], which rules have all be listed in this work. We have seen that the leading power contribution , corresponds to $\lambda = 0$[34] and we with a full set of power counting rules in our side we are prepared to extract the corresponding reduced diagram. Corresponding of Wilson lines and eikonal approximation is the last asset we will need in our attempt to produce a factorization formula for the leading power. The procedure will be done in a photon annihilation process to two massless partons, in covariant gauge, therefore two Jet subdiagrams will appear. A generalization to n final partons is not straightforward and this will be discussed at the end, whereas it also will act as a stepping stone for the further.

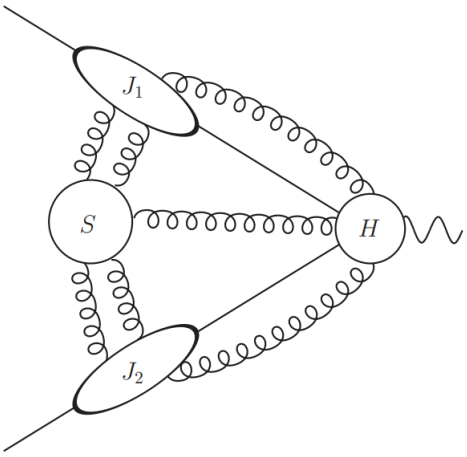

Figure 3.1: Reduced diagram for 2-hard particles in the final state.No quarklines connectining subdiagrams up to LP due to power counting.[10]

At this point, it is useful to remember that the final goal of decoupling Soft, Hard and Jet subdiagrams is translated in an effort to have a reduced diagram, in which no subdiagram is connected to any other.

The first observation that can immediately be made is that there are no quark lines between the blobs. This follows from our power counting procedure as any such line would not survive power counting .

3.1 The Soft Function

The goal in each of these subsections will therefore be to decouple the subdiagram in question from the rest of the blobs. We already have seen that for soft emitted gauge bosons , we can use the eikonal approximation and the Wilson lines to simplify and interpret the radiating effects.

Since the goal of this section is a factorization formula only up to LP , there is no soft gluon connection between the Hard subdiagram and the Soft one. This is also due to the power counting. When a soft gluon attaches to an internal off-shell propagator in the Hard subdiagram, it splits the propagator into two parts. This splitting introduces an additional off-shell propagator, resulting in contributions that exceed the leading power. Consequently, soft gluons cannot establish connections between the hard and soft subdiagrams.

It is now time , for the eikonal approximation to be used in this work . For the moment let's concentrate our efforts in the remaining soft gluon connection between the Soft and Collinear reduced diagrams .

A soft gluon , can only couple to a collinear jet with its longitudinal polarization[35]. This observation leads us to apply the Non-Abelian Ward Identities[53], which are revealing that the coupling of the soft gluon is analogous to the quark coupling bridging J and H, as well as to the coupling of the soft gluon to the hard reduced diagram. As previously noted, the latter is not existent in leading power. Consequently, we are left with a soft gluon coupled to the quark line linking the Jet and the Hard blobs. Hence, the previously discussed eikonal approximation straightforwardly applies. The soft radiation thus decouples from the Jet and attaches to an eikonal line.

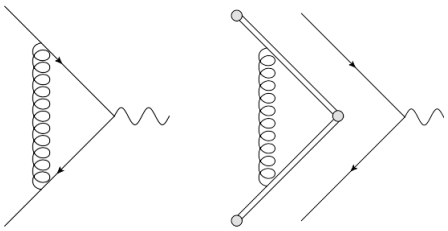

Figure 3.2: Decoupling of a soft gluon correction in the electromagnetic vertex , via the eikonal approximation .[10]

What has been done so far is a complete factorization of the soft effects included in the reduced soft blob with the use of the, defined as follows, Wilson line:

$$S(n,\bar{n}) = \langle 0|Y_n^\dagger(0)Y_{\bar{n}}^\dagger(0)|0\rangle$$

Here n and are the directions of the two final Jets . For an event with n final Jets, the soft function would be

$$S(n_i) = \langle 0|\prod_i Y_{n_i}^\dagger(0)|0\rangle$$

if QED was the case in question . *We shall see that the non abelian nature of colour generators do not allow for a naive expression like the one mentioned .*

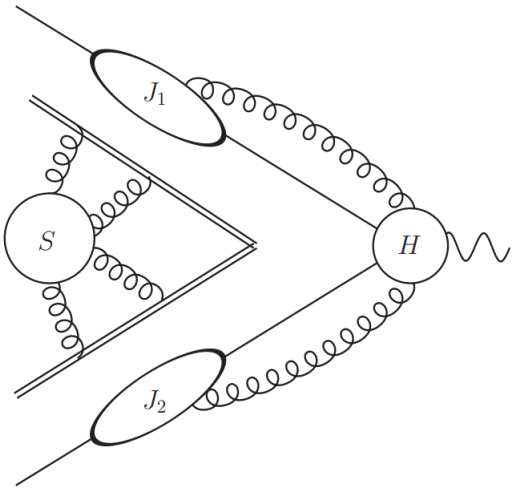

Reduced diagram for 2-hard particles in the final state after decoupling of the Soft subdiagram .

3.2 The Jet Function

The Jet subdiagrams are still connected with the Hard one .We focus now to a collinear gluon attached to the Hard subdiagram and keep in mind that it can do so only with its longitudinal polarization .Then using the Ward Identities , we can extract a situation where the eikonal approximation can be applied .

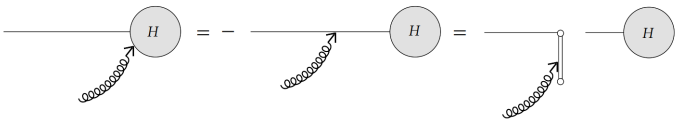

Reduced diagram for 2-hard particles in the final state after decoupling of the Soft subdiagram[10].

The Ward identites[41] ,

$$k^{\mu} M_{\mu} = 0 \tag{3.1}$$

sum over the longitudinal polarizations on the Amplitude to be zero. Therefore (see figure) the collinear gluon coupled to the Hard function, added to a collinear gluon coupled to the quark line that connects the Jet with the hard blob should equal to zero. That is depicted in the first equality of the figure .

Grammer and Yennie [10], [50], [15], have shown that the collinear gluon attached to the quark off shell line can be detached from it and attached to an eikonal line (second equality) of the figure.

Consider a QCD correction to the EM vertex

In [10], it is shown that in the collinear pinch surface for the first momentum, in which the other one is off shell and in the Norton picture is reduced to a point using a simple rearrangement of the virtual momentum

$$A^{-}B^{+} = A^{-}\frac{k^{+}}{k^{+}}B^{+} = (k \cdot A)\frac{B \cdot n}{k \cdot n} \quad \text{(n is } \bar{n} \text{ here)}$$

and working in the lightcone coordinates, the gluon can be detached from the hard off shell part and attach to a Wilson line as one can see from the scattering amplitude calculated in their work [10], [15].

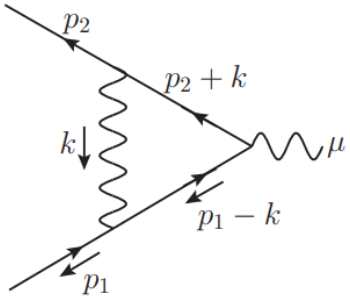

Figure 3.3: Typica QCD correction to photon , quark antiquark vertex

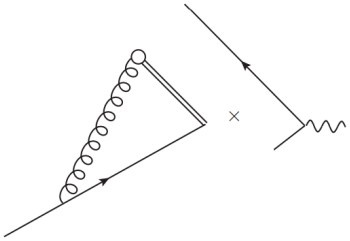

Figure 3.4: Collinear gluon deatachment from the hard part and factorization of the amplitude to a hard and a jet function [10]

$$\int \frac{d^4k}{(2\pi)^4}\bar{u}(P_2)\gamma^\mu \frac{(\not{P}_1 - \not{k})\gamma\cdot n}{(P_1-k)^2k^2}\frac{1}{k\cdot n}u(P_1)$$

where we can easily see the decoupling of the gluon from p2 and the corresponding eikonal feynman rule that appears.

From this point everything is clear, we can repeat the same procedure as many times as we need and decouple all the collinear gluons from the subdiagram of H.Adopting the Wilson line nomenclature for the afforementioned procedure we can have the following formula for the Jet function[34], [10].

$$J(p) = \langle 0|W_l^\dagger(0)\psi(0)|p\rangle \tag{3.2}$$

3.3 Jet-soft Factorization

We are almost done. Almost, because of a small detail that is not taken care of yet. Namely, we did not consider soft gluons that turn collinear, or conversely collinear gluons that become soft. Their effect is captured in both S and J matrix elements and that, obviously is a double counting. We resolve this situation with the use of an overlapping factor that captures and deletes the double contributions either from the Jets or from the Soft functions. Now, consider the Jet function by defining an eikonal Jet function[10], [34] as follows,

$$\mathscr{J} = \langle 0|W_l^\dagger(0)Y_n^\dagger(0)|0\rangle \tag{3.3}$$

By doing so, we eliminate the redundant contributions and can ultimately represent the total factorization formula up to leading power as [10], [34]:

$$M^\mu\left(\frac{\mu^2}{Q^2}\right) = H\left(\frac{\mu^2}{Q^2}, p\right)S(n,\bar{n})\prod_{i=1}\left(\frac{J_i(p,l)}{\mathscr{J}(l,\bar{n})}\right) \tag{3.4}$$

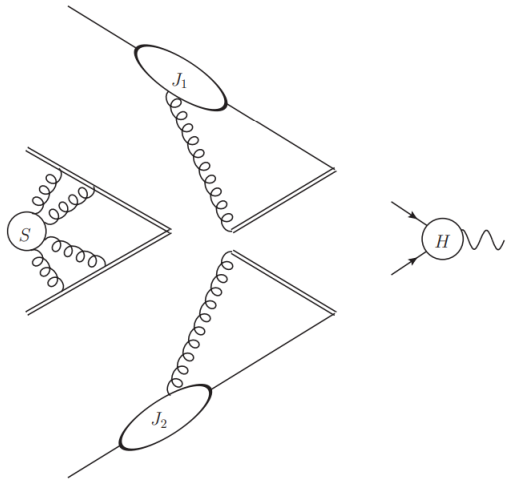

Figure 3.5: Reduced diagram for 2-hard particles in the final state. Factorization is complete and Jets are also decoupled[10]

[10], [2]

Commentary

- Soft and Jet functions are *universal*, and as such they depend only on quantum numbers of the external particles.
- The hard function is process dependent, and as such it can contain new UV divergencies, even if it is IR finite as we already declared.
- To avoid spurious singularities in the Jet function, we define $n^2 \neq 0$.

4 Next to Leading Power Factorization. QED and extensions

4.1 $e^+ + e^- \to \gamma^*$ Factorization

In recent years there is a growing emphasis on the study of power corrections in the theory of gauge invariant scattering events. This is driven by the anticipated precision demands, which the upcoming experimental facilities in Europe[1][11] and the US[32] will necessitate.

At the beginning of this chapter, we derive a factorization formula up to and including next-to-leading power (NLP) for a QED scattering event with the emission of a soft photon, following the work of Laenen et al. [34]. This includes power counting of the relevant to the infrared divergences pinch surfaces and constructing the reduced diagrams corresponding to those. The geometry of these reduced diagrams will also guide the formulation of a suitable factorization formula.

Drawing inspiration from the work done in [34], I will extend the methodology and its results to QCD corrections for the same process and for Higgs production via gluon fusion [4]. I will adjust the procedure to be consistent with the properties of QCD and present my efforts in direct parallelism with the derivation of the original QED procedure [34]. This will allow for qualitative comments on the technical differences and explore how fundamental differences between the theories might affect factorization.

4.1.1 QED: Soft scale expansion

The process considered in [34] is a generic n-particles final state QED scattering event mediated by abelian gauge bosons and dressed with the emission of a soft photon of momentum k. Such processes are characterized by the fact they occur near threshold, and the energy of the initial states is predominantly shared among the final states, thus limiting the radiating photon to be soft. The amplitude is conveniently described as a power expansion in the ratio $\xi \sim E/Q \ll 1$, where E represents the energy of the soft photon, and Q is the invariant mass of the final state. In particular, the authors succesfully factorize the elastic amplitude[1] of the procedure in more manageable parts depending on their different energy scalings.

$$\mathcal{M}_{n+1} = \mathcal{M}_{n+1}^{\mathrm{LP}} + \mathcal{M}_{n+1}^{\mathrm{NLP}} + \mathcal{O}(E),$$

[1] Elastic amplitude is simply the remainder of the radiative amplitude when the radiated photon is stripped off

The leading power(LP) term scales like $\mathcal{M}^{\mathrm{LP}}_{n+1} \sim 1/\xi$, and the NLP contribution's scaling is $\mathcal{M}^{\mathrm{NLP}}_{n+1} \sim \xi^0$

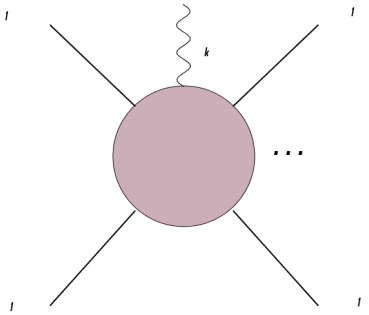

Figure 4.1: QED n-final states event dressed with radiation

In the initial study[34], the authors concentrate on two particular instances, one regarding massless fermions and a second where extremely low masses are assigned to the involved fermions. These cases have specific interest as they are the cases in which the Low-Burnett-Kroll (LBK) theorem fails[5], [39].

4.1.2 Failure of LBK theorem

Correctly using the LBK theorem one can decompose the radiative amplitude in two separated amplitudes as shown as in 4.2: one in which the photon is radiated from an external leg and a second where radiation is originating from a particle in the hard scattering kernel[5].

$$\mathcal{M}_{n+1} = \mathcal{M}^{ext}_{n+1} + \mathcal{M}^{int}_{n+1},$$

The relation mentioned is of particular interest because:

- $\mathcal{M}^{int}_{n+1}$ can be derived via the application of Ward identities to $\mathcal{M}^{ext}_{n+1}$.
- Factorization of $\mathcal{M}^{\mathrm{ext}}_{n+1}$ can be achieved from the corresponding non-radiative amplitude, $\mathcal{M}_n$.

The limits of LBK are highlighted in the mass region $m^2/Q < k^0 < m.$ where the expansion overlooks a particular situation in which the soft photon is emitted from a collinear to the external leg internal particle. Such a physical situation can neither be included in M^{ext}_{n+1} nor M^{int}_{n+1}.

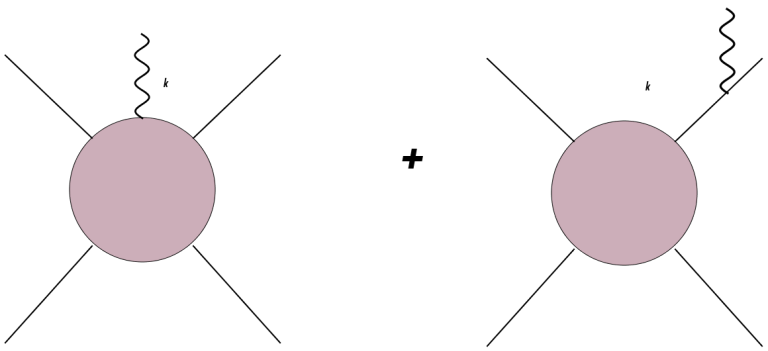

Figure 4.2: Amplitude decomposition into one with radiation from external leg a) and one with radiation from the hard part b)

In this chapter, I follow and extend the analysis done in the massless case. Comparisons and parallelisms with the parametrically small mass case will be made.

Extension of the work done in [34] involves finally a proposal for a factorization theorem up to and including NLP contributions for Drell-Yan and Higgs Production via gluon fusion. As in the original paper I will follow certain steps. Working in a lightcone frame, I will use power counting analysis of relevant pinch surfaces at NLP, which represent the soft and collinear divergences we strive to describe in terms of soft hard and Jet functions. After extracting the most generic power counting formula, I will make use of this, creating the relevant reduced diagrams for each possible scenario, physically relevant and mathematically feasible. Finally those reduced diagrams will allow for a proposed factorization formula up to second order.

4.2 Overview of Factorization

In this section, I will outline the steps followed in [34]. My goal is to introduce, motivate, and become familiar with the procedure before the detailed application and potential extension I will attempt in the subsequent section. The following provides a short sequence of steps and results.

4.2.1 Power Counting Methodology

The authors in [34] adopt a careful method for power counting the degree of infrared divergence. This thorough approach is justified by the infamous complexity of the infrared structure. Here, I will only briefly summarize the steps of their methodology. A comprehensive examination and application will follow in later sections.

Lightcone Coordinate System

As in the majority of related literature a lightcone coordinate frame is favoured. Earlier, I have thoroughly defined this frame, motivating its advantages. A concise review of the key components used in this context follows:

For each momentum vector p_i, we introduce two lightlike vectors n_i and $\bar{n}_i$:

$$n_i^\mu = \frac{1}{\sqrt{2}}\left(1, \frac{\overrightarrow{p_i}}{|\overrightarrow{p_i}|}\right), \quad \bar{n}_i^\mu = \frac{1}{\sqrt{2}}\left(1, -\frac{\overrightarrow{p_i}}{|\overrightarrow{p_i}|}\right),$$

$$\text{with } n_i \cdot \bar{n}_i = 1, \quad n_i^2 = \bar{n}_i^2 = 0.$$

These lightlike vectors can, of course, be used for any generic vector u^μ:

$$n_i^\mu = \frac{1}{\sqrt{2}}\left(1, \frac{\overrightarrow{u_i}}{|\overrightarrow{u_i}|}\right), \quad \bar{n}_i^\mu = \frac{1}{\sqrt{2}}\left(1, -\frac{\overrightarrow{u_i}}{|\overrightarrow{u_i}|}\right).$$

The decomposition of a vector u_i^μ in terms of these lightlike vectors is:

$$u_i^\mu = u^+ n_i^\mu + u^- \bar{n}_i^\mu + u_{1\perp}^\mu,$$

where

$$u^+ = u \cdot \bar{n}_i, \quad u^- = u \cdot n_i.$$

A scalar product between two vectors u^μ and ω_μ is now defined as:

$$u^\mu \omega_\mu = u^+ \omega^- + u^- \omega^+ + u_\perp \cdot \omega_\perp.$$

This decomposition and the associated scalar product are useful in various contexts, particularly in high-energy physics and the study of scattering amplitudes, where lightlike vectors simplify the calculations involving collinear and soft emissions.

4.2.2 Power Counting of individual components

A succesful power-counting should provide the superficial degree of divergence (λ-scaling) for reduced diagrams $\mathcal{G}$ as those depicted in Figure 4.3.

$$\mathcal{G} \sim \lambda^{\gamma_{\mathcal{G}}}$$

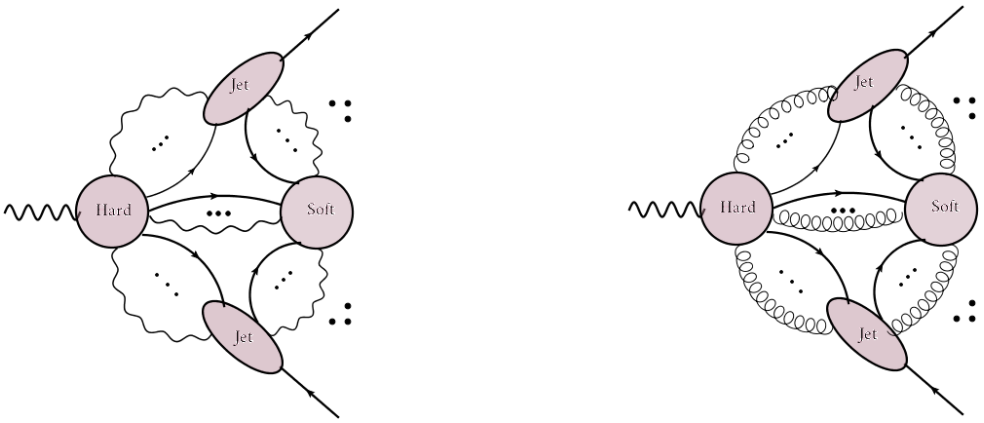

Figure 4.3: Reduced diagrams for QED and QCD corrections respectively

As in [34], the first step is to use the different scalings for collinear, soft or hard momenta to evaluate the scaling of the components of the theory. Only afterward should we combine our results to determine the total divergence of the diagram. As mentioned in the introduction, using the ansatz $k^\mu = \left(k^+, \vec{k}_\perp, k^-\right)$ along with the list of λ scalings, while adhering to the theory's rules, enables us to understand the contribution of each part to the total infrared divergence. In [34] Axial gauge is prefered.

Scaling Type	Momenta Configuration
Hard	$k^\mu = Q(1,1,1)$
Collinear	$k^\mu = Q(1,\lambda,\lambda^2)$
Soft	$k^\mu = Q(\lambda^2,\lambda^2,\lambda^2)$

In [34] this procedure leads to the following scalings for each component :

Category	QED
Collinear Fermion	λ^{-2}
Soft Fermion	λ^{-2}
Soft Photon	λ^{-4}
Collinear Photon	λ^{-2}
Collinear Loop	λ^4
Soft Loop	λ^8
All Collinear Vertex	λ
Rest of Vertices	λ^0

4.2.3 Infrared degree of divergence: From one to whole

Equipped with power counting rules which determine the scaling of individual components participating in the diagrams of the theory, the authors in [34] make use of them to approach a total superficial degree of infrared divergence $\mathcal{G} \sim \lambda^{\gamma_{\mathcal{G}}}$.

To achieve this, it is necessary to initially derive power counting equations for the subdiagrams that collectively constitute the reduced diagram we aim to align with a power counting equation. Specifically, by employing the individual scalings, we examine the infrared level of divergence of the soft, hard and jet subdiagrams and also the extra supression caused by the lines connecting the above.

γ_S:	Soft subdiagram
$\gamma_{S\leftrightarrow H}$:	Fermionic and bosonic lines that connect the soft subdiagram with the hard one.
γ_{J_i}:	Jet subdiagram
$\gamma_{J_i\leftrightarrow H}$:	Fermionic and bosonic lines that connect every Jet to the hard subdiagram.
$\gamma_{J_i\leftrightarrow S}$:	Fermionic and bosonic lines that connect the soft subdiagram with Jets.
$\gamma_{J_i}^{\text{ext}}$:	Fermionic and bosonic lines that connect Jets with external particles.

The most generic power counting formula corresponding to a n-final states event is the sum over all the individual formulas:

$$\gamma_{\mathcal{G}} = \gamma_S + \gamma_{S\leftrightarrow H} + \sum_{i=1}^{n} \left(\gamma_{J_i} + \gamma_{J_i\leftrightarrow H} + \gamma_{J_i\leftrightarrow S} + \gamma_{J_i}^{\text{ext}}\right)$$

This step of the procedure is not free from subtleties and as for every step, there will be detailed derivation during the following sections as well as applications to QED and extensions to QCD corrections and Higgs production.

4.2.4 Reduced diagrams

The formula resulting from the sequence of prior steps serves as a sufficient method of generating reduced diagrams which correspond to various power contributions, reflecting the distinct infrared structure of each physical scenario.

Since the goal is a factorization formula up to NLP in λ we should constrain our focus in the cases of $\gamma = 0, 1, 2$. By definition[34], [48] but motivated as well in Chapter 2 of this thesis leading power contributions correspond to $\gamma = 0$. Higher values of γ correspond to the subleading power corrections we are after. In this work, following the work of the authors in [34] we consider as NLP contributions of $\gamma = 2$ and $\sqrt{NLP}$ those contributions encoded in $\gamma = 1$. Investigating which possible combinations of individual components lead in those values we can reconstruct the relevant reduced diagrams. In the following table, I present all the individual components which will arise in the procedure and their conventionally assigned names which I will use now on.

4.2.5 Hard-Collinear Factorization

In the final part of this procedure the authors of [34] map the reduced diagrams corresponding to $\sqrt{NLP}$ and NLP contributions to a factorization formula based on the work in[16].

Table 4.1: Description of Variables

Variable	Description
$I = \tilde{I}_f + \tilde{I}_\gamma$	Fermion and photon lines internal to the isolated subdiagrams
L	Number of loops
V	Number of vertices
Euler's identity	$L = 1 + \tilde{I}_f + \tilde{I}_\gamma - V$
$m_{f,\gamma}$	Fermion, photon lines connecting soft and hard subdiagrams
$N_{f,\gamma}$	Fermion, photon lines connecting jets and hard subdiagrams
$n_{f,\gamma}$	Fermion, photon lines connecting jets and soft subdiagrams

$$\mathcal{M}_{\rm coll}^{\rm NLP} = \sum_{i=1}^{n}\left(\prod_{j\neq i} J^j_{(f)}\right)\left[J^i_{(f\gamma)}\otimes H^i_{(f\gamma)} + J^i_{(f\partial\gamma)}\otimes H^i_{(f\partial\gamma)}\right] + \sum_{i=1}^{n}\left(\prod_{j\neq i} J^j_{(f)}\right) J^i_{(f\gamma\gamma)}\otimes H^i_{(f\gamma\gamma)} S$$
$$+ \sum_{i=1}^{n}\left(\prod_{j\neq i} J^j_{(f)}\right) J^i_{(fff)}\otimes H^i_{(fff)} S + \sum_{1\leq i\leq j\leq n}\left(\prod_{k\neq i,j} J^k_{(f)}\right) J^i_{(f\gamma)} J^j_{(f\gamma)}\otimes H^{ij}_{(f\gamma)(f\gamma)} S.$$

The four terms in the formula above are directly translated from the reduced diagrams of Figure 4.4. There are three more reduced diagrams contributing NLP suppresions but those arise from the soft function. Therefore and as the primary goal of this paper was a hard-collinear factorization they are not taken into consideration. The exact derivation, and the special treatment of this formula will be studied in detail in the forthcoming chapters.

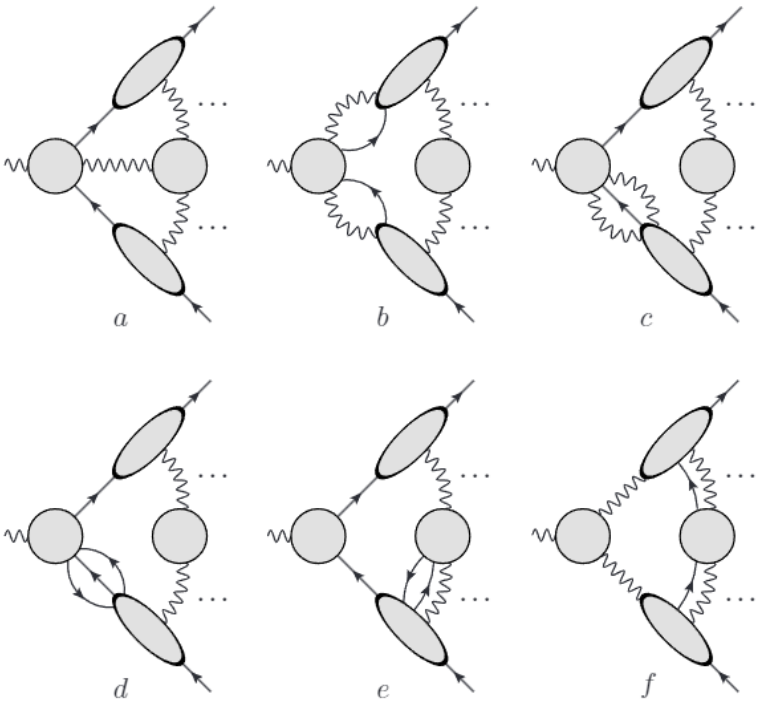

Figure 4.4: Reduced diagrams corresponding to NLP contributions. Diagrams a, e, f are not considered as even if they are NLP contributions those originate from the soft subdiagram [34]

4.3 Extension: QCD corrections

Building on the work done for QED in [34], I aim to extend the methodology to non-Abelian gauge theories. This will be performed by closely following the steps outlined in the aforementioned paper and discussed in prior sections.It will become clear that some steps can be reproduced straightforwardly while for others we need to employ some ”tricks” or modify the procedure. After power counting the relevant pinch surfaces which relate to the soft and collinear divergences arising from QCD corrections, I will compare results with QED[34] and propose a factorization formula.

Our goal, to construct a factorization formula for NLP QCD corrections passes from the derivation of the total formula for power counting a reduced diagram G in the Norton-Coleman picture λ^{γ_G} and in order to achieve that we have to express γ in terms of the fermionic and gluonic connections, between the hard, soft and jet subdiagrams. Such a formula tells us, which pinch surfaces contribute up to NLP and guides us in setting up a consistent and compact NLP framework for factorization in QCD.

4.3.1 Power counting of individual components

QED

Fermionic Propagator

$$i \cdot \frac{\not{p}}{p^2} \to \frac{\gamma^+ p^- + \gamma^- p^+ + \gamma_\perp p_\perp}{2p^+p^- + p_\perp^2}$$

Collinear: $i\frac{\not{p}}{p^2} \to \frac{1}{\lambda^2} = \lambda^{-2}$

Soft: $i\frac{\not{p}}{p^2} \to \frac{\lambda^2}{\lambda^4} = \lambda^{-2}$

Photon Propagator in Axial Gauge[2]

$$\Delta_{\mu v}(k,r) = \frac{i}{k^2 + i\varepsilon} \times \times \left(-n_{\mu v} + \frac{r_\mu k_v + r_v k_\mu}{r \cdot k} - \frac{r^2 k_\mu k_v}{(r \cdot k)^2} \right)$$

We have the scaling from the common factor:
Soft Photon: λ^{-4} **Collinear Photon**: λ^{-2}

Loops

$$\int d\ell_\perp^2 d\ell_+ d\ell_-$$

Soft: λ^8 **Collinear**: λ^4

QCD

Fermionic Propagator

$$i \cdot \frac{\not{p}}{p^2} \to \frac{\gamma^+ p^- + \gamma^- p^+ + \gamma_\perp p_\perp}{2p^+p^- + p_\perp^2}$$

Collinear: $i\frac{\not{p}}{p^2} \to \frac{1}{\lambda^2} = \lambda^{-2}$

Soft: $i\frac{\not{p}}{p^2} \to \frac{\lambda^2}{\lambda^4} = \lambda^{-2}$

Photon Propagator in Axial Gauge[3]

$$\Delta_{\mu v}(k,r) = \frac{i}{k^2 + i\varepsilon} \times \times \left(-n_{\mu v} + \frac{r_\mu k_v + r_v k_\mu}{r \cdot k} - \frac{r^2 k_\mu k_v}{(r \cdot k)^2} \right)$$

We have the scaling from the common factor:
Soft Photon: λ^{-4} **Collinear Photon**: λ^{-2}

Loops

$$\int d\ell_\perp^2 d\ell_+ d\ell_-$$

Soft: λ^8 **Collinear**: λ^4

[3]Working in axial gauge is inherently important, because as we derived in past chapters, no longitudinal or scalar polarizations are allowed. This soon will be of tremendous help not only computationally wise, but also in deriving physically sensible predictions

Vertices

The last component of the theory, which requires a power counting rule, is also the most complex, as the suppressions in the numerator depend on the spin. In [34] it is proven that in QED the only contributing vertex is the all-collinear (QED vertex with all legs scaling collinear) giving an extra suppression of λ. In [48] this is generalized for every all-collinear three-vertex existent in gauge theories. Of course this naturally includes the three-gluon QCD all collinear vertex. Finally, in the soft limit, [14] only all-soft three gluon vertices contribute, being linear in momenta, suppressing the numerator with λ^2.The four gluon vertex is not contributing any extra supression[47].

Contributing vertices in each theory

QED	QCD
All-collinear vertex: λ	**All-collinear vertices:** λ (quark-antiquark gluon or three gluon) **All-soft three gluon vertex:** λ^2

A deeper examination of the all-collinear vertex, will help us appreciate the interplay of the spin structure as well as underline the effect of using an axial gauge choice in extracting physically sensible predictions. Consider a collinear fermion line emitting a boson, which can be soft or collinear. We could as well have a hard gauge boson, but using the Zombie Lemma [47] immediately we state that the vertex is not contributing a suppression. The numerator structure is:

$$
\begin{aligned}
&(\not{p}-\not{k})\gamma^{\mu}\not{p} = \\
&=(p-k)_{\rho}\gamma^{\rho}\gamma^{\mu}\not{p} = (p_{\rho}-k_{\rho})(2n^{\mu\rho}-\gamma^{\mu}\gamma^{\rho})\not{p} = \\
&=2(p-k)^{\mu}\not{p} - p_{\rho}\gamma^{\mu}\gamma^{\rho}\not{p} + k_{\rho}\gamma^{\mu}\gamma^{\rho}\not{p} = \\
&= -p^2\gamma^{\mu} + \gamma^{\mu}\not{k}\not{p} + 2(p^{\mu}-k^{\mu})\not{p}
\end{aligned}
$$

- **First term**: Contributing per definition λ^2, as the emitting fermion is collinear.
- **Second term**: Contributing λ if the photon emission is collinear or ^{2} for soft photon emission:

$$
\begin{aligned}
\gamma^{\mu}\not{k}\not{p} &= \gamma^{\mu}(k^{+}\gamma^{-}+k^{-}\gamma^{+}+k_{\perp}\gamma_{\perp})(p^{+}\gamma^{-}+p^{-}\gamma^{+}+p_{\perp}\gamma_{\perp}) \\
&\eqsim \gamma^{\mu}(1\gamma^{-}+\lambda^2\gamma^{+}+\lambda\gamma_{\perp})(1\gamma^{-}+\lambda^2\gamma^{+}+\lambda\gamma_{\perp}) \\
&\text{but } (\gamma^{-})^2 = 0
\end{aligned}
$$

- **Last term:** Unsuppressed. Even if the boson is soft $p^{\mu}\not{p}$ is dominant and ”contaminates ” the whole numerator in IR insensitivy.

On a more physical argument, we have to realize that the index μ will be contracted with the neighboring gluon (photon) propagator and in the collinear limit, since the jets in $-$ direction, the only surviving polarization would be $+$ which corresponds to unphysical cases.

There is also a third way to interpret the λ suppression of an all collinear vertex: If all three lines are in a jet, in the limit where p, k are parallel and on-shell, p is proportional to k, and the line carrying k has an effective longitudinal polarization. We could not expect an IR divergence to rise from an unphysical polarization, since these divergences result from **degeneracies among physical** states. Dropping the unphysical polarizations, we obtain λ as a suppression again.

Summary

Category	**QED**	**QCD**
Collinear Fermion	λ^{-2}	λ^{-2}
Soft Fermion	λ^{-2}	λ^{-2}
Soft Photon/Gluon	λ^{-4}	λ^{-4}
Collinear Photon/Gluon	λ^{-2}	λ^{-2}
Collinear Loop	λ^{4}	λ^{4}
Soft Loop	λ^{8}	λ^{8}
All Collinear Vertex	λ	λ
Rest of Vertices	λ^{0}	All Soft Three Gluon Vertex λ^{2}

4.3.2 Derivation of a total power counting formula for QED and QCD

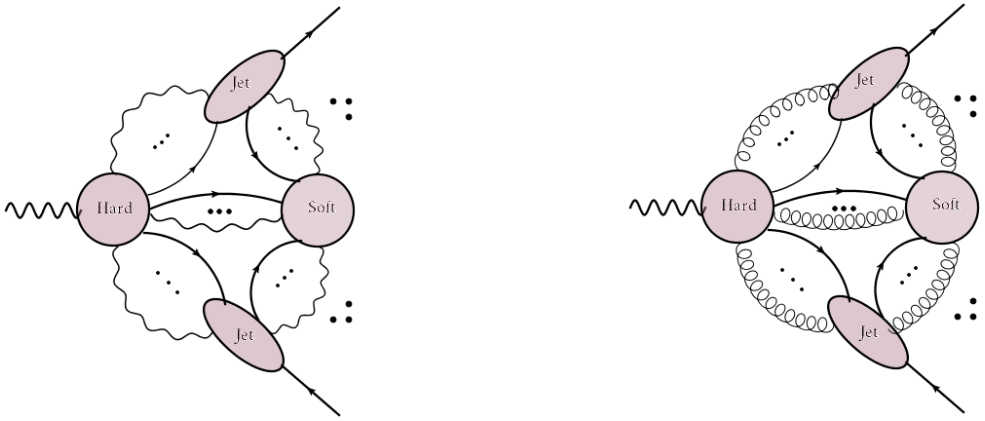

Figure 4.5: Reduced diagrams for QED and QCD corrections

Based on the work of [34], I will follow the authors' methodology to derive an analogous formula for a $2-$jet final state QCD scattering event. Work will be displayed side to side and potential differences will be underlined and discussed. Before I start, two crucial differences in underlying theories should be underlined and taken care of:

In QCD there is an extra contributing vertex, the three gluon vertex which scales as λ if all collinear and as λ^2 if all soft.

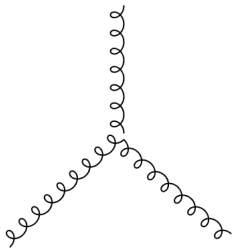

A second variation from the original work, concerning the three-gluon vertex absent in QED, impacts the power counting applied to the connecting lines between the sub-diagrams in picture.

In the following I present how these variations arise and what effects do they really have on power counting, and on factorization. Then I will modify the procedure to adapt to the new information and proceed to find the reduced diagrams. In summary the appearance of a three gluon vertex, is responsible for two major scenery changes:

1) New possible bubble diagrams.

2) New possible scaling for soft gluon connections.

Internal Propagator Relations in QCD vs QED

QED

In QED the only loop bubble diagrams to consider are:

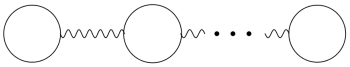

where

$$\boxed{I_{\text{fermion}} = 2I_{\text{photon}} = V}$$

we can easily check this relation either with induction or using

$$E + 2I = \sum_{k=3}^{\infty} kV_k \text{ for } E = 0$$

QCD

In QCD we encounter a second type of diagrams: Except from

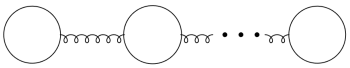

satisfying

$$\boxed{I_{\text{quark}} = 2I_{\text{gluon}} = V_{qqg}}$$

the existence of the three gluon vertex is responsible for the "new"

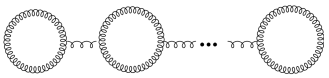

for which $\boxed{I_{\text{gluon}} = \frac{3}{2}V_{ggg}}$

In QED: The degree of divergence arises not only from the lines themselves but also from their effect on the associated blobs. More precisely, when lines attach to sub-diagrams, they split internal propagators and introduce new vertices to both sub-diagrams.

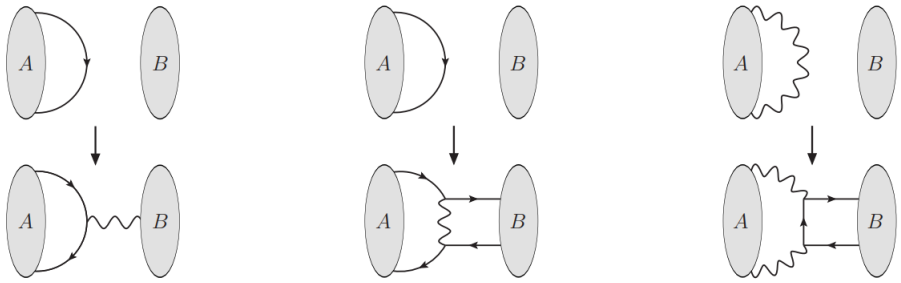

In this figure we see how this happens. Note that adding a fermionic connection must be partnered with its corresponding antifermionic connection for charge conservation.

Calculation of contributions originating from connections of blobs.

	Jet-Hard	Soft-Hard	Jet-External
$\alpha)$	$\frac{(-2)\times3-2+2\times1}{2} = -3$	$\frac{(-2)\times3-4}{2} = -5$	-1
$\beta)$	$\frac{(-2)\times3-2+2\times1}{2} = -3$	$\frac{(-2)\times3-4}{2} = -5$	-1
$\gamma)$	$-2-2+1 = -3$	$-4-2 = -6$	-1

Note: The scaling of connections between Jets and external particles is -1 in all cases. It is easy to calculate it if you have in mind that these subdiagrams are amputated and hence we just ignore the contribution of the external propagator.

In QCD: Four possible configurations due to the three gluon vertex.

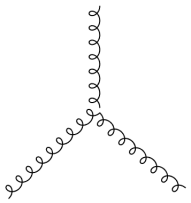

In Jet-Hard connections, this has no impact but when the gluon turns soft, the total scaling is affected.

Calculation of contributions originating from connections of blobs.

	Jet-Hard	Soft-Hard	Jet-External
$\alpha)$	$\frac{(-2)\times3-2+2}{\frac{2}{-3}}$	$\frac{(-2)\times3-4}{2} = -5$	-1
$\beta)$	-3	$\frac{(-2)\times3-4}{2} = -5$	-1
$\gamma)$	$-4+1 = -3$	$-4-2 = -6$	-1
$\delta)$	$-2(2)+1 = -3$	$-4\times2+1\times2 = -6$	-1

4.4 Strategy for Power Counting

To power count the pinch surfaces and adapt to the new scenery I will employ a modified version of the conventional method. For each component of the diagram I want to power count γ, we will discern two distinct contributions: $\gamma = \gamma_1 + \gamma_2$. Specifically, γ_1 accounts for the subdiagram components featuring loops as depicted in  , while γ_2 includes loops like  .

This approach introduces gluon lines with subscripts $g_i, i = 1, 2$, where:

- $i = 1$: denotes gluons present in quark-gluon vertices,
- $i = 2$: signifies gluons in three-gluon vertices.

For a reduced diagram with n–jets (where $n = 2$ for the QCD case), the degree of divergence is expressed as:

$$\gamma = \gamma_s + \gamma_{s\leftrightarrow H} + \sum_{i=1}^{n} \left(\gamma_{J_i} + \gamma_{J_i\leftrightarrow H} + \gamma_{J_i\leftrightarrow s} + \gamma_{J_i}^{ext}\right) \text{[4]}$$

[4] the γ's here have the same interpretation as explained in the previous chapter

4.4.1 Power-Counting subdiagrams

Degree of divergence in a subdiagram which contains collinear lines[5]

QED

Using the rules for components

$$\gamma_{J_i} = -2\left(\tilde{I}_f + \tilde{I}_\gamma\right) + 4L + V$$

We have shown $V = I_f = 2I_\gamma$
Used with the Euler identity : $L = 1 + (\tilde{I}_f + \tilde{I}_\gamma) - V$

$$\begin{aligned}\Rightarrow \gamma_{J_i} &= -2\left(\tilde{I}_f + \tilde{I}_\gamma\right) \\ &\quad + 4\left(1 + \tilde{J}_f + \tilde{I}_\gamma - V\right) + V \\ &= -2\left(\tilde{3}I_\gamma\right) + 4\left(1 + \tilde{I}_\gamma\right) + 2\tilde{I}_\gamma \\ &= 4\end{aligned}$$

Degree of divergence of a collinear subdiagram is **independent** of its internal structure.

QCD

Here I calculate γ_1 and γ_2
γ_1 : includes only quark-gluon loops

$$\gamma_1 = -2\left(\tilde{I}_q + \tilde{I}_{g_1}\right) + 4L + V_{qqg} =$$

$$= 4 \quad \left(\begin{array}{c} \text{The same exact rules} \\ \text{are applied like QED} \end{array} \right)$$

γ_2 : includes only three-gluon vertex induced loops

$$\begin{aligned}\gamma_2 &= -2\tilde{I}_{g_2} + 4L + V_{ggg} = \\ &= -2 \cdot \frac{3}{2} V_{ggg} + 4\left(1 + \frac{3}{2} V_{ggg} - V_{ggg}\right) \\ &\quad + V_{ggg} \\ &= 4\end{aligned}$$

where I used $I_{g_2} = \frac{3}{2} V_{ggg}$ and Euler Identity.

Degree of divergence **independent** in QCD also!

[5] External lines are not into consideration in this degree of divergence

Degree of divergence in a subdiagram which contains soft lines

QED

Using the component scaling and ignoring any contribution from vertices as we have shown before that soft vertices do not contribute in QED we have:

$$\begin{aligned}\gamma_s &= -2\tilde{I}_f - 4\tilde{I}_\gamma + 8L \\ &= -2\tilde{I}_f - 4\cdot\frac{1}{2}\tilde{I}_f + \\ &\quad + 8\left(\tilde{I}_f + \tilde{I}_\gamma + 1 - V\right) \\ &= -4\tilde{I}_f + 8\left(\frac{3}{2}\tilde{I}_f + 1 - \tilde{I}_f\right) \\ &= 8\end{aligned}$$

where I used the Euler identity $L = 1 + I - V$ and the relations $I_f = 2I_\gamma = V$.

QCD

$$\gamma_s = \gamma_{s_1} + \gamma_{s_2}$$

γ_{s_1} : concerns only scales in quark gluon vertices.

Enjoying the same component rules as the associated vertex in QED

$\gamma_{s_1} = 8$.

γ_{s_2} : for loops induced from the three gluon vertices.

$$\begin{aligned}\gamma_{s_2} &= -4\tilde{I}_{g_2} + 8L + 2V_{ggg} \\ &= -4\tilde{I}_{g_2} + 8\left(1 + \tilde{I}_{g_2} - V\right) + 2V \\ &= -4\tilde{I}_{g_2} + 8\left(1 + \tilde{I}_{g_2} - \frac{2}{3}\tilde{I}_{g_2}\right) + \frac{4}{3}\tilde{I}_{g_2} \\ &= 8.\end{aligned}$$

Apart from Euler identity, I have used that $V_{ggg} = \frac{2}{3}I_{g_2}$. Furthermore, **a scaling for the soft gluon vertex** has been introduced for the first time.

Once more, we see that for massless fermions the internal structure of soft subdiagram **does not affect power counting**.

Degree of divergence from lines connecting hard subdiagrams and jets

QED

$N^{(i)}$: Total lines
$N_\gamma^{(i)}$: Total photon connections
$N_1^{(i)}$: Total fermion connections

$$\begin{aligned}\gamma_{J_{i_l\to H}} &= -3N_\gamma^{(i)} - 3N_f^{(i)} \\ &+ 4(N_\gamma^{(i)} + N_f^{(i)} - 1) \\ &= N_\gamma^{(i)} + N_f^{(i)} - 4\end{aligned}$$

This is counted as -3 for each connection as shown in [1] and $N_\gamma^{(i)} + N_f^{(i)} - 1$ loops.

QCD

γ_1 : As usual the same vertex structure leads to same as in QED result

$$\gamma_1 = N_{g_1}^{(i)} + N_q^{(i)} - 4$$

γ_2 : Where $N_{g_2}^{(i)}$ is the number of gluon connections that only participate in three-gluon vertices.

$$\begin{aligned}\gamma_2 &= -3N_{g_2}^{(i)} + 4(N_{g_2}^{(i)} - 1) \\ &= N_{g_2}^{(i)} - 4\end{aligned}$$

where we have $N_{g_2}^{(i)} - 1$ loops created.

Degree of divergence from lines connecting hard and soft subdiagrams

The first thing to consider is that there is no vertex suppression in this case. This is a result of the discussed scaling of vertices, which lead to the conclusion that a vertex has to be all collinear to present a λ scaling, or all soft and linear to momentum to have λ^2. Finally again we will take into consideration, loops created from the connections, $m_\gamma + m_f - 1$ in QED case, $(m_{g_1} + m_q - 1)$ and, or $(m_{g_2} - 1)$ in QCD case.

QED

$$\begin{aligned}\gamma_{s_{l\to H}} &= 6m_\gamma - 5m_f + \\ &+ 8(m_\gamma + m_f - 1) = \\ &= 2m_\gamma + 3m_f - 8\end{aligned}$$

where I just used the scaling for soft attachments shown in the previous.

QCD

$\gamma_1 = 2m_{g_1} + 3m_q - 8$
as usual
$\gamma_2 = -6m_{g_2} + 8(m_{g_2} - 1) = -8 + 2m_{g_2}$

Degree of divergence from lines connecting soft subdiagrams and jets

Finally, the scaling of lines connecting the Jet and Soft subdiagrams. The loops created are increased by 1, as an extra loop is created between the Jet, soft and hard subdiagram.

QED

$$\gamma = -2(\overbrace{n_\gamma^{(i)} + n_f^{(i)}}^{\text{collinear effect}}) - \\ - (\overbrace{6n_\gamma^{(i)} + 5n_f^{(i)}}^{\text{soft effect}}) + \\ + 8(n_\gamma^{(i)} + n_f^{(i)}) = n_f^{(i)}$$

QCD

$\gamma_1 = n_q^{(i)}$, as usual

and

$$\gamma_2 = -2n_{g_2}^{(i)} - \\ - 6n_{g_2}^{(i)} + 8(n_{g_2}^{(i)}) = \\ = 0$$

Contributions to the degree of divergence

	QED	QCD	
$2\cdot\gamma_{J_i}$	$2\cdot 4$	γ_1	4
		γ_2	4
$2\cdot\gamma_s$	$2\cdot 8$	γ_1	8
		γ_2	8
$2\cdot\gamma_{J_i-H}$	$2\cdot N_f + N_\gamma - 4$	γ_1	$N_q + N_g - 4$
		γ_2	$Ng_2 - 4$
$\gamma_{J_i}^{\text{ext}}$	-1		-1
$2\cdot\gamma_{J_i-s}$	$2\cdot n_f$	γ_1	n_q
		γ_2	0
γ	$2m_\gamma + 3m_f + \sum_{i=1}^{n}\left(N_f^{(i)} + N_\gamma^{(i)} + n_f^{(i)} - 1\right)$		$2m_{g_1} + 3m_q + 2m_{g_2} + \sum_{i=1}^{2}\left(N_q^{(i)} + N_{g_1}^{(i)} + N_{g_2}^{(i)} + n_q^{(i)} - 1\right)$
			$2m_g + 3m_q + \sum_{i=1}^{2}\left(N_q^{(i)} + N_g^{(i)} + n_q^{(i)} - 1\right)$

In [34], the authors combined the above to estimate the total degree of divergence:

$$\gamma = 2m_\gamma + 3m_f + \sum_{i=1}^{n}\left(N_f^{(i)} + N_\gamma^{(i)} + n_f^{(i)} - 1\right)$$

After summing the contributions, I found one reads,

$$\gamma = 2(m_{g_1} + m_{g_2}) + 3m_q + \sum_{i=1}^{2}\left(N_q^{(i)} + N_g^{(i)} + n_q^{(i)} - 1\right)$$

which, conveniently, works out as:

$$\gamma = 2m_g + 3m_q + \sum_{i=1}^{2}\left(N_q^{(i)} + N_g^{(i)} + n_q^{(i)} - 1\right)$$

after using:

$$\left[\begin{array}{l} m_g = m_{g_1} + m_{g_2} : \text{ gluon lines connecting soft and hard,} \\ N_g = N_{g_1} + N_{g_2} : \text{ gluon lines connecting jet and hard,} \\ n_g = n_{g_1} + n_{g_2} : \text{ gluon lines connecting jetsoft.} \end{array}\right.$$

and keeping in mind:

$$\left[\begin{array}{l} \text{Subscript 1 indicates gluon which only participates in quark-gluon vertices,} \\ \text{Subscript 2 indicates gluon which only participates in three-gluon vertices.} \end{array}\right.$$

Notes, comments, conclusions

- The formula is identical to the QED one, up to a type of bosons.
- The formula reproduces the known, result for leading power, in axial gauge. In covariant gauges multiple gluons may connect jets to the Hard subdiagram. This would mean that such gluons would carry unphysical polarizations. Of course, when computing a gauge invariant quantity, these configurations will be suppressed by means of the Ward Identities, after summing over all relevant gauge invariant diagrams but since this work relies on a diagram-diagram basis, this is not a compatible choice.
- We see that the introduction of the ”two types” of gluons, not only provides a way to power count but also they add up together finally, allowing us to not worry for peculiar contributions.

4.5 Factorization: QCD corrections

We now have a total power counting formula for the process:

$$e^+e^- \to \gamma^* \to 2 \text{ jets}$$

$$\gamma = 2m_g + 3m_q + \sum_{i=1}^{2}\left(N_g^{(i)} + N_q^{(i)} + n_1^{(i)} - 1\right)$$

Where:

$$\begin{bmatrix} m_g = m_{g_1} + m_{g_2} : \text{ gluon lines connecting soft and hard,} \\ N_g = N_{g_1} + N_{g_2} : \text{ gluon lines connecting jet and hard,} \\ n_g = n_{g_1} + n_{g_2} : \text{ gluon lines connecting jetsoft.} \end{bmatrix}$$

- Subscript 1 indicates gluons which only participate in quark-gluon vertices.
- Subscript 2 indicates gluons which only participate in three-gluon vertices.

Following [34] we will use our findings to reproduce the reduced diagrams. It is obvious from the formula, that $\gamma \geqslant 0$. Also $\gamma = 0$ corresponds to logarithmic singularities and $\gamma > 0$ vanishes in the $\lambda \to 0$ limit. We identify $\gamma = 0$ as leading power contributions and $\gamma > 0$ as power corrections.

Since, for quite a long time now, we examine elastic non-radiative, amplitudes it is rather advisable to have in mind that the final goal is to resum NLP threshold logarithms associated with soft final state radiation. For this purpose we consider a dressing of the non-radiative graphs with a single soft emission. This defects the divergence with -2.

4.5.1 Reduced diagrams

Table 4.2: Contributing diagrams in subleading power

γ	$N_q^{(1)}$	$N_q^{(2)}$	$N_g^{(1)}$	$N_g^{(2)}$	$n_q^{(1)}$	$n_q^{(2)}$	m_q	m_g
1	1	1	1	0	0	0	0	0
2	1	1	2	0	0	0	0	0
2	3	1	0	0	0	0	0	0
2	1	1	1	1	0	0	0	0
2	1	1	0	0	0	0	0	1
2	1	1	0	0	2	0	0	0
2	1	1	0	0	1	1	0	0

The leading power configuration, $\gamma = 0$, corresponds to $N_q^{(i)} = 1$ and $\left\{N_j^{(i)}, n_1^{(n)}, m_1, m_{s\theta}\right\} = 0$. In cases where the number of connections among the two jets is different, we can interchange them. For instance in the $\gamma = 1$ case, we get equivalent diagrams for $N_q^{(1)} = 1,\ N_q^{(2)} = 0$ and for $N_q^{(1)} = 0,\ N_q^{(2)} = 1$. We also verify that the number of quarks connecting hard and soft blobs, do never have a non vanishing value, completely in agreement with literature[15]. They start contributing beyond NLP. It is nice to see that the derived formula is in complete agreement with work done [8], [48], [15] and more identification with the theory is collected here:

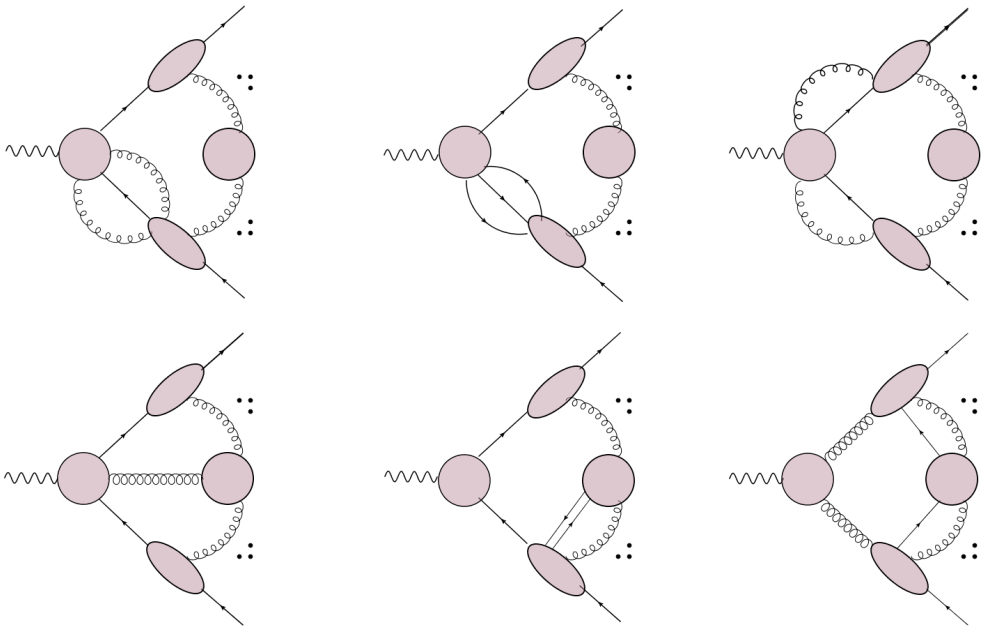

Figure 4.6: NLP reduced diagrams which correspond to $\gamma = 2$ based on power counting.

1. The superficial degree of divergence is non-negative, $\gamma \geqslant 0$. That means that the derived formula correctly showcases that only logarithmic divergences are to be expected.
2. The reduced diagram for LP is in complete correspondence with work done[48],
3. The number of gluons connecting the Jet subdiagrams and the soft one is arbitrary.
4. The reduced diagrams in which, lines connect directly the soft and the hard blob, are finite and contribute beyond LP. In fact, as we noticed fermionic lines of this family contribute from **NNLP**.
5. In LP, only gluons connect Jets and Soft diagrams.

Also, we see that working in axial gauge, in LP, every Jet subdiagram must be connected to the hard subdiagram with one line, which must carry the same quantum numbers as the external line exiting the graph. In covariant gauges, further unphysical, ”scalar-polarised” gluons could be in picture.

4.5.2 Factorization formulas: LP and NLP

We now aim to use the same thinking as in [34] to extract factorization formulas for LP and NLP in hard-collinear factorization of QCD corrections. In our case we use a configuration with two final state particles for which there are already proposed factorization formulas in the literature which can be used for validating our whole procedure [15][51].

Leading Power Contribution

$\gamma = 0$

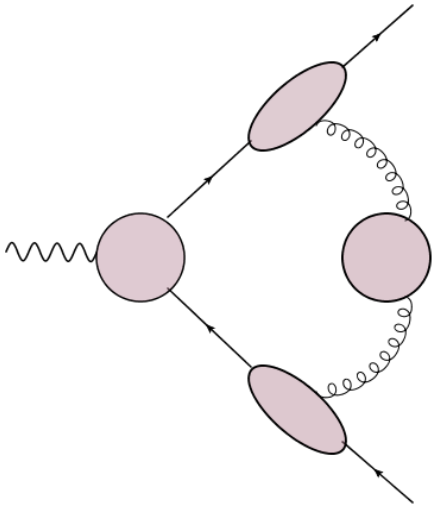

Figure 4.7: Reduced diagram for the QCD process $\gamma = 0$, corresponding to LP contributions.

The leading power configuration arises for $\gamma = 0$. Only one combination is possible based on the extracted formula when $N_q^{(i)} = 1$ and all components $\{N_g^{(i)}, n_q^{(i)}, m_q, m_g, I_q\}$ are set to zero, where g denotes gluons and f refers to fermions. In this case, the already established in the previous chapter factorisation formula applies perfectly and also serves as a validity check of what we have done:

$$\mathcal{M}^{\mathrm{LP}} = \left(\prod_{i=1}^{2} J_{(q)}\left(\hat{p_i}\right)\right) \otimes H\left(\hat{p_1}, \ldots, \hat{p_n}\right) S\left(n_i n_j\right) \text{[6]}$$

The hatted vectors contain the dominant momentum component and are imposed in this formula in a way which allows us to pick only the dominant contribution to the amplitude, leaving the subleading suppresions to be included in formulas concerning NLP factorization and beyond.

$$\hat{p_i}^{\mu} = p_i^{+} n_i^{\mu}$$

The included in the factorization formula Jet and Soft functions are of the same form as introduced in Chapter 3 and their motivation is similar. This is because we are lucky, or canny enough to apply this work on a two final jets event. Having more final states would make the construction of matrix elements a way more complicated business than in QED mainly because of the non-commutativity of the SU(3) generators.

$$J_{(q)}\left(p_i\right) = \left\langle p_i \left| \bar{\psi}(0) \Phi_{\bar{n}_i}(0, \infty) \right| 0 \right\rangle$$

$$S\left(n_i \cdot n_j\right) = \left\langle 0 \left| \prod_{i=1}^{2} \Phi_{n_i}(0, \infty) \right| 0 \right\rangle$$

[6](⊗): Contraction of spin and colour indices

Notice that the Wilson line in the Jet function does not have the direction of the flowing momentum, as the ones which are relevant to soft function. It is important also to be aware that the Jet functions in the formula are practically the redefinition we employed earlier, where in the sake of cancelling potential double counting due to soft-collinear overlapping, each Jet function was divided with its eikonal counterpart.

$$J_{(q)}\left(\hat{p}\right) = \frac{J_{(q)}\left(\hat{p}\right)}{J_{EIK_{(q)}}\left(\hat{p}\right)}$$

Hard-Collinear Factorization | Extension to NLP

The generalization and focus on the hard-collinear factorization is consistent only under the assumption that for each class of the reduced diagrams, relevant, the jet functions are different.

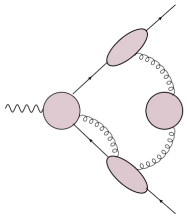

Figure 4.8: Reduced diagram for the QCD process $\gamma = 1$, corresponding to $NLP^{\frac{1}{2}}$ contributions

$$M_{\text{coll}}^{NLP} = \sum_{i=1}^{2}\left(\prod_{j\neq i} J_{(q)}^{j}\right)\left(J_{(qg)}^{i}\otimes H_{(qg)}^{i} + J_{(q\partial g)}^{i}\otimes H_{(q\partial g)}^{i}\right)S$$

$$+\sum_{i=1}^{2}\left(\prod_{j\neq i} J_{(q)}^{i}\right) J_{(qgg)}^{i}\otimes H_{(qgg)}^{i} S + \sum_{i=1}\left(\prod_{J+i} J_{(q)}^{i}\right)$$

$$\times\, J_{(\text{qgg})}^{i}\otimes H_{(qgg)}^{i} S + \sum_{1\leq i\leq j\leq 2}\left(\prod_{k\neq i,j} J_{(q)}^{4}\right) J_{(qg)}^{i} J_{(qg)}^{j} H_{(qg)(qg)}^{ij} S$$

To improve readability, arguments are suppressed and $i,\ j$ correspond to the collinear sectors.

This is inspired from the reduced diagrams we extracted the power counting formula. In particular, the first using term corresponds to the contribution of (β), whereas the second third and fourth to $(\gamma),\ (\delta),\ (\epsilon)$ respectively. Since, we examine hard-collinear factorization for the moment, the formula is not supplement with the contributions from the rest of the diagrams which include further connections to the soft function. Therefore, the soft function will be unsuppressed and always have the LP definition given of in the previous page.

Before diving deeper in this framework, let us point out that we now have formula for hard collinear factorization to every order in perturbation theory, consisting of four parts. Each part is reflecting a different possible NLP contribution, based on the reduced diagrams we have. The soft function is always in LP and has the same matrix element form, when the Jet functions have to be crafted differently for each case.

Shorthand index notation

The explanations and remarks on the notation used, which will be presented here are showcased only in the most trivial **qg** term. Everything can be used equivalently to any term of the equation.

$$J^i_{(qg)} = J_{(qg)}\left(p_i - \hat{\ell}_i, \hat{\ell}_i; \epsilon\right)$$
$$H^i_{(qg)} = H_{(qg)}\left(p_1 \ldots; p_i - \hat{\ell}_i, \hat{\ell}_i; \ldots p_n; \epsilon\right)$$

The first two arguments in the Jet function denote the momentum flowing through the quark and gluon leg, respectively, while in the hard function the index i also specifies which of the n hard momenta has been shifted in presence of the additional collinear gluon. What is more, we could replace p_i with $\hat{p}_i$, in the argument of the hard function, as in contrary with the massive fermion case, the jet functions contribution starts from $O\left(\lambda^2\right)$, and no room for an additional subleading suppresion from the hard part is available.

$\otimes$ Product in NLP factorisation formula

There is also a redefinition of the $\otimes$ product in the NLP factorization formula. Now apart from spin and colour indices contraction, the product involves convolutions over the leading components and additional Lorentz contractions over spacetime indices carried from the gluon leg.

$$\begin{aligned}
&\left(\prod_{j\neq i} J^j_{(q)}\right)\left[J^i_{(qg)} \otimes H^i_{(qg)} + J^i_{(q\partial g)} \otimes H^i_{(q\partial g)}\right] S \equiv \\
&\equiv S\left(\hat{p}_i \cdot \hat{p}_j; \epsilon\right)\left(\prod_{j\neq i} J_{(q)}\left(p_j; \epsilon\right)\right)\int_0^{p_i^+} d\ell_i^+ \\
&+\left[J^\nu_{(qg)}\left(p_i - \hat{\ell}_i, \hat{\ell}_i; \epsilon\right) H_{(qg)\nu}\left(p_1 \ldots; p_i - \hat{\ell}_i, \hat{\ell}_i; \ldots p_n; \epsilon\right) + \right. \\
&\left. +J^{\nu\rho}_{(q\partial g)}\left(p_i - \hat{\ell}_i, \hat{\ell}_i; \epsilon\right) H_{(q\partial g)\nu\rho}\left(p_1 \ldots; p_i - \hat{\ell}_i, \hat{\ell}_i; \ldots p_n; \epsilon\right)\right].
\end{aligned}$$

Finally, while the second, third and fourth term start contributing at $O(\lambda^2)$, the first one does so from $O(\lambda)$. This, implies a potential dependence of the hard function on the perpendicular momentum of the gluon, that emerges from it. To take care of that, we expand the hard function:

$$\begin{aligned}
&\widetilde{H}^i_{(qg)\nu}\left(p_1 \ldots p_n; \ell_i; \epsilon\right) = \\
&= \widetilde{H}^i_{(qg)\nu}\left(p_1 \ldots p_n; \hat{\ell}_i; \epsilon\right) + \ell^\rho_\perp\left[\frac{\partial}{\partial \ell^\rho_\perp}\widetilde{H}^i_{(qg)\nu}\left(p_1 \ldots p_n; \ell_i; \epsilon\right)\right]_{\ell_\perp = 0} + \mathcal{O}\left(\lambda^2\right) \\
&\equiv H_{(qg)\nu}\left(p_1 \ldots; p_i - \hat{\ell}_i, \hat{\ell}_i; \ldots p_n; \epsilon\right) + \ell^\rho_\perp H_{(q\partial g)\nu\rho}\left(p_1 \ldots; p_i - \hat{\ell}_i, \hat{\ell}_i; \ldots p_n; \epsilon\right)
\end{aligned}$$

A hard function should have dependence only in the leading momentum component. The unique scenario here suggests a subleading contribution from the hard part, which can occur only if there is a dependence on the transverse momentum component of the connection. We can then isolate this λ suppression from the hard part and appropriately transfer it to the jet using a Taylor expansion as described above. This establishes the definition of the matrix elements and permits perturbative analysis of the short-distance elements.

4.5.3 Intermezzo and discussion

By suitably modifying the work in QED while ensuring the principles of QCD are maintained, and temporarily introducing two distinct types of gluons to facilitate the calculations, which ultimately cancelled each other out, we obtained a result for massless quarks that closely resembles the QED scenario. That should not be counted as a big surprise as the Feynman diagrams considered are also present in electrodynamical processes like electron positron annihilation to a charged pair of a muon and an antimuon and should differ only via a colour factor. In QED production of a charged pair is divergent , emitting a photon or not. The difference between the theories lies on the fact that unlike in QED, where we can calculate further and realise that a charged pair production cross section always vanishes except in the case of a soft emission, in QCD the very same soft emission disables us from calculating perturbatively. This is a result of asymptotical freedom or, its reverse, confinement. Therefore, in order to effectively make predictions for this case we have to somehow factor out the effects of the soft emission from the hard process.

The next step should be to identify operator matrix elements for Jet and Soft functions, in order to approach universally and utilize them so as to generate soft and collinear divergences for all fixed angle amplitudes, regardless of the particular hard process .

For now, we will extract the Jet functions from our diagrams and check the consistency of the formula at one loop level.

5 Further extensions: Higgs production

5.1 Introduction

The discovery of the scalar Higgs boson in 2012[13], [1] at the Large Hadron Collider (LHC) was a major milestone in particle physics, completing the Standard Model. This discovery confirmed the existence of the Higgs field, which gives mass to elementary particles and explains electroweak symmetry breaking. Higgs boson production at the LHC occurs through several main mechanisms, as shown in Figure 5.1:

1. **Vector Boson Fusion (VBF):** In this process, two quarks each emit a weak boson (W or Z), which then interact to produce a Higgs boson. This process is marked by forward jets and low central hadronic activity, making it easier to identify among background events [46].

2. **Associated Production with a Vector Boson (VH):** Also known as Higgs-strahlung, this involves the production of a Higgs boson with a W or Z boson. The vector boson can decay into leptons, providing a clear signature to detect the Higgs boson, especially useful for studying Higgs decays into b-quark pairs [28].

3. **Associated Production with a (Anti)Top Quark Pair (ttH):** In this channel, the Higgs boson is produced with a top quark pair. This process directly probes the top-Higgs Yukawa coupling, testing the Standard Model's predictions. The signature includes multiple jets and b-jets, plus possible leptons from top decays [17].

4. **Gluon Fusion (ggF):** The dominant production mode at the LHC, gluon fusion occurs when two gluons interact via a top quark loop to produce a Higgs boson. The large gluon density in protons results in the highest production cross-section, though significant QCD background complicates signal extraction [27].

Each production mechanism is essential for studying the Higgs boson. Examining these channels allows physicists to test Standard Model predictions, search for new physics, and measure Higgs properties like mass, width, and couplings [20].

Gluon fusion is particularly important due to its high production rate, making it the primary source of Higgs bosons at the LHC [19]. However, its significant QCD background requires precise calculations

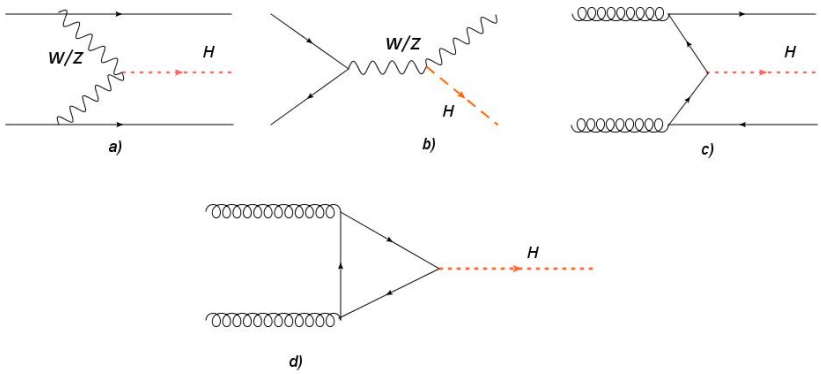

Figure 5.1: Main Higgs production channels at the LHC: The dominant gluon fusion channel is depicted in d).

and advanced techniques to accurately identify the Higgs signal. These include higher-order QCD corrections and effective field theory methods to distinguish signal from background [29].

Experimental measurements at the LHC have confirmed theoretical predictions with high precision, validating the Standard Model for gluon fusion. These measurements are crucial for probing Higgs properties and potential new physics [13]. The High-Luminosity LHC (HL-LHC) will further improve measurement precision, allowing for stricter tests of the Standard Model and the discovery of new phenomena. Ongoing theoretical developments ensure that predictions match experimental capabilities [30].

In summary, the various Higgs production mechanisms at the LHC provide complementary insights into the Higgs particle and its role in the Standard Model. Utilizing each channel's strengths allows for thorough exploration of Higgs physics, testing the Standard Model's limits, and searching for new physics beyond it.

5.2 Main Channel: Gluon-Fusion

For the gluon fusion tree-level amplitude, we apply the Feynman rules to the two diagrams in Figure 5.3 :

$$M^{\mu\nu} = -i\frac{\alpha_s}{2\pi v}\delta^{ab}\varepsilon_\mu(k_1)\varepsilon_\nu(k_2)\left(k_1\cdot k_2 g^{\mu\nu} - k_1^\nu k_2^\nu\right)\left(\frac{4m_t^2}{m_h^2}\right)\left(1+\left(1-\frac{4m_t^2}{m_h^2}\right)\tan^{-1}\left(\frac{1}{\sqrt{\frac{4m_t^2}{m_h^2}-1}}\right)^2\right)$$

Observing that the mass of the (anti)top quark is not significantly larger than the Higgs boson's, we can justify an expansion in $m_t \to \infty$ formulated in powers of $1/\frac{m_h^2}{4m_t^2} \simeq 0.13$. The main reasoning behind a need for an approximation like this is the infamous difficulty involved in procedures of calculating radiative corrections using the Lagrangian of the Standard Model [53].

The simplified amplitude is:

$$M^{\mu\nu} = -i\frac{\alpha_s}{3\pi v}\delta^{ab}\varepsilon_\mu\left(k_1\right)\varepsilon_\nu\left(k_2\right)\left(k_1\cdot k_2 g^{\mu\nu} - k_1^\nu k_2^\nu\right)$$

This expanded amplitude, which is independent of quark mass, effectively illustrates a local interaction between the Higgs boson and gluons, as shown in Figure 5.2 . This interaction is derived from the effective Lagrangian [20]::

$$\mathcal{L}_{\text{eff}} = -\frac{1}{4}\frac{\alpha_s}{3\pi v}hG_a^{\mu\nu}G^a_{\mu\nu}$$

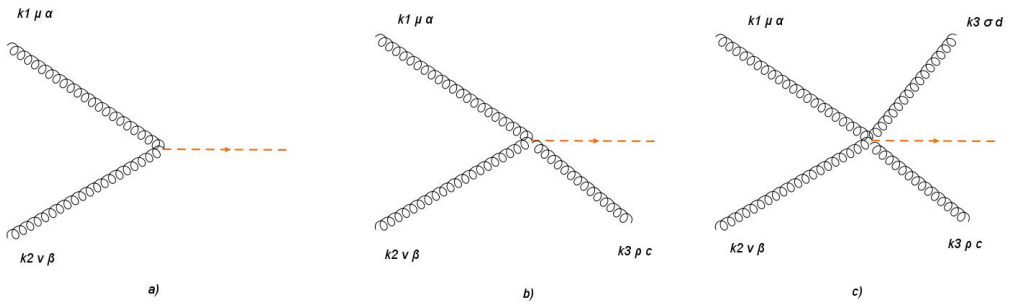

Figure 5.2: Effective Higgs-Gluon vertices

5.2.1 Effective (and usual) Feynman rules

The effective Lagrangian $\mathcal{L}_{\text{eff}}$ generates the vertices shown in 5.2 corresponding to the following Feynman rules:

a) $i\delta_{ab}\left(k_1 \cdot k_2 g_{\mu\nu} - k_{1\nu} k_{2\mu}\right)$

b) $-g_s f_{abc}\left[\left(k_1 - k_2\right)_\rho g_{\mu\nu} + \left(k_2 - k_3\right)_\mu g_{\rho\nu} + \left(k_3 - k_1\right)_\nu g_{\rho\mu}\right]$

c) $-ig_s^2\left\{f_{abe} f_{cde}\left(g_{\mu\rho} g_{\nu\gamma} - g_{\mu\gamma} g_{\nu\rho}\right)\right.$
$+f_{\text{ace}}\, f_{bde}\left(g_{\mu\nu} g_{\rho\gamma} - g_{\mu\gamma} g_{\nu\rho}\right)$
$\left.+\text{f}_{\text{ade}}\, f_{bce}\left(g_{\mu\nu} g_{\rho\gamma} - g_{\mu\rho} g_{\nu\gamma}\right)\right.$

Standard Model Feynman rules

$$g^{\mu v} = (+,-,-,-)$$

Quark Propagator

$= \frac{i(\not{p}+m)}{p^2-m^2+i\varepsilon}$

Gluon Propagator

$= \frac{i\delta^{\alpha\beta}}{k^2+i\varepsilon}\left(-n_{\mu v} + \frac{r_\mu k_v + r_v k_\mu}{r\cdot k} - \frac{r^2\mu}{(r\cdot u)^2}\right)$

Scalar Higgs Propagator

$= \frac{i}{k^2+i\varepsilon}$

QCD Quark Gluon Vertex

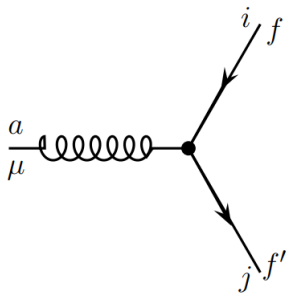

$= igt^c_{ji}\gamma^\mu, c, i, j$ colour indices

2

QCD
3 gluon Vertex

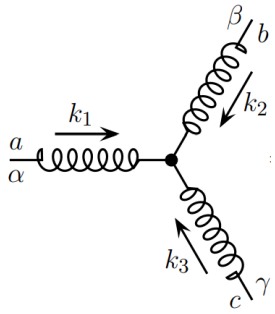

$$= g f^{a\beta c} \left(g^{\mu v}(k-p)^{p} + g^{vp}(p-q)^{\mu} + g^{p\mu}(q-k)^{v}\right)$$

QCD
4 gluon Vertex

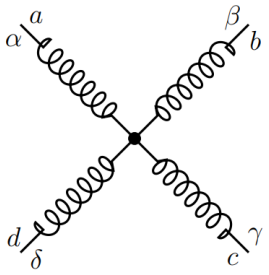

$$\begin{aligned} = -ig^2 \Big(& f^{abe} f^{cde} \left(g^{\mu p} g^{v\beta} - g^{\mu\beta} g^{vp}\right) \\ & + f^{ace} f^{bde} \left(g^{\mu v} g^{p\beta} - g^{\mu}\beta g^{vp}\right) \\ & + f^{ade} f^{bce} \left(g^{\mu v} g^{p\beta} - g^{\mu p} g^{v\beta}\right)\Big) \end{aligned}$$

Quark Higgs Vertex

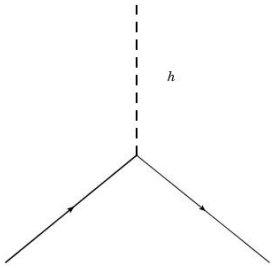

$$\sim -i\frac{m_f}{v} = \frac{-igm_f}{2M_W}$$

Triple Higgs Self Coupling

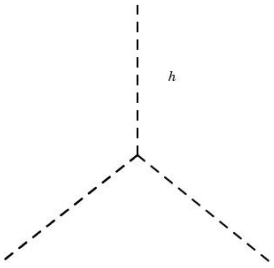

$$\sim -i\frac{-3igm_H{}^2}{2M_W}$$

Four Higgs Self Coupling

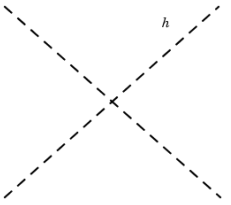

$$\sim -i\frac{-3ig^2 m_H{}^2}{4M_W{}^2}$$

5.3 Higgs production via gluon fusion: Power Counting

As planned I will once again apply the procedure of the previous chapter's examples to gluon fusion. I use the same lightcone frame and the same λ parametrization of soft and collinear momentum components:

Table 5.1: Lightcone coordinate frame

Definitions	Expressions	Comments
Lightlike vectors n_i and $\bar{n}_i$	$n_i^\mu = \frac{1}{\sqrt{2}}\left(1, +\frac{\vec{p}_i}{\lvert\vec{p}_i\rvert}\right)$, $\bar{n}_i^\mu = \frac{1}{\sqrt{2}}\left(1, -\frac{\vec{p}_i}{\lvert\vec{p}_i\rvert}\right)$	$n_i \cdot \bar{n}_i = 1, n_i^2 = \bar{n}_i^2 = 0$
Vector decomposition	$v^\mu = v^+ n_i^\mu + v^- \bar{n}_i^\mu + v_{\perp i}^\mu$ *	$v^+ = v \cdot \bar{n}_i, v^- = v \cdot n_i$
Scalar product	$v \cdot w = v^+ w^- + v^- w^+ + v_\perp^\mu w_{\perp\mu}$ **	

Always using the ansatz $k^\mu = (k^+, \vec{k}_\perp, k^-)$, we assign the same divergence scaling to the corresponding collinear and soft lines.

Soft	$k^\mu = (\lambda^2, \lambda^2, \lambda^2) \cdot Q$
Collinear	$k^\mu = (1, \lambda, \lambda^2) \cdot Q$

Predicting a reliable factorization formula which includes NLP power supressions, demands the derivation of a generic formula for power counting a reduced diagram G in the Norton-Coleman picture λ^{γ_G}. As in Chapter 4, to achieve that we have to express γ in terms of fermion and gluon connections, between the hard, soft and jet subdiagrams. Such a formula tells us, in any perturbative order, which pinch surfaces contribute up to NLP and guides us in setting up a consistent and compact NLP framework for factorization.

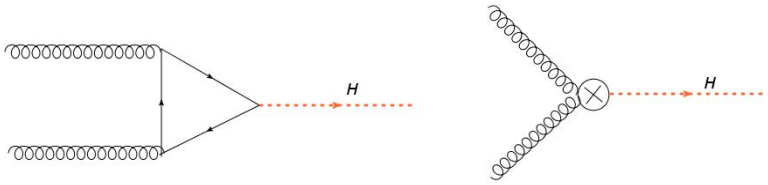

Figure 5.3: SM and Effective Diagrams, Leading order contributions $H \to gg$

Once the Higgs boson decays into two gluons within the effective vertex 5.3, any corrections thereafter are computed exclusively in a QCD framework. This means that the individual components and their scaling are the same with those calculated for QCD corrections in Chapter 4. As a result the power counting formula will be the same as well. What we expect to be different is the factorization formula and the reduced diagrams as those are the ingredients which are different for different processes within the same theory. Therefore the procedure of power counting will be presented very briefly as typically has been derived in chapter 4:

IR degree of divergence - Constituents			
	Lightcone frame expression	**Soft**	**Collinear**
Quark	$i \cdot \frac{\not{p}}{p^2} \to \frac{\gamma^+ p^- + \gamma^- p^+ + \gamma_\perp p_\perp}{2p^+p^- + p_\perp^2}$	λ^{-2}	λ^{-2}
Gluon	$\frac{i}{k^2+i\varepsilon}\left(-n_{\mu\upsilon} + \frac{r_\mu k_\nu + r_\upsilon k_\mu}{r\cdot k} - \frac{r^2 k_\mu k_\nu}{(r\cdot u)^2}\right)$	λ^{-4}	λ^{-2}
Higgs	$\frac{i}{p^2+i\varepsilon}$	λ^{-4}	λ^{-2}
Loops	$\int d\ell_\perp^2 d\ell_+ d\ell_-$	λ^8	λ^4

Table 5.2: QCD vertices infrared degree of divergence

Types	All Soft *	All Collinear
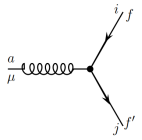	0	λ
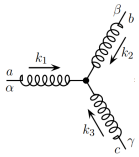	λ^2	λ
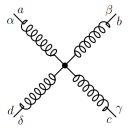	0	0

QCD: Two loop diagrams.

Loop Type 1

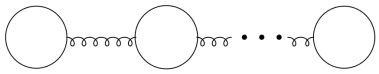

$$I_{quark} = 2I_{gluon} = V_{qqg}$$

Loop Type 2

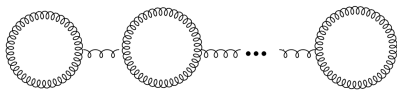

$$I_{gluon} = \frac{3}{2}V_{ggg}$$

$$\gamma = 2m_g + 3m_q + \sum_{i=1}^{2}\left(N_g^{(i)} + N_q^{(i)} + n_q^{(i)} - 1\right)$$

$$\left[\begin{array}{l} m_g = m_{g_1} + m_{g_2}: \text{ gluon lines connecting soft and hard,} \\ N_g = N_{g_1} + N_{g_2}: \text{ gluon lines connecting jet and hard,} \\ n_g = n_{g_1} + n_{g_2}: \text{ gluon lines connecting jetsoft.} \end{array}\right.$$

Naturally the formula giving the infrared degree of divergence coincides with the one we found in Chapter 4. We will see now, that there is difference in the reduced diagrams and as a result in the

factorization formula which is emerging from their geometrical characteristics. Of course we expect a situation like this as the reduced diagrams are resembling the full event and the factorization formula is nothing else but the scattering amplitude reexpressed. Hence, instead of a generic qcd components power counting which is of course similar to any scenario, an amplitude and a diagram carry identifying properties of the event.

The fundamental difference, which is responsible for separating the two events is the jet content. In Chapter Four we examined a QED vertex which lead to two jets initiated by leptons, and external leptonic particles electrically charged. Now the jets and the external particles are gluonic and carry neutral electrical charge.

Conservation of charge will play a major role and will limit the available reduced diagrams, as some of the possibilities allowed in the vertex corrections are not conserving the electrical charge in our case.

5.4 Reduced diagrams

We now proceed in the determination of the reduced diagrams necessary to capture all the contributions up to and including next to leading power contributions. We notice once more, that the power counting formula derived is bound to be higher or equal to zero, equipping us with the presposition of anticipating only infrared divergencies. We consider as leading power contributions diagrams with total degree of divergence $\gamma = 0$ and as next to leading power $\gamma = 2$. As before, a specific case of diagrams contributing to $\gamma = 1$ arise and will be treated accordingly. The diagrams will be notated loosely as $\sqrt{NLP}$.

5.4.1 Leading Power Factorization

The leading power configuration $\gamma = 0$, corresponds to $N_g^{(i)} = 1$ and $\left\{N_q^{(i)}, n_q^{(n)}, m_q, m_g\right\} = 0$ for $i = 1, 2$.

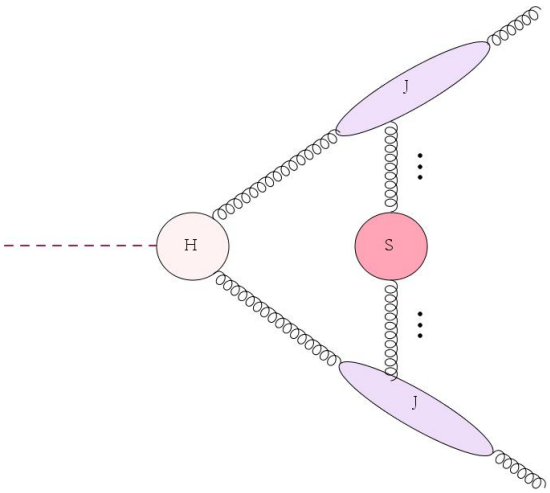

Figure 5.4: Leading power corresponding reduced diagram

5.4.2 Next to Leading Power Factorization

Now, using the same philosophy as we did in the previous chapters we make use of the power counting formula to extract all the possible configurations which, respecting the power counting formula, contribute in subleading powers.

We highlight the following:

- Charge conservation plays an inherently important role here. Since the lines contributing to leading power are bosonic and neutral in terms of electric charge, we have a smaller pool of allowed diagrams than the corresponding ones in $e^+e^- \to \gamma$.
- For example, diagrams contributing to NLP with 2 quarks connecting the soft part with the jets, existent in the previous procedures, violate charge conservation here and shall not be considered. Similarly, we cannot add a single quark line between the hard part and a jet.
- In the diagrams which follow, as always there is no competition between jets when only one connection is present. With that I mean that for example in the $\sqrt{NLP}$ diagram there are two gluon connections between the hard part and the upper jet while a single line connects the other jet with the hard part. This is equivalent to a mirror setup.

Table 5.3: Contributing diagrams in subleading power

γ	$N_q^{(1)}$	$N_q^{(2)}$	$N_g^{(1)}$	$N_g^{(2)}$	$n_q^{(1)}$	$n_q^{(2)}$	m_q	m_g
1	1	0	2	1	0	0	0	0
2	0	0	2	2	0	0	0	0
2	0	0	3	1	0	0	0	0
2	2	0	1	1	0	0	0	0
2	0	0	1	1	0	0	0	1
2	0	0	1	1	1	1	0	0

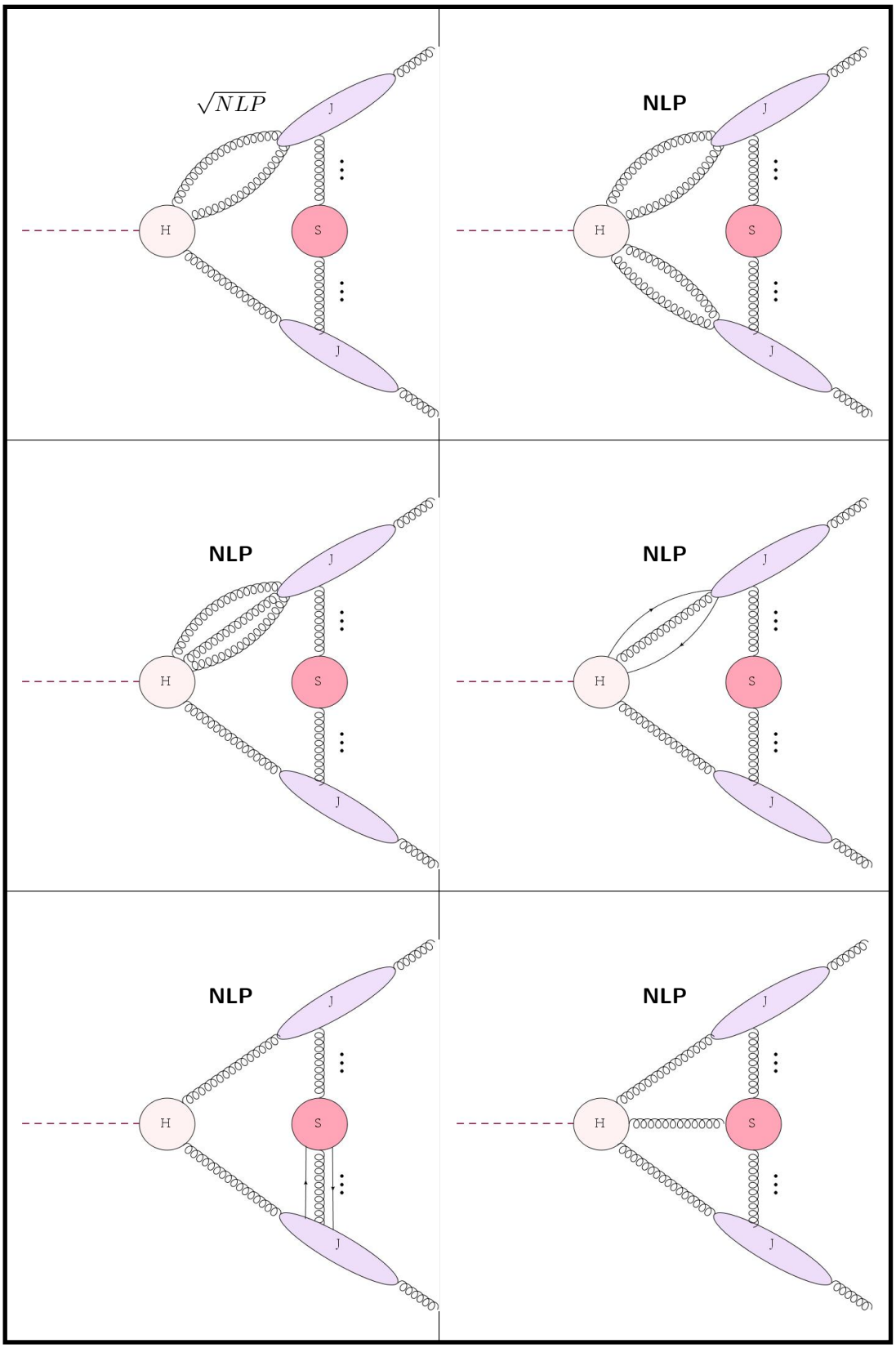

Figure 5.5: Reduced diagrams up to and including NLP

5.5 Factorization formula

$$
\begin{aligned}
M_{\text{coll}}^{NLP} = & \sum_{i=1}^{2} \left(\prod_{j \neq i} J^{j}_{(g)} \right) \left(J^{i}_{(gg)} \otimes H^{i}_{(gg)} + J^{i}_{(g\partial g)} \otimes H^{i}_{(g\partial g)} \right) S \\
& + \sum_{i=1}^{2} \left(\prod_{j \neq i} J^{i}_{(g)} \right) J^{i}_{(ggg)} \otimes H^{i}_{(ggg)} S + \sum_{i=1} \left(\prod_{J+i} J^{i}_{(g)} \right) \\
& \times J^{i}_{(\text{qqg})} \otimes H^{i}_{(qqq)} S + \sum_{1 \leq i \leq j \leq 2} \left(\prod_{k \neq i,j} J^{j}_{(g)} \right) J^{i}_{(gg)} J^{j}_{(gg)} H^{ij}_{(gg)(gg)} S
\end{aligned}
$$

Part II

Higher Twist Contributions

6 Power Corrections in inclusive Deep Inelastic Scattering.

6.1 Framework

The decision to opt for a covariant gauge, in contrast with the Axial gauge choice of Ellis, Furmanski, Petronzio[24] $(n \cdot A = 0)$, with n^μ being a constant lightlike vector, is motivated by the primary objective of most related works in inclusive DIS. In particular we aim to associate the non-perturbative matrix elements derived easier in DIS with similar terms in Drell-Yan, SIDIS or other relevant processes based on the universality of those parts. Since Drell-Yan(DY) is the case of interest in my situation I chose to work in Feynman gauge, a natural choice for DY.

We will use lightcone coordinate and the relevant decomposition for the momenta involved.[1]:

$$n^\mu = (0,1,0,0)$$
$$\overline{n}^\mu = (1,0,0,0)$$
$$n^\mu_{1\perp} = (0,0,1,0)$$
$$n^\mu_{2\perp} = (0,0,0,1),$$

In this framework any momentum can be written as $k^\mu = (k^+, k^-, \overrightarrow{k_\perp})$ and $k^\mu p^\nu n_{\mu\nu} = k^+ p^- + p^- k^+ + \overrightarrow{k_\perp} \cdot \overrightarrow{p_\perp}$

DIS Related Momenta	
Momentum of hadron p^μ	$p^\mu = p^+ \overline{n}^\mu$
Transverse Momentum of Lepton l	$l^\mu_{1\perp} = \overrightarrow{l_{1\perp}} n^\mu_{\perp 1}$
Virtual Photon Momentum q	$q^\mu = -x_B p^\mu - n^\mu \frac{q^2}{2x_B P^+}$
Parton (Incoming) Momentum k	$k^\mu = (xp^+, k^-, k_\perp), x = \frac{k^+}{p^+}$
* The choice of frame is the Breit-Bart[14] (brickwall) frame, setting the mass of hadron to 0 $(M = 0)$ x_B is the Bjorgen scaling $(x_B = \frac{Q_2}{2P \cdot s})$	

[1] Note a difference with the first part of the thesis, n and $\overline{n}$ are reversed.

The inclusive DIS, under consideration is $e^- P \to e^- X$ [14]. The differential cross-section for this process is:[2]

$$E' \frac{d\sigma}{d^3 l'} = \frac{\pi e^4}{2s} \sum_X \delta^4(P_x - p - q) \cdot | < l' | J_l l^{\text{lept}} | l > \frac{1}{q^2} < x | J^l | p > |^2 = \frac{2a^2}{sQ^4} L_{\mu\nu}(l, l') W^{\mu\nu}(q, p, s)$$

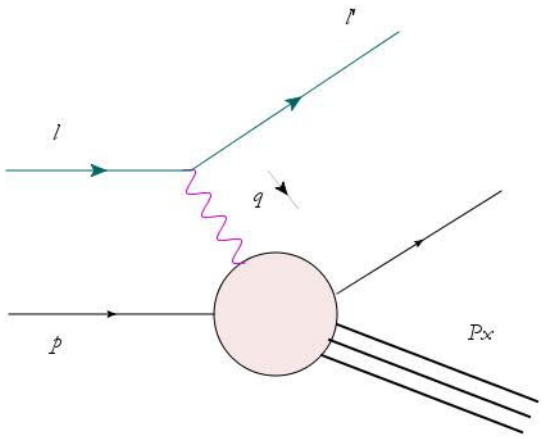

Figure 6.1: "Inclusive deep-inelastic scattering"

Leptonic tensor: For massless leptons, with helicities $h,\ h'$:

$$L^{\mu\nu} = \sum_h (\overline{u}(\ell', h') \gamma^\mu u(l, h)) * (\overline{u}(e', h') \gamma^\nu u(l, h)) = 4(l^\mu \ell'^\nu + \ell'^\mu l^\nu - l \cdot l' n^{\mu\nu} + hi\epsilon^{\mu\nu al} l_a l_{\beta'})$$

Hadronic tensor:

$$W^{\mu\nu} = \frac{1}{4\pi} \sum_x < P | J_\mu(0) | x >< x | J_\nu(0) | P > \times (2\pi)^4 \delta(p + q - P_x) *$$

Via the optical theorem[47], the hadronic tensor is related to the virtual photon-hadron forward scattering amplitude[38], as $W^{\mu\nu} = \frac{1}{2\pi} \text{Im}(M^{\mu\nu})$ and using that $\text{Im}[M^{\mu\nu}] = \frac{Disc(M^{\mu\nu})}{2}$ we find the useful relation $\boxed{W^{\mu\nu} = \frac{1}{4\pi} Disc(M^{\mu\nu})}$, where $Disc(M^{\mu\nu})$, refers to the discontinuity of the amplitude.

In our effort to organise and collect non leading power contributions, we will use the diagrammatic expansion shown in6.3 combined with the relation among the imaginary parts of those amplitudes to the hadronic tensor .

[2] $\sum_x$ corresponds in a Lorentz invariant sum and integration over all hadronic final states.

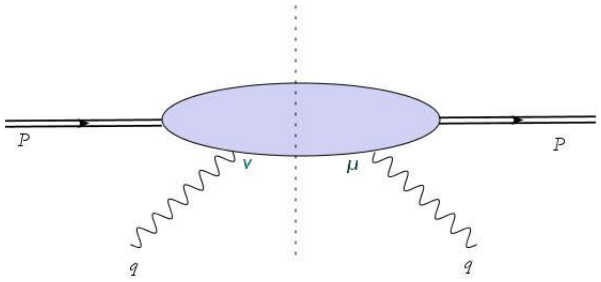

Figure 6.2: Forward scattering amplitude of virtual photon-hadron

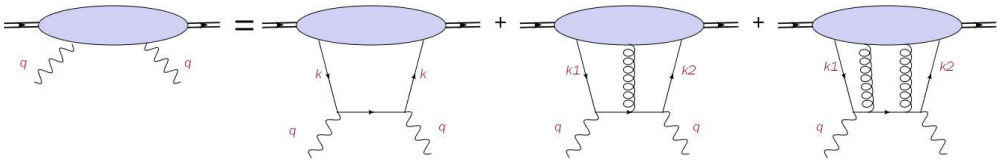

Figure 6.3: Diagrammatic expansion of the forward-scattering amplitude.

6.2 Framework and kinematics: Corrections up to $\frac{1}{Q^2}$

The factorized contributions to the hadronic tensor $W^{\mu\nu}$ can be expressed as a convolution between short-distance components, which can be calculated using perturbation theory, and long-distance matrix elements corresponding to the "upper" parts of the diagrams, which cannot be calculated using perturbation theory. The coupling constant g and the relative color matrices are included in the matrix elements. One of the most interesting and conceptually insightful results, proven later, shows that a naive treatment of the lower parts as hard components will lead to an inaccurate description of the theory. This is because short-distance parts will still be present in the supposedly long-distance matrix elements. Fixing this with various techniques, we analyse in detail in the following will lead to the emergence of the so-called higher twist contributions. Initially, the 'hard' parts are defined as the segments of the diagram that transport the virtual photon momentum q. The leading contribution from the hard part arises when the lines entering the hard part are on-shell and collinear to the initial hadron momentum. This orients our effort in expanding the involved momenta around this large part to extract the subleading contributions. Indeed, one of the trickiest parts in separating such a procedure in energy scales is exactly the fact that diagrams of any order contribute in all powers. However, grasping the conceptual rationale and employing it to refine the method is promising deeper understanding and potentially adressing additional problems. We start with writing down the contributions from each diagram following J. Qiu and G. Sterman [43]. The current chapter consists of a self-consistent guide to acquire the higher-twist [23] contributions to inclusive DIS. It is heavily influenced and follows works like [42], [43], [23], [37] while also provides derivations not accesible as well as new ways to proceed towards deriving those power corrections.

6.2.1 Quark-gluon diagrams relevant to $\frac{1}{Q^2}$ corrections

Diagram 1

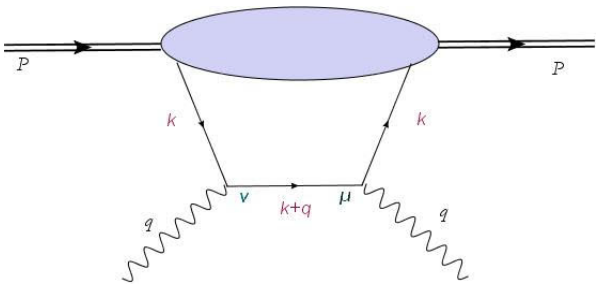

Relevant kinematics

$$p^\mu = \left(p^+, 0, \vec{0}\right)$$

$$k^\mu = (xp^+, k^-, \vec{k_\perp})$$

$$k'^\mu = \left((x - x_B)p^+, \frac{Q^2}{2x_B p^+} + k, \vec{k_\perp}\right) =$$

$$= k^\mu + q^\mu$$

$$W^{\mu\nu}_{(a)} = \frac{1}{4\pi} \int \frac{d^4k}{(2\pi)^4} Tr(\widehat{H}^{\mu\nu}(k)\widehat{M}(k))$$

Matrix Element $\widehat{M}(k) = \int d^4y e^{iky} < p|\overline{\Psi}(0)\Psi(y)|p >$
Hard Part $\widehat{H}^{\mu\nu}(K) = \gamma^\mu(\not{k} + \not{q})\gamma^\nu \times \delta_+((\not{k} + q)^2)$

To determine the hard part, it is sufficient to extract the discontinuity of the virtual photon-hadron forward scattering amplitude. In our case, this discontinuity pertains solely to the hard part.

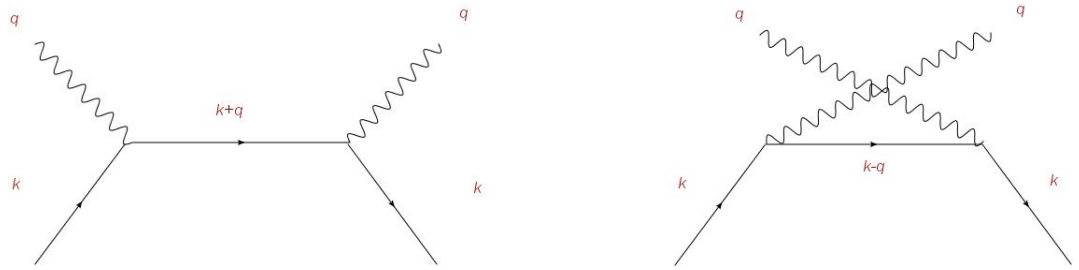

Figure 6.4: "Virtual photon - hadron forward scattering amplitude in leading power"

Aplying Feynman rules:[3]

[3]Note: The second diagram can be acquired from the first replacing $q \to -q$ and $\mu \to \nu$.

$$\frac{i}{2}\left(\gamma_\mu \frac{i}{\not k+\not q}\gamma_\nu + \gamma_\nu \frac{i}{\not k-\not q}\gamma_\mu\right) = \left(\gamma_\mu \frac{i}{\not k+\not q}\gamma_\nu\right)$$

In order to pick the discontinuity we apply the Cutkosky rules[16]:

$$\widehat{H}^{\mu\nu}(k) = \gamma^\mu(\not k + \not q)\gamma^\nu \times \delta_+((k+q)^2)$$

Diagram 2

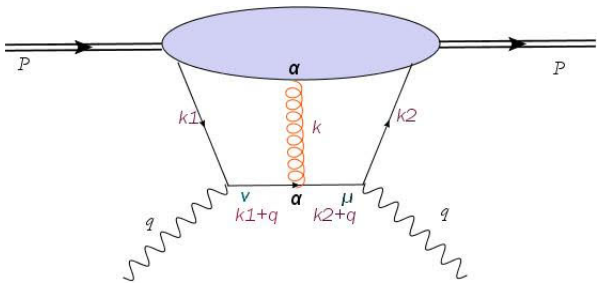

Relevant kinematics

Momentum of gluon $k^\mu = k_1^\mu - k_2^\mu = \left((x_1 - x_2)p^+, (k_1^- - k_2^-), (\overrightarrow{k_{11}} - \overrightarrow{k_{22}})\right)$

$$k_1^{'\mu} = k_1^\mu - q^\mu$$
$$k_2^{'\mu} = k_2^\mu + q^\mu$$
$$k_1^{'\mu} = \left((x_1 - x_B)p^+, \frac{q^2}{2x_B p^+} + k_1^-, \overrightarrow{k_{\perp 1}}\right)$$
$$k_2^{'\mu} = \left((x_2 + x_B)p^+, \frac{-q^2}{2x_B p^+} + k_2^-, \overrightarrow{k_{\perp 2}}\right)$$

$$W^{\mu\nu}_{(\beta)} = \frac{1}{4\pi}\int \frac{d^4k_1}{(2\pi)^4}\frac{d^4k_2}{(2\pi)^4} T_r(\widehat{H_a}^{\mu\nu}(k_1,k_2)\widehat{M^a}(k_1,k_2))$$

with,

$$\widehat{M_a}(k_1,k_2) = \int d^4y_1 d^4y_2 e^{ik_1y_1 + ik_2(y_2-y_1)} \times < p|\overline{\Psi}(0)gA_a(y_1)\Psi(y_2)|p >$$
$$\hat{H}^a_{\mu\nu}(k_1,k_2,q) = \gamma_\mu(\not k_1 + \not q)\gamma^\alpha \frac{\not k_2 + \not q}{(k_2+q)^2 - i\epsilon}\gamma_\nu(2\pi)\delta_+\left((k_1+q)^2\right) +$$
$$+ \gamma_\mu(\not k_1 + \not q)\gamma^\alpha \frac{\not k_2 + \not q}{(k_1+q)^2 + i\epsilon}\gamma_\nu(2\pi)\delta_+\left((k_2+q)^2\right)$$

Again, the hard part is calculated using the Cutkosky rules and summing over the two different cuts. In this case we can have two cuts, a left and a right since the sole gluon is the only object in the cut diagram which would alter the amplitude for different choice of cut.

Diagram 3

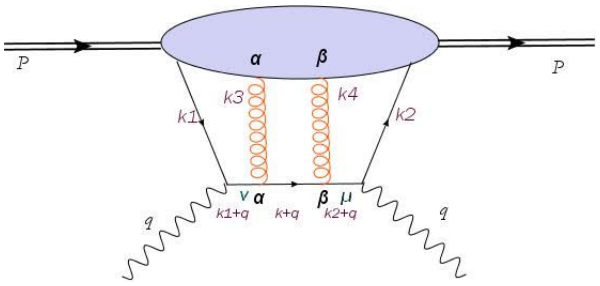

Gluon momenta $k_3^\mu = k^\mu - k_1^\mu$, $k_4^\mu = k^\mu - k_2^\mu$

$$W^{\mu\nu}_{(\alpha\beta)} = \frac{1}{4\pi}\int \frac{d^4k_1}{(2\pi)^4}\frac{d^4k}{(2\pi)^4}\frac{d^4k_2}{(2\pi)^4} T_r(\widehat{H}^{\mu\nu}_{\alpha\beta}(k_1,k,k_2)\widehat{M}^{\alpha\beta}(k_1,k,k_2))$$

$$\widehat{M}_{\alpha\beta}(k_1,k,k_2) = \int d^4y_1 d^4y d^4y_2 e^{ik_1y_1} e^{ik(y_2-y_1)} e^{ik_2(y_2-y_1)} < p|\bar{\psi}(0) g^2 A^\alpha(y_1) A^b(y)\psi(y_2)|p>$$

The hard part is given from the sum of three cuts, one in the right of the two gluon, one in the left of them and one in the middle. ssdsSince none of the matrix-elements are secured with gauge invariance, a collinear expansion as in [43] will be introduced, to rearrange them in gauge invariant parton correlators.

6.3 Towards colour gauge invariance: A first rearrangement of power corrections

The leading contribution, as we said and as stated in [43] is acquired when the lines entering the hard part are on shell and collinear to the momentum of the hadron. Therefore, to capture subleading effects and to isolate the contributions we will expand the partonic momenta around its collinear component.

6.3.1 Collinear expansion toolset

The projection operator

First we define $\boxed{\omega^\alpha_{\alpha'} = g^\alpha_{\alpha'} - \overline{n}^\alpha n_{\alpha'}}$, a projection operator, which upon acting on the parton momenta, strips them off their collinear component $k^+ = xp^+, x = \frac{k^+}{p^+}$.

$$\omega^\alpha_{\alpha'} = (g^\alpha_{\alpha'} - \overline{n}^\alpha n_{\alpha'})k^{\alpha'} = (k^\alpha - \overline{n}^\alpha(k_+)) = (k - xp)^\alpha$$

Taylor expansion

Thereafter, and to pick subleading power contributions induced from the transverse component of the partonic momenta, we expand the Hard parts around the dominant collinear components $k = xp$ which are responsible for leading power corrections:

$$\widehat{H}^{\mu\nu}(k) = \widehat{H}^{\mu\nu}(xp) + \frac{\partial \widehat{H}^{\mu\nu}(xp)}{\partial k^a}(k-xp)^a + \frac{1}{2}\frac{\partial^2 \widehat{H}^{\mu\nu}(xp)}{\partial k^a \partial k^\beta}(k-xp)^a(k-xp)^\beta =$$

$$= \widehat{H}^{\mu\nu}(xp) + \frac{\partial \widehat{H}^{\mu\nu}(xp)}{\partial k^a} w^a_{a'} k^a + \frac{1}{2}\frac{\partial^2 H^{\mu\nu}(xp)}{\partial k^a \partial k^\beta} w^a_{a'} w^\beta_{\beta'} k^{a'} k^{\beta'} + O(\frac{1}{Q^n}, n>2)$$

$$\widehat{H}^{\mu\nu}_a(k_1,k_2) = \widehat{H}^{\mu\nu}_a(x_1 p, x_2 k_2) + \frac{\partial \widehat{H}^{\mu\nu}(x_1 p, x_2 p)}{\partial k_1^\beta} w^\beta_{1\beta'} k_1^{\beta'} + \frac{\partial \widehat{H}^{\mu\nu}(x_1 p, x_2 p)}{\partial k_2^\beta} \times$$

$$\times w^\beta_{2\beta'} k_2^{\beta'} + O(\frac{1}{Q^n}, n>2)$$

$$\widehat{H}^{\mu\nu}_{\alpha\beta}(k_1,k,k_2) = \widehat{H}^{\mu\nu}_{\alpha\beta}(x_1 p, xp, x_2 p) + O(\frac{1}{Q^n}, n>2)$$

Note that I keep only the necessary terms from each expansion, and ignore the NNLP terms.

Evaluation of Hard parts in the collinear expansion

Expanding around the collinear momenta for all contributions from the hadronic tensor results in Hard parts that are solely dependent on these momenta throughout the process. Consequently, assessing these Hard parts in the collinear limit is beneficial. Additionally, this limit brings about notable simplifications that are crucial for subsequent steps. I now proceed with the evaluations:

$$\begin{aligned}
\widehat{H}^{\mu\nu}(xp) &= \gamma^\mu (x\not{p} + \not{q})\gamma^\nu \times \delta_+((x\not{p}+q)^2) = \\
&= \gamma^\mu (x\not{p} + \not{q})\gamma^\nu \times (2\pi)\delta\left(-Q^2 + 2xp^+\frac{Q^2}{2x_B p^+}\right) = \\
&= \gamma^\mu (x\not{p} + \not{q})\gamma^\nu \times (2\pi)\delta\left(\frac{Q^2}{x_B}(x-x_B)\right) = \\
&= \gamma^\mu (x\not{p} + \not{q})\gamma^\nu (2\pi)\frac{x_B}{Q^2}\delta(x-x_B)
\end{aligned}$$

Where we used the virtual photon momentum $q^\mu = -x_B p^\mu - n^\mu \frac{q^2}{2x_B P^+}$
Likewise we find

$$\widehat{H}^{a}_{\mu\nu}\left(x_1 p, x_2 p, q\right) = \gamma_\mu \left(x_1 \not{p} + \not{q}\right) \gamma^\alpha \frac{x_2 \not{p} + \not{q}}{\left(x_2 p + q\right)^2 - i\epsilon} \gamma_\nu (2\pi) \delta_+ \left(\left(x_1 p + q\right)^2\right) +$$
$$+ \gamma_\mu \left(x_1 \not{p} + \not{q}\right) \gamma^\alpha \frac{x_2 \not{p} + \not{q}}{\left(x_1 p + q\right)^2 + i\epsilon} \gamma_\nu (2\pi) \delta_+ \left(\left(x_2 p + q\right)^2\right) =$$
$$= \gamma_\mu \left(x_1 \not{p} + \not{q}\right) \gamma^\alpha \frac{x_2 \not{p} + \not{q}}{\left(x_2 p + q\right)^2 - i\epsilon} \gamma_\nu (2\pi) \frac{x_B}{Q^2} \delta\left(x_1 - x_B\right) +$$
$$+ \gamma_\mu \left(x_1 \not{p} + \not{q}\right) \gamma^\alpha \frac{x_2 \not{p} + \not{q}}{\left(x_1 p + q\right)^2 + i\epsilon} \gamma_\nu (2\pi) \frac{x_B}{Q^2} \delta\left(x_2 - x_B\right)$$

Ward Identities

Using the generalized Ward-Takahashi identities is crucial when implementing the collinear expansion. Moreover their use will be highly helpful in later parts of this section. Therefore, and in order to have all the needed identities handy, I present here a list of useful examples that will be used now or later on.

Ward identities relating derivatives of Hard parts to higher order Hard parts

- $\dfrac{\partial \widehat{H}_{\mu\nu}(xp)}{\partial k_a} = -H^{a}_{\mu\nu}(xp, xp)$
- $\dfrac{1}{2}\dfrac{\partial^2 \widehat{H}_{\mu\nu}(xp)}{\partial k_a \partial k_\beta} = H^{\alpha\beta}_{\mu\nu}(xp, xp, xp)$
- $\dfrac{\partial^2 \widehat{H}^{a}_{\mu\nu}(x_1 p, x_2 p)}{\partial k_{2\beta}} = -H^{\alpha\beta}_{\mu\nu}(x_1 p, x_2 p, x_2 p)$
- $\dfrac{\partial^2 \widehat{H}^{a}_{\mu\nu}(x_1 p, x_2 p)}{\partial k_{1\beta}} = -H^{\beta\alpha}_{\mu\nu}(x_1 p, x_1 p, x_2 p)$

In tree level this identity follows immediately,

$$\frac{\partial}{\partial k^a}\frac{i}{\not{k} - m} = \frac{i}{\not{k} - m} i\gamma_a \frac{i}{\not{k} - m},$$

and is also proven in all orders in [52].

Ward identities relating the product of the hard part with p with a lower order hard part.

- $p_\alpha \widehat{H}^{\alpha}_{\mu\nu}(x_1 p, x_2 p) = -\dfrac{H_{\mu\nu}(x_1 p)}{x_2 - x_B - i\varepsilon} - \dfrac{H_{\mu\nu}(x_2 p)}{x_1 - x_B + i\varepsilon}$
- $p_\alpha \widehat{H}^{\alpha\beta}_{\mu\nu}(x_1 p, x_2 p, xp) = -\dfrac{H^{\beta}_{\mu\nu}(x_1 p, x_1 p)}{x - x_1 - i\varepsilon} - \dfrac{H^{\beta}_{\mu\nu}(xp, x_1 p)}{x_1 - x + i\varepsilon}$
- $p_\alpha \widehat{H}^{\alpha\beta}_{\mu\nu}(x_1 p, x_2 p, xp) = -\dfrac{H^{\alpha}_{\mu\nu}(x_1 p, xp)}{x_2 - x - i\varepsilon} - \dfrac{H^{\alpha}_{\mu\nu}(x_1 p, x_2 p)}{x - x_2 + i\varepsilon}$

The proof of those relationships is not very complicated: First we rearrange $\widehat{H}^a_{\mu\nu}(x_1p, x_2p, q)$ as follows:

$$
\begin{aligned}
&\widehat{H}^a_{\mu\nu}(x_1p, x_2p, q) = \gamma_\mu (x_1 \not{p} + \not{q}) \gamma^\alpha \frac{x_2 \not{p} + \not{q}}{(x_2p+q)^2 - i\epsilon} \gamma_\nu (2\pi) \delta_+ \left((x_1p+q)^2\right) + \\
&+ \gamma_\mu (x_1 \not{p} + \not{q}) \gamma^\alpha \frac{x_2 \not{p} + \not{q}}{(x_1p+q)^2 + i\epsilon} \gamma_\nu (2\pi) \delta_+ \left((x_2p+q)^2\right) = \\
&= \gamma_\mu (x_1 \not{p} + \not{q}) \gamma^\alpha \frac{x_2 \not{p} + \not{q}}{(x_2p+q)^2 - i\epsilon} \gamma_\nu (2\pi) \frac{x_B}{Q^2} \delta(x_1 - x_B) + \\
&+ \gamma_\mu (x_1 \not{p} + \not{q}) \gamma^\alpha \frac{x_2 \not{p} + \not{q}}{(x_1p+q)^2 + i\epsilon} \gamma_\nu (2\pi) \frac{x_B}{Q^2} \delta(x_2 - x_B) = \\
&= \gamma_\mu (x_1 \not{p} + \not{q}) \gamma^\alpha (x_2 \not{p} + \not{q}) \gamma_\nu \frac{1}{(x_2p+q)^2 - i\epsilon} (2\pi) \frac{x_B}{Q^2} \delta(x_1 - x_B) + \\
&+ \gamma_\mu (x_1 \not{p} + \not{q}) \gamma^\alpha (x_2 \not{p} + \not{q}) \gamma_\nu \frac{1}{(x_1p+q)^2 + i\epsilon} (2\pi) \frac{x_B}{Q^2} \delta(x_2 - x_B) = \\
&= \gamma_\mu (x_1 \not{p} + \not{q}) \gamma^\alpha (x_2 \not{p} + \not{q}) \gamma_\nu (2\pi) \left(\frac{\delta(x_1 - x_B)}{(x_2p+q)^2 - i\epsilon} + \frac{\delta(x_2 - x_B)}{(x_1p+q)^2 + i\epsilon} \right) \frac{x_B}{Q^2} = \\
&= \gamma_\mu (x_1 \not{p} + \not{q}) \gamma^\alpha (x_2 \not{p} + \not{q}) \gamma_\nu (2\pi) \left(\frac{\delta(x_1 - x_B)}{x_2 - x_B - i\epsilon} + \frac{\delta(x_2 - x_B)}{x_1 - x_B + i\epsilon} \right)
\end{aligned}
$$

Contracting with p_a and using some basic algebra we finalize the proof:

$$
\begin{aligned}
&p_a \widehat{H}^a_{\mu\nu}(x_1p, x_2p, q) = \\
&= \gamma_\mu (x_1 \not{p} + \not{q}) \not{p} (x_2 \not{p} + \not{q}) \gamma_\nu (2\pi) \left(\frac{\delta(x_1 - x_B)}{x_2 - x_B - i\epsilon} + \frac{\delta(x_2 - x_B)}{x_1 - x_B + i\epsilon} \right) = \\
&= -\gamma^\mu (x_1 \not{p} + \not{q}) \gamma^\nu (2\pi) \frac{x_B}{Q^2} \frac{\delta(x_1 - x_B)}{x_2 - x_B - i\epsilon} - \\
&- \gamma^\mu (x_2 \not{p} + \not{q}) \gamma^\nu (2\pi) \frac{x_B}{Q^2} \frac{\delta(x_2 - x_B)}{x_1 - x_B + i\epsilon} = \\
&= -\frac{H_{\mu\nu}(x_1p)}{x_2 - x_B - i\varepsilon} - \frac{H_{\mu\nu}(x_2p)}{x_1 - x_B + i\varepsilon}
\end{aligned}
$$

Using the Ward identities we now can express the expansions as[44]:

- $\widehat{H}^{\mu\nu}(k) = \widehat{H}^{\mu\nu}(xp) - \widehat{H}^{\mu\nu}_\alpha(xp, xp) w^\alpha_{\alpha'} k'^{\alpha'} + \widehat{H}^{\mu\nu}_{\alpha\beta}(xp, xp, xp) w^\alpha_{\alpha'} w^\beta_{\beta'} k'^\alpha_{\alpha'} k^{\beta'}$
- $\widehat{H}^{\mu\nu}_\alpha(k_1, k_2) = \widehat{H}^{\mu\nu}(x_1p, x_1p) - \widehat{H}^{\alpha\beta}_{\mu\nu}(x_1p, x_2p, x_2p) w^\beta_{\beta'} k^{\beta'} - \widehat{H}^{\beta\alpha}_{\mu\nu}(x_1p, x_1p, x_2p) w^\beta_{\beta'} k^\beta$
- $\widehat{H}^{\mu\nu}_{\alpha\beta}(k_1, k, k_2) = \widehat{H}^{\mu\nu}_{\alpha\beta}(x_1p, x, x_2p)$ + higher orders

6.4 Collinear expansion: Applied to the hadronic tensor

We now have a well-defined route to follow as well as a fully equipped toolset in our disposal. In what follows, I implement every step of the collinear expansion previously discussed, addressing the three corrections depicted in the three diagrams while establishing newly structured relationships.

Diagram 1

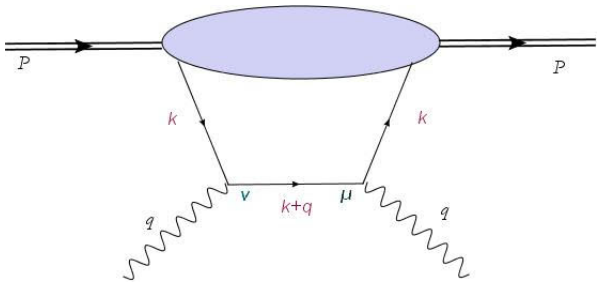

$$W_a^{\mu\nu} = \frac{1}{4\pi}\int \frac{d^4k}{(2\pi)^4}\,\mathrm{Tr}\left(\widehat{H}^{\mu\nu}(k)\widehat{M}(k)\right)$$

Steps

- First we introduce $1 = \int dx\delta\left(x - \frac{k^+}{p^+}\right)$ in order to use the fact that the hard function is now **independent of the transverse partonic momenta**. In this way, we can reduce the $\int d^4k$ dimension-four momentum integral to a single-dimensional integral over the momentum fraction x.
- To perform this reduction we also will need the aid of the identity[45]

$$\int \frac{\mathrm{d}^4k}{(2\pi)^4}\mathrm{e}^{iky}\delta(x - \tfrac{k^+}{p^+}) = \int \frac{p^+\mathrm{d}y^-}{2\pi}\mathrm{e}^{i(xp^+)y^-}\delta^4(y - y^-)$$

- We replace the Hard parts with the Taylor expansion around the collinear component of partonic momenta as we expressed it using the projection operators and the Ward Identities.
- We replace $k^{\alpha'}$ with $\left(-i\partial^{\alpha'}\right)$

The procedure is identical for the three corrections and is as follows:

$$\begin{aligned}
W_{(a)}^{\mu\nu} &= \frac{1}{4\pi}\int dx\,\mathrm{Tr}\left(\hat{H}^{\mu\nu}(xp) - H_\alpha^{\mu\nu}(xp,xp)w_{\alpha'}^{\alpha}\left(k^{\alpha'}\right) - H_{\alpha\beta}^{\mu\nu}(xp,xp,xp)w_{\alpha'}^{\alpha}w_{\beta'}^{\beta}\left(k^{\alpha'},k^{\beta'}\right)\right)\times \\
&\quad\times\int\frac{d^4kd^4y}{(2\pi)^4}\delta\left(x-\frac{k^+}{p^+}\right)e^{iky}\left\langle p\left|\bar{\psi}(0)\psi\left(y\right)\right|p\right\rangle \\
&= \frac{1}{4\pi}\int dx\,\mathrm{Tr}\left(\hat{H}^{\mu\nu}(xp) - H_\alpha^{\mu\nu}(xp,xp)w_{\alpha'}^{\alpha}\left(-i\partial^{\alpha'}\right) - H_{\alpha\beta}^{\mu\nu}(xp,xp,xp)w_{\alpha'}^{\alpha}w_{\beta'}^{\beta}\left(-i\partial^{\alpha'},-i\partial^{\beta'}\right)\right)\times \\
&\quad\times\int\frac{p^+d^4ydy^-}{2\pi}\delta^4\left(y-y^-\right)e^{i(xp^+)y^-}\left\langle p\left|\bar{\psi}(0)\psi\left(y^-\right)\right|p\right\rangle
\end{aligned}$$

$$= \frac{1}{4\pi}\int dx\,\mathrm{Tr}\left(\hat{H}^{\mu\nu}(xp)\cdot\int\frac{p^+dy^-}{2\pi}e^{i(xp^+)y^-}\left\langle p\left|\bar{\psi}(0)\psi\left(y^-\right)\right|p\right\rangle\right)+$$
$$+\frac{1}{4\pi}\int dx\,\mathrm{Tr}\left(\hat{H}^{\mu\nu}_{\alpha}(xp,xp)\cdot w^{\alpha}_{\alpha'}\int\frac{p^+dy^-}{2\pi}e^{i(xp^+y^-)}\times\left\langle p\left|\bar{\psi}(0)i\partial^{\alpha'}(y)\psi\left(y^-\right)\right|p\right\rangle+\right.$$
$$\left.+\frac{1}{4\pi}\int dx\,\mathrm{Tr}\left(\hat{H}^{\mu\nu}_{\alpha\beta}(xp,xp,xp)\cdot w^{\alpha}_{\alpha'}w^{\beta}_{\beta'}\int\frac{p^+dy^-}{2\pi}e^{i(xp^+y^-)}\left\langle p\left|\bar{\psi}(0)i\partial^{\alpha'}(y)i\partial^{\beta'}(y)\psi\left(y^-\right)\right|p\right\rangle\right)\right)$$

Diagram 2

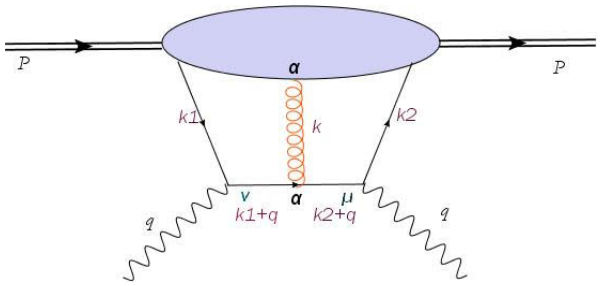

$$W^{\mu\nu}_{(b)} = \frac{1}{4\pi}\int\frac{d^4k_1}{(2\pi)^4}\frac{d^4k_2}{(2\pi)^4}T_r(\widehat{H_{\alpha}}^{\mu\nu}(k_1,k_2)\widehat{M^{\alpha}}(k_1,k_2))$$

$$
\begin{aligned}
&W_b^{\mu\nu} = \frac{1}{4\pi}\int dx_1 dx_2 \,\mathrm{Tr}\Big(\Big(H_\alpha^{\mu\nu}\left(x_1 p, x_2 p\right) - H_{\alpha\beta}^{\mu\nu}\left(x_1 p, x_2 p, x_2 p\right) w_{2_{\beta'}}^{\beta} k_2^{\prime\beta'} - \\
&-\hat{H}_{\beta\alpha}^{\mu\nu}\left(x_1 p, x_1 p, x_2 p\right) w_{1_{\beta'}}^{\beta} k_1^{\prime\beta'}\Big) \times \\
&\times \int d^4 y_1 d^4 y_2 \frac{d^4 k_1}{(2\pi)^4}\frac{d^4 k_2}{(2\pi)^4}\delta\left(x_1 - \frac{k_1^+}{p^+}\right)\delta\left(x_2 - \frac{k_2^+}{p^+}\right) e^{i k_1 y_1} e^{i k_2 (y_2 - y_1)} \times \\
&\times \left\langle p\left|\bar{\psi}(0) g A_\alpha\left(y_1\right)\psi\left(y_2\right)\right|p\right\rangle\Big) = \\
&= \frac{1}{4\pi}\int dx_1 dx_2 \,\mathrm{Tr}\Big(\Big(H_\alpha^{\mu\nu}\left(x_1 p, x_2 p\right) - H_{\alpha\beta}^{\mu\nu}\left(x_1 p, x_2 p, x_2 p\right) w_{2_{\beta'}}^{\beta} k_2^{\prime\beta'} - \\
&-\hat{H}_{\beta\alpha}^{\mu\nu}\left(x_1 p, x_1 p, x_2 p\right) w_{1_{\beta'}}^{\beta} k_1^{\prime\beta'}\Big) \times \\
&\times \int d^4 y_1 d^4 y_2 \frac{p^+ dy_1^-}{2\pi}\frac{p^+ dy_2^-}{2\pi}\delta^4\left(y_1 - y_1^-\right)\delta^4\left(y - y^-\right) e^{i\left(x_1 p^+\right) y_1^-} e^{i\left(x_2 p^+\right)\left(y_2^- - y_1^-\right)} \times \\
&\times \left\langle p\left|\bar{\psi}(0) g A_\alpha\left(y_1\right)\psi\left(y_2\right)\right|p\right\rangle\Big) = \\
&= \frac{1}{4\pi}\int dx_1 dx_2 \,\mathrm{Tr}\left(\hat{H}_\alpha^{\mu\nu}\left(x_1 p, x_2 p\right)\cdot\int \frac{p^+ dy_1^-}{2\pi}\frac{p^+ dy_2^-}{2\pi}\times\right. \\
&\left.\times e^{i\left(x_1 p^+\right) y_1^-} e^{i\left(x_2 p^+\right)\left(y_2^- - y_1^-\right)} \times \left\langle p\left|\bar{\psi}(0) g A^\alpha\left(y_1^-\right)\psi\left(y_2^-\right)\right|p\right\rangle\right) + \\
&+ \frac{1}{4\pi}\int dx_1 dx_2 \,\mathrm{Tr}\left(\hat{H}_{\alpha\beta}^{\mu\nu}\left(x_1 p, x_2 p, x_2 p\right)\cdot w_{\beta'}^{\beta}\times\right. \\
&\times \int \frac{dy_1^- p^+}{2\pi}\frac{dy_2^- p^+}{2\pi} e^{i\left(x_1 p^+\right) y_1^-} e^{i\left(x_2 p^+\right)\left(y_2^- - y_1^-\right)} \times \\
&\left.\times \left\langle p\left|\bar{\psi}(0) g A^\alpha\left(y_1^-\right) i\partial^{\beta'}\left(y_2\right)\psi\left(y_2^-\right)\right|p\right\rangle\right) + \\
&+ \frac{1}{4\pi}\int dx_1 dx_2 \cdot \mathrm{Tr}\left(\hat{H}_{\beta\alpha}^{\mu\nu}\left(x_1 p, x_1 p, x_2 p\right) w_{\beta'}^{\beta}\times\right. \\
&\times \int \frac{dy_1^- p^+}{w\pi}\frac{dy_2^- p^+}{w\pi} e^{i\left(x_1 p^+\right) y_1^-} e^{i\left(x_2 p^+\right)\left(y_2^- - y_1^-\right)} \times \\
&\left.\times \left\langle p\left|\bar{\psi}(0) i\partial^{\beta'}\left(y_1\right) g A^\alpha\left(y_1^-\right)\bar{\psi}\left(y_2^-\right)\right|p\right\rangle\right)
\end{aligned}
$$

Diagram 3

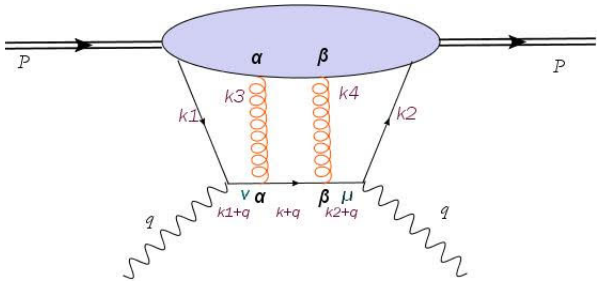

$$W_c^{\mu\nu} = \frac{1}{4\pi}\int \frac{d^4k_1}{(2\pi)^4}\frac{d^4k}{(2\pi)^4}\frac{d^4k_2}{(2\pi)^4}\,\mathrm{Tr}\left(\hat{H}_{ab}^{\mu v}\left(k_1,k,k_2\right)\times\right.$$

$$\left.\times\int d^4y_1 d^4y d^4y_2 e^{ik_1y_1}e^{ik(y_2-y_1)}e^{ik_2(y_2-y_1)} < p\left|\bar{\psi}(0)g^2A^{\alpha}\left(y_1\right)A^{b}\left(y\right)\psi(y_2)\right|p >\right)$$

$$\begin{aligned}
W_c^{\mu\nu} &= \frac{1}{4\pi}\int dx_1 dx dx_2\,\mathrm{Tr}\left(\hat{H}_{ab}^{\mu v}\left(x_1p,xp,x_2p\right)\right.\\
&\times\int d^4y_1 d^4y d^4y_2\frac{d^4k_1}{(2\pi)^4}\frac{d^4k}{(2\pi)^4}\frac{d^4k_2}{(2\pi)^4}\delta\left(x_1-\frac{k_1^+}{p^+}\right)\\
&\times\delta\left(x-\frac{k^+}{p^+}\right)\delta\left(x_2-\frac{k_2^+}{p^+}\right)e^{ik_1y_1}e^{ik(y_2-y_1)}e^{ik_2(y_2-y_1)}\\
&\times < p\left|\bar{\psi}(0)g^2A^{\alpha}\left(y_1\right)A^{b}\left(y\right)\psi(y_2)\right|p >\Big) =\\
&= \frac{1}{4\pi}\int dx_1 dx dx_2\,\mathrm{Tr}\left(\hat{H}_{ab}^{\mu v}\left(x_1p,xp,x_2p\right)\right.\\
&\times\int d^4y_1 d^4y d^4y_2\frac{dy_1p^+}{2\pi}\frac{dy^-p^+}{2\pi}\frac{dy_2^-p^+}{2\pi}e^{i(x_1p^+)y_1^-}\\
&\times e^{i(xp^+)(y^--y_1^-)}e^{i(x_2p^+)(y^--y_2^-)}\delta^4\left(y_1-y_1^-\right)\\
&\times\delta^4\left(y-y^-\right)\delta^4\left(y_2-y_2^-\right)\\
&\times < p\left|\bar{\psi}(0)g^2A^{\alpha}\left(y_1\right)A^{b}\left(y\right)\psi(y_2)\right|p >\Big) =\\
&= \frac{1}{4\pi}\int dx_1 dx dx_2\,\mathrm{Tr}\left(\hat{H}_{ab}^{\mu v}\left(x_1p,xp,x_2p\right)\right.\\
&\times\int\frac{dy_1p^+}{2\pi}\frac{dy^-p^+}{2\pi}\frac{dy_2^-p^+}{2\pi}e^{i(x_1p^+)y_1^-}\\
&\times e^{i(xp^+)(y^--y_1^-)}e^{i(x_2p^+)(y^--y_2^-)} < p\left|\bar{\psi}(0)g^2A^{\alpha}\left(y_1^-\right)A^{b}\left(y^-\right)\psi(y_2^-)\right|p >\Big)
\end{aligned}$$

6.5 Collinear expansion of the gluon

We have successfully re-expressed the hadronic tensor and its related corrections using the collinear expansion introduced in [26] and in chapter 6.3. The acquired form is lacking colour gauge invariance and also is not particularly useful as it contains terms which can not be combined. To merge terms efficiently, we collinearly expand the gluon field as in [43]:

$$A^{\alpha} = \omega^{\alpha}_{\alpha'} A^{\alpha'} + \frac{p^{\alpha}}{p\cdot n}\cdot(n\cdot A) = \\ = \omega^{\alpha}_{\alpha'} A^{\alpha'} + \frac{p^{\alpha}}{p^{+}}\cdot A^{+}$$

With the gluon field, successfully separated in a transverse and a scalar longitudinal component we will exploit both parts for further rearrangement. The transverse part $\omega^{\alpha}_{\alpha'} A^{\alpha'}$ will be combined with terms $\omega^{\alpha}_{\alpha'}\partial^{\alpha'}$ and form "transverse" covariant derivatives, of the form $\omega^{\alpha}_{\alpha'} D(y) = \Big(i\partial^{\alpha'}(y) - gA^{\alpha'}(y)\Big)$, while the p^{α} momentum in the longitudinal part of the gluon field can contract with and via the aforementioned generalized Ward identities lower the order of Hard diagrams. We will also use the following identity [42]:

$$p_{\alpha}\omega^{\alpha}_{\alpha'} = 0 = p_{\alpha}\left(g^{\alpha}_{\alpha'} - \overline{n}^{\alpha} n_{\alpha'}\right) = \left(p_{\alpha'} - p^{+} n_{\alpha'}\right) = 0$$

6.5.1 Further rearrangement of the corrections

Since $W^{\mu\nu}_{a}$ does not contain any gauge fields, we start the modification of the corrections from $W^{\mu\nu}_{b}$. To that end we replace

$$A^{\alpha} = w^{\alpha}_{\alpha'} A^{\alpha'} + \frac{p^{\alpha}}{p\cdot n}\cdot(n\cdot A) = \\ = w^{\alpha}_{\alpha'} A^{\alpha'} + \frac{p^{\alpha}}{p^{+}}\cdot A^{+}$$

in the derived formula for $W^{\mu\nu}_{b}$. Afterwards we apply a new set of Ward identities and separate terms depending on the gauge field component each term contains. In particular, we separate terms including the collinear part of the gauge field from terms dependent on its transverse component.

Our reward will be the ability to combine terms from different hadronic corrections into covariant derivatives and gauge links. This will be only possible if we lower the order of some hard contributions using Ward identities.

$$
\begin{aligned}
W^{\mu\nu}_{(b)} = & \frac{1}{4\pi}\int dx_1 dx_2 Tr\left(H^{\mu v}_{\alpha}\left(x_1 p_1, x_2 p\right)\cdot\int\frac{p^+dy_1}{2\pi}\frac{p^+dy_2^-}{2\pi}\; e^{i\left(x_1p^+\right)y_1^-}e^{i\left(x_2p^+\right)\left(y_2^- - y_1^-\right)}\times\right.\\
& \times < p\mid\bar{\psi}(0)\left(\omega^{\alpha}_{\alpha'}A^{\alpha'}\left(y_1\right) - p^{\alpha}\frac{A^+\left(y_1^-\right)}{p^+}\right)\psi\left(y_2^-\right)|p\rangle +\\
& + \frac{1}{4\pi}\int dx_1 dx_2 Tr\left(H^{\mu\nu}_{\alpha\beta}\left(x_1 p, x_2 p, x_2 p\right)\omega^{\alpha}_{\alpha'}\int\frac{p^+dy_1}{2\pi}\frac{p^+dy_2}{2\pi}\; se^{i\left(x_1p^+\right)y_1^-}e^{i\left(x_2p^+\right)\left(y_2^- - y_1^-\right)}\times\right.\\
& \left.\left.\times < p\mid\bar{\psi}(0)g\left(\omega^{\alpha}_{\alpha'}A^{\alpha'}\left(y_i\right) - \frac{p^{\alpha}}{p^+}A^+\left(y_1^-\right)\left(i\partial_b'\left(y_2^-\right)\right)\psi\left(y_2^-\right)|p\rangle\right)\right)+\right.\\
& + \frac{1}{4\pi}\int dx_1 dx_2\,\mathrm{Tr}\left(H^{\mu\nu}_{ba}\left(x_1 p, x_2 p, x_2 p\right)w^{b}_{b'}\times\right.\\
& \times\int\frac{p^+dy_1^-}{2\pi}\frac{p^+dy_2^{-}}{2\pi}e^{i\left(x_1p^+\right)y_1^-}e^{i\left(x_2p^+\right)\left(y_2^- - y_1^-\right)}\times\\
& \left.\times < p|\bar{\psi}_0\left(i\partial_{b'}\left(y_1\right)\right)g\left(w^{\alpha}_{\alpha'}A^{\alpha'}\left(y_1^-\right) - \frac{p^{\alpha}A^+\left(y_i^-\right)}{p^+}\right)\psi\left(y_2^-\right)|p>\right)\\
= & \frac{1}{4\pi}\int dx_1 dx_2 Tr\left(H^{\mu\nu}_{\alpha b}\left(x_1 p, x_2 p\right)\times\right.\\
& \times\int\frac{p^+dy_1^+}{2\pi}\frac{p^+dy_2^-}{2}e^{i\left(x_1p^+\right)y_1^-}e^{i\left(x_2p^+\right)\left(y_2^- - y_1^-\right)}\times\\
& \left.\times < p\left|\bar{\psi}(0)g\omega^{\alpha}_{\alpha}A^{\alpha'}\left(y_1^-\right)\psi\left(y_2^-\right)\right|p> +\right.\\
& + \frac{1}{4\pi}\int dx_1 dx_2\left(H^{\mu\nu}_{ba}\left(x_1 p, x_1 p, x_2 p\right)\times\right.\\
& \times w^{\alpha}_{\alpha'}w^{b}_{b'}\int\frac{p^+dy_1^-}{2\pi}\frac{p^+dy_2^-}{2\pi}e^{i\left(x_1p^+\right)y_1^-}e^{i\left(x_2p^+\right)\left(y_2^- - y_1^-\right)}\times\\
& \left.\times < p\left|\bar{\psi}(0)i\partial_{b'}\left(y_1^-\right)g\omega^{\alpha}_{\alpha'}A^{\alpha'}\left(y_i\right)\psi\left(y_2^-\right)\right|p> +\right.\\
& + \frac{1}{4\pi}\int dx_1 dx_2\,\mathrm{Tr}\left(H^{\mu\nu}_{ab}\left(x_1 p, x_2 p, x_2 p\right).\times\right.\\
& \left.\times w^{\alpha}_{\alpha'}w^{b}_{b'}\int\frac{p^+dy_1^-}{2\pi}\frac{p^+dy_2^-}{2\pi}e^{i\left(x_1p^+\right)y_1^-}e^{i\left(x_2p^+\right)\left(y_2^- - y_1^-\right)}+\right.\\
& + \frac{1}{4\pi}\int dx_1 dx_2\,\mathrm{Tr}\left(\left(\frac{H^{\mu v}\left(x_1 p\right)}{x_2 - x_B - i\varepsilon} + \frac{H^{\mu\nu}\left(x_2 p\right)}{x_1 - x_B + i\varepsilon}\right)\times\right.\\
& \times\int\frac{p^+dy_1^-}{2\pi}\frac{p^+dy_2^-}{2\pi}e^{i\left(x_1p^+\right)}e^{i\left(x_2p^+\right)\left(y_2^- - y_i^-\right)}\times\\
& \left.\times < p\left|\bar{\psi}(0)gA^+_{a'}\left(y_1^-\right)\psi\left(y_2\right)\right|p> +\right.\\
& + \frac{1}{4\pi}\int dx_1 dx_2\,\mathrm{Tr}\left(\left(\frac{H^{\mu\nu}_{b}\left(x_1 p, x_2 p\right)}{x_2 - x_1 - i\varepsilon} + \frac{H^{\mu\nu}_{b}\left(x_2 p, x_2 p\right)}{x_1 - x_2 + i\varepsilon}\right)\times\right.\\
& \times\int\frac{p^+dy_1^-}{2\pi}\frac{p^+dy_2^-}{2\pi}e^{i\left(x_1p^+\right)}e^{i\left(x_2p^+\right)\left(y_2^- - y_i^-\right)}\times\\
& \left.\times < p\left|\bar{\psi}(0)gA^+_{a'}\left(y_1^-\right)i\partial_{b'}\left(y_2\right)\psi\left(y_2\right)\right|p> +\right.\\
& + \frac{1}{4\pi}\int dx_1 dx_2\,\mathrm{Tr}\left(\left(\frac{H^{\mu\nu}_{b}\left(x_1 p, x_2 p\right)}{x_1 - x_2 - i\varepsilon} + \frac{H^{\mu\nu}_{b}\left(x_1 p, x_1 p\right)}{x_2 - x_1 + i\varepsilon}\right)\times\right.\\
& \times\int\frac{p^+dy_1^-}{2\pi}\frac{p^+dy_2^-}{2\pi}e^{i\left(x_1p^+\right)}e^{i\left(x_2p^+\right)\left(y_2^- - y_i^-\right)}\times\\
& \left.\times < p\left|\bar{\psi}(0)gA^+_{a'}\left(y_1^-\right)i\partial_{b'}\left(y_2\right)\psi\left(y_2\right)\right|p>
\end{aligned}
$$

where we used the following Ward identities:

$$H_a^{\mu\nu}(x_1p, x_2p)\cdot p^a = -\frac{H^{\mu\nu}(x_1p)}{x_2 - x_B - i\varepsilon} - \frac{H^{\mu\nu}(x_2p)}{x_1 - x_B + i\varepsilon}$$

$$H_{ab}^{\mu\nu}(x_1p, x_1p_1x_2p)\,p^a = -\frac{H_b^{\mu\nu}(x_1p, x_2p)}{x_2 - x_1 - i\varepsilon} - \frac{H_b^{\mu\nu}(x_2p, x_2p)}{x_1 - x_2 + i\varepsilon}$$

$$H_{ba}^{\mu\nu}(x_1p, x_1p, x_2p)\,p^a = -\frac{H_b^{\mu\nu}(x_1p, x_2p)}{x_1 - x_2 - i\varepsilon} - \frac{H_b^{\mu\nu}(x_1p, x_1p)}{x_2 - x_1 + i\varepsilon}$$

Now we likewise expand the gluon fields encapsulated in the matrix elements of $W_c^{\mu\nu}$:

$$W_c^{\mu\nu} = \frac{1}{4\pi}\int dx_1 dx dx_2\,\mathrm{Tr}\left(\hat{H}_{ab}^{\mu\nu}(x_1p, xp, x_2p)\int \frac{dy_1p^+}{2\pi}\frac{dy^-p^+}{2\pi}\frac{dy_2^-p^+}{2\pi}e^{i(x_1p^+)y_i^-}e^{i(xp^+)(y_2^- - y_1^-)}\times\right.$$
$$\times < p\left|\bar{\psi}(0)g^2\left(w_\alpha^\alpha\cdot A^{\alpha'}(y_1^-) - p^2\frac{A^+(y_1^-)}{p^+}\right)\cdot\left(w_{b'}^b A^{b'}(y_2^-) - p^b\frac{A^+(y_2^-)}{p^+}\right)\psi(y)\right|p>\Big) =$$
$$= \frac{1}{4\pi}\int dx_1 dx dx_2\,\mathrm{Tr}\left(\hat{H}_{ab}^{\mu\nu}(x_1p, xp, x_2p)\int \frac{dy_1}{2\pi}\frac{dy^-p^+}{2\pi}\frac{dy_2^-p^+}{2\pi}e^{i(x_1p^+)y_i^-}e^{i(xp^+)(y_2^- - y_1^-)}\times\right.$$
$$\times < p\left|\bar{\psi}(0)g^2 w_{\alpha'}^\alpha w_{b'}^b A^{\alpha'}(y_1^-)\,A^{b'}(y_2^-)\,\psi(y)\right|p>\Big) +$$
$$+\frac{1}{4\pi}\int dx_1 dx dx_2\,\mathrm{Tr}\left(\left(\frac{H_{\mu\nu}^\alpha(x_1p, xp)}{x_2 - x_1 - i\varepsilon} - \frac{H_{\mu\nu}^\alpha(x_2p, x_p)}{x_1 - x_2 + i\varepsilon}\right)\int \frac{dy_1p^+}{2\pi}\frac{dy^-p^+}{2\pi}\frac{dy_2^-p^+}{2\pi}e^{i(x_1p^+)y_i^-}e^{i(xp^+)(y_2^- - y_1^-)}\times\right.$$
$$\times < p\left|\bar{\psi}(0)g^2 A^+(y_1^-)\,w_{b'}^b A^{b'}(y_2^-)\,\psi(y_2^-)\right|p>\Big) +$$
$$+\frac{1}{4\pi}\int dx_1 dx dx_2\,\mathrm{Tr}\left(\left(\frac{H_{\mu\nu}^\alpha(x_1p, x_2p)}{x - x_2 - i\varepsilon} - \frac{H_{\mu\nu}^\alpha(x_1p, xp)}{x_2 - x + i\varepsilon}\right)\int \frac{dy_1p^+}{2\pi}\frac{dy^-p^+}{2\pi}\frac{dy_2^-p^+}{2\pi}e^{i(x_1p^+)y_i^-}e^{i(xp^+)(y_2^- - y_1^-)}\times\right.$$
$$\times < p\left|\bar{\psi}(0)g^2 w_{a'}^a A^{\alpha'}(y_1^-)\,A^+(y_2^-)\,\psi(y_2^-)\right|p>\Big) +$$
$$+\frac{1}{4\pi}\int dx_1 dx dx_2\,\mathrm{Tr}\left(\left(\frac{H^{\mu\nu}(x_1p)}{(x - x_B - i\varepsilon)(x_2 - x_1 - i\varepsilon)} + \frac{H^{\mu\nu}(x_2p)}{(x - x_B - i\varepsilon)(x_1 - x_2 + i\varepsilon)} + \right.\right.$$
$$\left.+\frac{H^{\mu\nu}(xp)}{(x_1 - x_B + i\varepsilon)(x_2 - x_1 - i\varepsilon)} + \frac{H^{\mu\nu}(xp)}{(x_2 - x_B + i\varepsilon)(x_1 - x_2 + i\varepsilon)}\right)\times$$
$$\left.\times\int \frac{dy_1^-}{2\pi}\frac{dy_2^-}{2\pi}\frac{dy^-p^+}{2\pi}\quad\left\langle p\left|\bar{\psi}(0)g^2 A^+(y_1^-)\,A^+(y_2^-)\,\psi(y)\right|p\right\rangle\right.$$

Ward identities used above:

$$H_{ab}^{\mu\nu}(x_1p, xp, x_2p)\,p^\alpha = -\frac{H_b^{\mu v}(x_1p, xp)}{x_2 - x_1 - i\varepsilon} - \frac{H_b^{\mu v}(x_2p_1, xp)}{x_1 - x_2 + i\varepsilon}$$

$$H_{ab}^{\mu\nu}(x_1p, xp, x_2p)\,p^b = -\frac{H_a^{\mu\nu}(x_1p, x_2p)}{x - x_2 - i\varepsilon} - \frac{H_a{}^{\mu\nu}(x_1p, xp)}{x_2 - x + i\varepsilon}$$

$$\frac{H_b^{\mu\nu}(x_1, x_1p)}{x_2 - x_1 - i\varepsilon}p^b = \left(-\frac{H^{\mu\nu}(x_1p)}{x - x_B - i\varepsilon} - \frac{H^{\mu v}(xp)}{x_1 - x_B + i\varepsilon}\right)\frac{1}{x_2 - x_1 - i\varepsilon}$$

$$\frac{H_b{}^{\mu v}(x_2p, xp)}{x_1 - \lambda_2 + i\varepsilon}p^b = \left(-\frac{H^{\mu v}(x_2p)}{x - x_B - i\varepsilon} - \frac{H^{\mu\nu}(xp)}{x_2 - x_B + i\varepsilon}\right)\frac{1}{x_1 - x_2 + i\varepsilon}$$

6.6 Finally: Colour gauge invariance.

Now the result of our actions can become clear and the back to back refinements of the Hadronic Tensor corrections to showcase their substance. Indeed their current form allows for combinations between parts of the different power corrections with each other, and for the emergence of gauge links which make colour invariance manifest.

To do this I will first combine the first term of $W_a^{\mu\nu}$, in which I will assign the name $M_1^{\mu\nu}$ and the fourth term of $W_b^{\mu\nu}$ which I will call $\Lambda_{4\alpha}^{\mu\nu}$ in the following.

$M_1^{\mu\nu}$	$\frac{1}{4\pi}\int dx\,\mathrm{Tr}\left(\widehat{H}^{\mu\nu}(xp)\cdot\int\frac{p^+dy^-}{2\pi}e^{i(xp^+)y^-}\langle p\vert\overline{\psi}(0)\psi(y^-)\vert p\rangle\right)$
$\Lambda_{4\alpha}^{\mu\nu}$	$\frac{1}{4\pi}\int dx_1dx_2\,\mathrm{Tr}\left(\left(\frac{H^{\mu v}(x_1p)}{x_2-x_B-i\varepsilon}+\frac{H^{\mu\nu}(x_2p)}{x_1-x_B+i\varepsilon}\right)\times\right.$ $\times\int\frac{p^+dy_1^-}{2\pi}\frac{p^+dy_2^-}{2\pi}e^{i(x_1p^+)}e^{i(x_2p^+)(y_2^--y_i^-)}\times$ $\left.\times<p\left\vert\bar{\psi}(0)gA_{a'}^+(y_1^-)\,\psi(y_2)\right\vert p>\right)$

For the sake of simplicity in our process, and only for a brief fraction of our procedure, I will rescale the integration variable as $\lambda_i = y_i^- p^+$:

$$\begin{aligned}\Lambda_{(4\alpha)}^{\mu\nu} = &\frac{1}{4\pi}\int dx_1dx_2\int\frac{d\lambda_1}{2\pi}\frac{d\lambda_2}{2\pi}\frac{1}{p^+}\,\mathrm{Tr}\left(\left(H^{\mu\nu}(x_1p)\,\frac{1}{x_2-x_B-i\varepsilon}\right)\times\right.\\ &\times e^{i\lambda_1x_1}e^{i(\lambda_2-\lambda_1)x_2}<p\left\vert\bar{\psi}(0)gA^+(\lambda_1^-)\,\psi(\lambda_2^-)\right\vert p>\Big)\\ &+\frac{1}{4\pi}\int dx_1dx_2\int\frac{d\lambda_1}{2\pi}\frac{d\lambda_2}{2\pi}\frac{1}{p^+}\,\mathrm{Tr}\left(\left(H^{\mu v}(x_2p)\,\frac{1}{x_1-x_B+i\varepsilon}\right)\times\right.\\ &\left.\times e^{i\lambda_1x_1}e^{i(\lambda_2-\lambda_1)x_2}<p\left\vert\bar{\psi}(0)gA^+(\lambda_1^-)\,\psi(\lambda_2^-)\right\vert p>\right)\Big)\end{aligned}$$

Now we replace the hard part with its collinear limit estimated previously:

$$H_{\mu v}(xp) = \gamma_\mu(x\not{p}+\not{q})\gamma_v(2\pi)\frac{x_B}{Q^2}\delta(x-x_B)$$

There is no deeper underlying reason behind this subtitution besides of the technical assistance offered in later steps from the delta function.

Therefore:

$$\Lambda^{\mu\nu}_{(4\alpha)} = \frac{1}{4\pi}\int dx_1 dx_2 \int \frac{d\lambda_1}{2\pi}\frac{d\lambda_2}{2\pi}\frac{1}{p^+}\,\mathrm{Tr}\left(\left(\gamma_\mu(x_1\not{p}+\not{q})\gamma_v(2\pi)\frac{x_B}{Q^2}\delta\left(x_1-x_B\right)\frac{1}{x_2-x_B-i\varepsilon}\right)\times\right.$$
$$\left.\times\, e^{i\lambda_1 x_1}e^{i(\lambda_2-\lambda_1)x_2} < p\left|\bar{\psi}(0)gA^+\left(\lambda_1^-\right)\psi\left(\lambda_2^-\right)\right|p>\right) +$$
$$+\frac{1}{4\pi}\int dx_1 dx_2 \int \frac{d\lambda_1}{2\pi}\frac{d\lambda_2}{2\pi}\frac{1}{p^+}\,\mathrm{Tr}\left(\left(\gamma_\mu(x_2\not{p}+\not{q})\gamma_v(2\pi)\frac{x_B}{Q^2}\delta\left(x_2-x_B\right)\frac{1}{x_1-x_B-i\varepsilon}\right)\times\right.$$
$$\left.\times e^{i\lambda_1 x_1}e^{i(\lambda_2-\lambda_1)x_2} < p\left|\bar{\psi}(0)gA^+\left(\lambda_1^-\right)\psi\left(\lambda_2^-\right)\right|p>\right)$$

Before we secure colour gauge invariance, some technicalities must be fixed. In particular we need to, somehow emerge some "Wilson line" type object which will ensure the gauge invariance, while simultaneously bring the hard parts in the exact same form as in $W_a^{\mu\nu}$ to combine the terms. To do this, except from an argument transformation, we have to get rid of the denominators we inherited from the Ward identities. The following line of thinking, involves the use of the theta step function definition, as it includes these type of denominators (so we can dispose them) and provides a path ordering necessary for any gauge link we aspire to construct for colour gauge invariance.

The θ function ploy

From the definition of the step function,

$$\theta(\mp\lambda) = \mp\int\frac{dx}{2\pi i}\frac{e^{i\lambda x}}{x\pm i\varepsilon} = \pm\int\frac{dx}{2\pi i}\frac{e^{-i\lambda x}}{\lambda\mp i\varepsilon}$$

we absorb inspiration for the trick :

$$\theta\left(\lambda_1\right) = -\frac{1}{2\pi i}\int dx_1\frac{e^{i\lambda_1(x_1-x_\beta)}}{x_1-x_\beta+i\varepsilon}\Leftrightarrow$$
$$\Leftrightarrow\int dx_1\frac{e^{i\lambda_1 x_1}}{x_1-x_B+i\varepsilon} = -2\pi i\theta\left(\lambda_1\right)e^{i\lambda_1 x_B}$$

Likewise:

$$\theta\left(\lambda_2-\lambda_1\right) = \int\frac{dx_2}{2\pi i}\frac{e^{i(x_2-x_B)(\lambda_2-\lambda_1)}}{x_2-x_B-i\varepsilon}\Leftrightarrow$$
$$\Leftrightarrow\int dx_2\frac{e^{ix_2(\lambda_2-\lambda_1)}}{x_2-x_B-i\varepsilon} = 2\pi i\cdot\theta\left(\lambda_2-\lambda_1\right)e^{ix_B(\lambda_2-\lambda_1)}$$

We now identify and replace the denominators, as well as the exponentials that are not similar with the expression of $M_{1a}^{\mu\nu}$. Further to that, appearence of theta functions eventually will lead to the path ordering required for building Wilson lines. Replacing the integrals and integrating over the delta functions we read:

$$\begin{aligned}
\Lambda_{4b}^{\mu\nu} &= \frac{1}{4\pi}\int dx_1 dx_2 \int \frac{d\lambda_1}{2\pi}\frac{d\lambda_2}{2\pi}\frac{1}{p^+}\,\mathrm{Tr}\left(\left(\gamma_\mu(x_1\not{p}+\not{q})\gamma_v(2\pi)\frac{x_B}{Q^2}\delta\left(x_1-x_B\right)\frac{1}{x_2-x_B-i\varepsilon}\right)\times\right.\\
&\left.\times\, e^{i\lambda_1 x_1}e^{i(\lambda_2-\lambda_1)x_2} < p\left|\bar{\psi}(0)gA^+\left(\lambda_1^-\right)\psi\left(\lambda_2^-\right)\right|p>\right) +\\
&+\frac{1}{4\pi}\int dx_1 dx_2 \int \frac{d\lambda_1}{2\pi}\frac{d\lambda_2}{2\pi}\frac{1}{p^+}\,\mathrm{Tr}\left(\left(\gamma_\mu(x_2\not{p}+\not{q})\gamma_v(2\pi)\frac{x_B}{Q^2}\delta\left(x_2-x_B\right)\frac{1}{x_1-x_B-i\varepsilon}\right)\times\right.\\
&\left.\times e^{i\lambda_1 x_1}e^{i(\lambda_2-\lambda_1)x_2} < p\left|\bar{\psi}(0)gA^+\left(\lambda_1^-\right)\psi\left(\lambda_2^-\right)\right|p>\right) =\\
&= \frac{1}{4\pi}\int dx_1 \int \frac{d\lambda_1}{2\pi}\frac{d\lambda_2}{2\pi}\frac{1}{p^+}\,\mathrm{Tr}\left(\gamma_\mu(x_1\not{p}+\not{q})\gamma_v(2\pi)\frac{x_B}{Q^2}\delta\left(x_1-x_B\right)e^{i\lambda_1 x_1}e^{i(\lambda_2-\lambda_1)x_B}(2\pi)\theta\left(\lambda_2-\lambda_1\right)\times\right.\\
&\left.\times < p\left|\bar{\psi}(0)igA^+\left(\lambda_1^-\right)\psi\left(\lambda_2^-\right)\right|p>\right) -\\
&-\frac{1}{4\pi}\int dx_2 \int \frac{d\lambda_1}{2\pi}\frac{d\lambda_2}{2\pi}\frac{1}{p^+}\,\mathrm{Tr}\left(\gamma_\mu(x_2\not{p}+\not{q})\gamma_v(2\pi)\frac{x_B}{Q^2}\delta\left(x_2-x_B\right)e^{i\lambda_1 x_B}e^{i(\lambda_2-\lambda_1)x_2}(2\pi)\theta\left(\lambda_1\right)\times\right.\\
&\left.\times < p\left|\bar{\psi}(0)igA^+\left(\lambda_1^-\right)\psi\left(\lambda_2^-\right)\right|p>\right) =\\
&= \frac{1}{4\pi}\int \frac{d\lambda_2}{2\pi}\frac{1}{p^+}\,\mathrm{Tr}\left(\gamma_\mu(x_B\not{p}+\not{q})\gamma_v(2\pi)\frac{x_B}{Q^2}e^{i\lambda_1 x_B} < p\left|\bar{\psi}(0)\int d\lambda_1 ig\theta\left(\lambda_2-\lambda_1\right)A^+\left(\lambda_1^-\right)\psi\left(\lambda_2^-\right)\right|p>\right) -\\
&-\frac{1}{4\pi}\int \frac{d\lambda_2}{2\pi}\frac{1}{p^+}\,\mathrm{Tr}\left(\gamma_\mu(x_B\not{p}+\not{q})\gamma_v(2\pi)\frac{x_B}{Q^2}e^{i\lambda_1 x_B} < p\left|\bar{\psi}(0)\int d\lambda_1 ig\theta\left(\lambda_1\right)A^+\left(\lambda_1^-\right)\psi\left(\lambda_2^-\right)\right|p>\right) =\\
&= \frac{1}{4\pi}\int \frac{d\lambda_2}{2\pi}\frac{1}{p^+}\,\mathrm{Tr}\left(\gamma_\mu(x_B\not{p}+\not{q})\gamma_v(2\pi)\frac{x_B}{Q^2}e^{i\lambda_1 x_B}\times\right.\\
&\left.\times < p\left|\bar{\psi}(0)\int_{-\infty}^{\infty} d\lambda_1 ig\left(\theta\left(\lambda_2-\lambda_1\right)-\theta\left(\lambda_1\right)\right)A^+\left(\lambda_1^-\right)\psi\left(\lambda_2^-\right)\right|p>\right) =\\
&= \frac{1}{4\pi}\int \frac{d\lambda_2}{2\pi}\frac{1}{p^+}\,\mathrm{Tr}\left(\gamma_\mu(x_B\not{p}+\not{q})\gamma_v(2\pi)\frac{x_B}{Q^2}e^{i\lambda_1 x_B} < p\left|\bar{\psi}(0)\int_0^{\lambda_2} d\lambda_1 igA^+\left(\lambda_1^-\right)\psi\left(\lambda_2^-\right)\right|p>\right)
\end{aligned}$$

Before finalizing the analysis we take care of some details of technical nature:

- **Restore:** $\lambda_i = y_i^- p^+$
- **Include unity:**$1 = \int dx\delta\left(x-x_B\right)$ Then we can restore the hard function from which we temporarily borrowed its delta function and seizing the opportunity assign to the hard function of Wb the argument of the hard function of Wa.
- **Rename variables:**$y_1^- \longrightarrow y'^-$ and $y_2^- \longrightarrow y^-$, also in order to match the variables of $M_1^{\mu\nu}$
- **Express the gluon field in its adjoint representation.** That is not necessary but on the grounds that we are seeking to create Wilson line type objects, we might as well include the colour generators for resemblance.
- **Change the order of the integration limits**, and add an appropriate minus sign.

Finally I use

$$1 = \int d\zeta\delta\left(\zeta-\zeta_N\right)$$

and restore the original form of the hard function, which includes the dirac delta. The exponentials are also fixed and after we restore $\xi = y_i\cdot l^+$ and invert the integration boundaries, a perfect form for this contributions has emerged:

$$\Lambda_{4b}^{\mu\nu} = \frac{1}{4\pi}\int dx\,\mathrm{Tr}\left(\widehat{H}^{\mu\nu}(xp)\int\frac{p^+dy^-}{2\pi}e^{i(xp^+)y^-}\langle p|\overline{\psi}(0)\mathrm{P}\left[-ig\int_{y^-}^{0}\mathrm{d}y'^-A_B^+(y'^-)\,t^B\right]\psi(y^-)|p\rangle\right)$$

Combined with the lower order contribution:

$$W_\alpha^{\mu\nu} = \frac{1}{4\pi}\int dx\,\mathrm{Tr}\left(\widehat{H}^{\mu\nu}(xp)\int\frac{p^+dy^-}{2\pi}e^{i(xp^+)y^-}\langle p|\overline{\psi}(0)\left(1-\mathrm{P}\left[-ig\int_{y^-}^{0}\mathrm{d}y'^-A_B^+(y'^-)\,t^B\right]y\right)\psi(y^-)|p\rangle\right) =$$
$$= \frac{1}{4\pi}\int dx\,\mathrm{Tr}\left(\widehat{H}^{\mu\nu}(xp)\cdot\int\frac{p^+dy^-}{2\pi}e^{i(xp^+)y^-}\langle p|\overline{\psi}(0)\mathrm{P}e^{\left[-ig\int_{y^-}^{0}\mathrm{d}y'^-A_B^+(y'^-)t^B\right]}\psi(y^-)|p\rangle\right)$$

$$W_\alpha^{\mu\nu} = \frac{1}{4\pi}\int dx\,\mathrm{Tr}\left(\widehat{H}^{\mu\nu}(xp)\cdot\int\frac{p^+dy^-}{2\pi}e^{i(xp^+)y^-}\langle p|\overline{\psi}(0)\mathrm{P}e^{\left[-ig\int_{y^-}^{0}\mathrm{d}y'^-A_B^+(y'^-)t^B\right]}\psi(y^-)|p\rangle\right)$$

For future simplicity as the subleading power calculations tend to get messier, we make use of the following definition for the gauge link

$$\mathcal{L}(y^-,y_2^-) = 1+ig\int_{y^-}^{y_2^-}dy_1^-A^+\left(0,y_1^-,\overrightarrow{0}_\perp\right)+(ig)^2\int_{y^-}^{y_2^-}dy_1^-\int_{y^-}^{y_1^-}dy'A^+\left(0,y_1^-,\overrightarrow{0}_\perp\right)A^+\left(0,y',\overrightarrow{0}_\perp\right)$$

$$\widetilde{W_\alpha}^{\mu\nu} = \frac{1}{4\pi}\int dx\,\mathrm{Tr}\left(\widehat{H}^{\mu\nu}(xp)\cdot\int\frac{p^+dy^-}{2\pi}e^{i(xp^+)y^-}\mathcal{L}(0,y^-)\langle p|\overline{\psi}(0)\psi(y^-)|p\rangle\right)$$

We now have achieved colour gauge invariance following works as [42], [23]. One would note that in axial gauge the gauge link providing the invariance would be simply 1. The next power contribution is calculated exactly the same way and the only trick needed is inserting and extra integration variable as

$$1 = \int dx\delta(x-x_1) = \frac{1}{2\pi}\int dxdy\exp\{(i(x-x_1)y)\}$$

so we can combine terms of different dimension in covariant derivatives. The reason we did not use something similar here is of course the p^a's accompanying the longitudinal components of the gauge fields, reducing the dimension of the Hard Part effectively via the Ward Takahashi identities.
Summing up what we achieved so far:

$$\begin{aligned}W^{\mu\nu} =& W_{\mathrm{a}}^{\mu\nu}+W_{\mathrm{b}}^{\mu\nu}+W_{\mathrm{c}}^{\mu\nu}\\ =&\frac{1}{4\pi}\int\mathrm{d}x\,\mathrm{Tr}\left[\hat{H}^{\mu\nu}(xp)\hat{T}(x)\right]\\ &+\frac{1}{4\pi}\int\mathrm{d}x_1\,\mathrm{d}x_2\,\mathrm{Tr}\left[\hat{H}_\alpha^{\mu\nu}(x_1p,x_2p)\,\omega_{\alpha'}^{\alpha}\hat{T}^{\alpha'}(x_1,x_2)\right]\\ &+\frac{1}{4\pi}\int\mathrm{d}x_1\,\mathrm{d}x\,\mathrm{d}x_2\,\mathrm{Tr}\left[\hat{H}_{\alpha\beta}^{\mu\nu}(x_1p,xp,x_2p)\,\omega_{\alpha'}^{\alpha}\omega_{\beta'}^{\beta}\hat{T}^{\alpha'\beta'}(x_1,x,x_2)\right]\end{aligned}$$

$$
\begin{aligned}
\hat{T}(x) = \int \frac{p^+ \mathrm{d}y^-}{2\pi} \mathrm{e}^{ixp^+y^-} \langle p|\mathrm{T}\{\bar{\psi}(0) \\
\times P\exp\left[-ig\int_{y^-}^{0} \mathrm{d}y'^- A_B^+(y'^-)\, t^B\right]\psi(y^-)\Big\}|p\rangle \\
\hat{T}^\alpha(x_1,x_2) = \int \frac{p^+\mathrm{d}y_1^-}{2\pi}\frac{p^+\mathrm{d}y_2^-}{2\pi} \mathrm{e}^{ix_1p^+y_1^-}\mathrm{e}^{i(x_2-x_1)p^+y_2^-}\langle p|\mathrm{T}\{\bar{\psi}(0) \\
\times P\exp\left[-ig\int_{y_2^-}^{0} \mathrm{d}y_2'^- A_B^+\left(y_2'^-\right)t^B\right] D^\alpha(y_2^-) \\
\times P\exp\left[-ig\int_{y_1^-}^{y_2^-} \mathrm{d}y_1'^- A_C^+(y_1'^-)\, t^C\right]\psi(y_1^-)\Big\}|p\rangle \\
\hat{T}^{\alpha\beta}(x_1,x,x_2) = \int \frac{p^+\mathrm{d}y_1^-}{2\pi}\frac{p^+\mathrm{d}y_2^-}{2\pi}\frac{p^+\mathrm{d}y^-}{2\pi} \mathrm{e}^{ix_1p^+y_1^-}\mathrm{e}^{i(x-x_1)p^+y^-}\mathrm{e}^{-i(x-x_2)p^+y_2^-} \\
\times \left\langle p\right|\mathrm{T}\left\{\bar{\psi}(0)D^\alpha(y_2^-)\, D^\beta(y^-)\,\psi(y_1^-)\right\}\left|p\right\rangle .
\end{aligned}
$$

6.7 Electromagnetic Gauge Invariance

With color gauge invariance secured, we can still find reasons for concern in our factorized definitions. In particular, although we have reformulated the hard part in terms of dominant momenta, ensuring they comprise appropriate short-distance elements, we have not been equally meticulous with the composition of the matrix elements. Consequently, it is still possible to identify short-distance contributions that, by definition, belong to the hard part.

Moreover the matrix elements being matrices in spinor space should be reduced and electromagnetic gauge invariance would disentangle them, also allowing for further mixing of the terms and simplifying their factorization.

To that end, we will introduce some new physical objects, the special propagator and the contact term. A special propagator is defined as the part of a normal propagator which does not propagate. What that really means and how it is useful will be discussed in the following.

Previously, we observed that leading-power contributions emerge when the parton momenta entering the hard part are all on-shell and collinear. Consequently, we expanded around the collinear component of their momenta and considered subleading contributions from non-collinear partons. We will demonstrate that even when on-shell and collinear partons enter the hard part, there remains potential for additional subleading contributions:

- Because the loop propagators have a **contact term**.
- If the loop propagators have **a non vanishing** intrinsic transverse component of the parton momenta.

Notation used below:

We notice $k^2 = 2k_-k_+ - k_\perp^2 \to k\bar{\eta} = \frac{(k^2+k_\perp^2)}{2k\eta}$. Replacing this in the Sudakov decomposition of the parton momentum $k^\mu = xp^\mu + \frac{k^2+k_\perp^2}{2k\cdot n}n^\mu + k_\perp^\mu$.

We express the momentum k as $\boxed{k^\mu = \hat{k}^\mu + \frac{k^2}{2k\cdot n}n^\mu}$, where $\hat{k}$ is an on-shell projection of the momentum:

- $\hat{k}^2 = 0$
- $\hat{k} = xp^\mu + \frac{k_\perp^2}{2k\cdot n}n^\mu + k_\perp^\mu$

Using the above, we can express a quark propagator of momentum k in the matrix element as:

$$S(k) \equiv \frac{i\gamma\cdot k}{k^2+i\epsilon} = \frac{i\gamma\cdot n}{2k\cdot n} + \frac{i\gamma\cdot\hat{k}}{k^2+i\epsilon}$$

6.7.1 The Special Propagator and the Contact Term

We define a contact term as one that lacks spatial separation in the + light-cone coordinate and, in our context, matches the propagator term $\frac{i\gamma\cdot n}{2k\cdot n}$, which does not propagate and is thus identified as a special propagator. This term, being extremely short-ranged, should be included in the hard part of the factorized hadronic tensor. From a dimensional analysis perspective, transferring a special propagator and its directly connected vertex to the hard part is equivalent to shifting a dimension unit of $\frac{1}{\text{Energy}}$ from the matrix element to the hard part. Consequently, the dimensionally enhanced hard part will contribute one twist higher. To achieve the twist 4 contribution, we need to transfer an appropriate number of such combinations from the matrix elements to the hard parts.

Previously, estimating the Hard part in the collinear limit led us to the conclusion that its value is either proportional to γp or $\gamma \eta$.

More educationally the Hard part when estimated in the leading power is either proportional to the collinear $\gamma \cdot \overline{\eta}$ or to the anticollinear directioned momentum $\gamma \cdot \eta$.

Let's imagine the following configuration : A quark propagator decomposed into a special and a collinear part, with origins in the matrix element, contracts with the collinearly evaluated hard part.

The hard part's term proportional to $\gamma \eta$ annihilates the special propagator term since $\eta^2 = 0$.

On the other hand when contracting the term proportional to γp with the decomposed propagator, annihilates the collinear component and has as a result a higher-twist contribution.

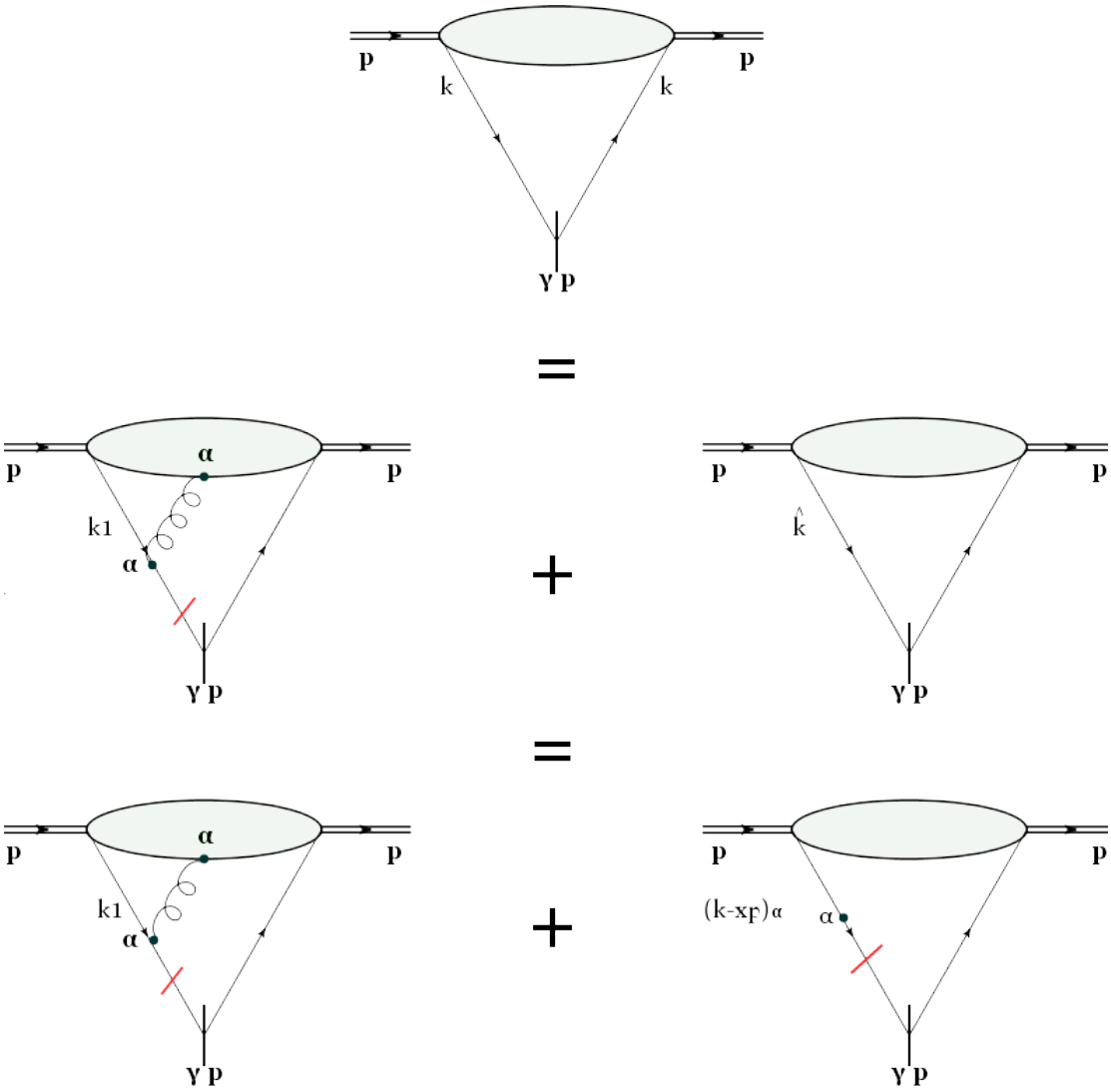

Figure 6.5: Result of contracting a quark propagator with γp

.

We need to understand the math involved in order to realise how this works: Contracting γp from the left with the quark propagator and using the parton momentum decomposition we mentioned we are lead to what is shown in 6.5 first equality:

$$\gamma \cdot p \cdot \frac{i\gamma k}{k^2} = \gamma \cdot p \cdot \left(\frac{i\gamma n}{2k \cdot n} + \frac{i\gamma \hat{k}}{k^2} \right)$$

First term: The contact term.

We discussed before about the contact term offering no space separation in the light-cone coordinate. Consequently such terms in the loop propagators as well as the vertices which connect them with the matrix element, should be moved in the Hard part. One can see this in 6.5, where the contact term (vertical line) and the quark gluon vertex in the first part of the right side of the figure are extracted from the matrix element and along with a unit of dimension they are taken to the Hard part, allowing this way, for a high twist contribution. The matrix element now is a three-parton target matrix element.

Feynman rule of contact term 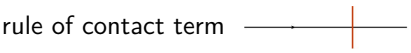 $= \frac{i\gamma\eta}{2k\eta}$

Contact term analysis, from J.Qiu [7]

To understand what is the meaning of a contact term not propagating in the lightcone direction we can study the light-cone coordinate dependence of a propagator of momentum k propagating from a vertex at light-cone coordinate y_1^+ to another vertex at y_2^+.

After we apply a Fourier transformation to pick up only the light-cone position coordinate we have we consider transformation

$$\frac{1}{2\pi}\int dk_- e^{-ik_-(y_1-y_2)_+}\frac{i\gamma\cdot k}{k^2+i\epsilon}$$
$$=\delta\left(y_1^+-y_2^+\right)\frac{i\gamma_+}{2k_+}+\theta\left(y_1^+-y_2^+\right)\frac{\gamma\cdot\hat{k}}{2k_+}$$
$$\times e^{-i\left(k_T^2/2k_+\right)\left(y_1^+-y_2^+\right)},$$

We can see how the special propagator has a delta function and does not propagate.

Second remainder term: The on shell remainder of the propagator

We now inspect the second term and what the effects of the contraction of γp are, on the ”on-shell” propagator:

$$
\begin{aligned}
&\gamma\cdot p\cdot\tfrac{i\gamma\hat{k}}{k^2}=\gamma\cdot p\tfrac{i\gamma\hat{k}}{k^2}i\gamma\cdot k\tfrac{i\gamma\cdot k}{k^2}=\\
&=\gamma\cdot pi\gamma\hat{k}\left(\tfrac{i\gamma n}{2k\cdot n}+\tfrac{i\gamma\hat{k}}{k^2}\right)\tfrac{i\gamma\cdot k}{k^2}=\\
&=\gamma\cdot pi\gamma\hat{k}\tfrac{i\gamma\eta}{2k\cdot n}\tfrac{i\gamma\cdot k}{k^2}=\\
&=\gamma\cdot pi\gamma\cdot\left(-xp^\mu+\tfrac{k_\perp^2}{2k\cdot n}+k_\perp^\mu\right)\tfrac{i\gamma\eta}{2k\cdot n}\tfrac{i\gamma\cdot k}{k^2}=\\
&=\gamma\cdot pi\left(\tfrac{i\gamma\cdot k_\perp\gamma\cdot n}{2kn}\right)\tfrac{i\gamma\cdot k}{k^2}=\\
&=\gamma\cdot pi\left(+i\tfrac{\gamma\cdot\eta\gamma\cdot k_\perp}{2k\cdot n}\right)\tfrac{i\gamma k}{k^2}=\\
&=\gamma\cdot p\tfrac{i\gamma\cdot n}{2k\cdot n}i\gamma_a\left(k_\perp^a+\left(\tfrac{k^2+k_\perp^2}{2k\cdot n}\right)\right)\tfrac{i\gamma k}{k^2}=\\
&=\gamma\cdot p\tfrac{i\gamma\cdot\eta}{2k\cdot n}i\gamma_\alpha\cdot(k-xp)^\alpha\tfrac{i\gamma k}{k^2}
\end{aligned}
$$

Using this also, we prove that the insertion of the special propagator does not interfere with gauge invariance.

We have used the following:

- First equality: $i\gamma\cdot k\cdot i\gamma\cdot k=k^2$
- Second equality: Definition of $S(k)$ expansion
- Third equality: $\hat{k}^2=0$
- Fourth equality: Definition of $\hat{k}$
- Fifth equality and seventh equality: $\eta^2=0$ in denominators (freely add or delete terms including $\frac{1}{2k\eta}$)
- Sixth equality: $\gamma\cdot\eta\gamma\cdot k_\perp=\gamma\cdot k_\perp\gamma\cdot\eta$
- Eighth equality: Definition of k^μ

All together:

$$\gamma\cdot p\left[\tfrac{i\gamma\cdot k}{k^2+i\epsilon}\right]=\gamma\cdot p\left(\tfrac{i\gamma\cdot n}{2k\cdot n}\right)\left[1+i\gamma_\alpha\cdot(k-xp)^\alpha\tfrac{i\gamma\cdot k}{k^2+i\epsilon}\right]$$

Accordingly:

$$\left[\tfrac{i\gamma\cdot k}{k^2+i\epsilon}\right]\gamma\cdot p=\left[1+\tfrac{i\gamma\cdot k}{k^2+i\epsilon}i\cdot(k-xp)^\alpha\gamma_\alpha\right]\left(\tfrac{i\gamma\cdot n}{2k\cdot n}\right)\gamma\cdot p$$

The result above is exactly representing the second equality of 6.5.

To see how this works, we consider the single pull shown in figure 6.5.
The relevant contributions are of the form:

- $\frac{1}{4\pi}\int dxdx_1 \,\mathrm{Tr}\left(\left(H_\alpha^{\mu v}\left(xp,x_1p\right)M^\alpha\left(xp,x_1p\right)\right)\right)$
- $\frac{1}{4\pi}\int dx \,\mathrm{Tr}\left(\left(H_\alpha^{\mu v}\left(xp,xp\right)\left(k-xp\right)\right)^\alpha M^\alpha\left(xp\right)\right)$

with matrix element definitions:

- $M^\alpha\left(xp,x_1p\right) = \int p^+dyp^+dy_2^- e^{i(xp^+)y^-}e^{i(x_1p^+)(y_1^- - y^-)} \times$
  $\times < p \mid \psi(0)\left(-gA^\alpha\left(y_1^-\right)\right)\psi\left(y^-\right)|p>$
- $M^\alpha\left(xp\right) = \int dy^- e^{ixp^+y^-}\left\langle p\left|\bar{\psi}(0)\psi(y^-)\right|p\right\rangle$

The three following tricks, will lead to a combination of the two terms upon their application. We will show now how combining those two terms which originate from the same initial leading-power contribution will give a higher-twist contribution. The effect of the second part of the decomposed diagram 6.5 is replacing the gluon which emerges from the contact term in the left part of the same diagram by the corresponding covariant derivative.

First rephrase:

$$(k-xp)^{\alpha}\widehat{M}(xp) = \omega^{\alpha}_{\alpha'}k^{\alpha'}\widehat{M}(xp)$$
$$= \omega^{\alpha}_{\alpha'}\int dy^{-}e^{ixp^{+}y^{-}}\left\langle p\left|\bar{\psi}(0)\left(i\partial^{\alpha'}\right)\psi(y^{-})\right|p\right\rangle$$

Then use the fact that the second term of

$$\omega^{\alpha}_{\alpha'}A^{\alpha'}\left(y_1^{-}\right) = A^{\alpha}\left(y_1^{-}\right)n - \frac{p^{\alpha}}{p\cdot n}\cdot(n\cdot A)$$

vanishes if contracted with $\gamma\cdot p$.
As well as the identity

$$1 = \int dx_1\delta\left(x-x_1\right) = \int p^{+}dx_1\int\frac{dy_1^{-}}{2\pi}e^{iy_1^{-}(xp_{+}-x_1p_{+})},$$

and add the terms to obtain:

$$\int dxdx_1\left[\hat{H}_{\alpha}\left(xp,x_1p\right)\omega^{\alpha}_{\alpha'}\widehat{M}^{\alpha'}\left(x,x_1\right)\right]$$

$$\hat{M}^{\alpha}\left(x,x_1\right) = \int\frac{dy^{-}}{2\pi}\frac{dy_1^{-}}{2\pi}e^{iy_{-}\cdot\left(xp^{+}-x_1p^{+}\right)}e^{iy_1^{-}x_1p^{+}}\left\langle p\left|\bar{\psi}(0)D^{\alpha}\left(y^{-}\right)\psi\left(y_1^{-}\right)\right|p\right\rangle$$

where the covariant derivative is $\left(i\partial^{\alpha}-gt^{B}A^{\alpha}_{B}\right)$.

We achieve the same repeating the procedure for the right loop propagator concluding that the diagram in 6.5 is equivalent to the first diagram in 6.7. The hard part is the leading nontrivial high-twist short-distance contribution given by $[\widehat{H}(xp)\gamma\cdot p]$.

6.7.2 Dimensional Analysis: Picking twist-4 Contributions

Since the goal is to group power contributions up to and including $\frac{1}{Q^2}$ the number of contact terms we should use is fixed. The suppresion such a "pull" adds to the total is $\frac{1}{Q}$ and based on this argument I will explain how we pick the configuration:

If we consider quark propagators in the matrix elements on both sides of diagram 1, contraction with $\gamma\cdot p$ will pull two contact terms and as a consequence the dimensional enhancement of the hard part will be double. The new hard part can be read from the diagram a) in 6.6. The matrix element is precisely $\hat{T}^{\alpha\beta}(x_1,x,x_2)$ as calculated previously.

In the case of $H^{\mu\nu}_{\alpha}$ dimensional analysis restricts us to pick maximum one contact term and this can happen with two separate ways as shown in b) c) of 6.6. The matrix element is precisely $\hat{T}^{\alpha\beta}(x_1,x,x_2)$ in alignment with before.

Dimensional analysis, does not allow for a contact term pull in $H^{\mu\nu}_{\alpha\beta}$ if we are restricted to $\frac{1}{Q^2}$ contributions. In 6.6 the complete set of hard diagrams contributing to $\frac{1}{Q^2}$.

Overall we have grouped the leading twist-4 contributions to $W^{\mu\nu}$ in the form:

$$W^{\mu\nu'}_{\text{twist}-4} = \int \mathrm{d}x_1\,\mathrm{d}x\,\mathrm{d}x_2\,\mathrm{Tr}\left[\hat{H}^{\mu\nu'}_{\alpha\beta}\left(x_1p,xp,x_2p\right)\omega^{\alpha}_{\alpha'}\omega^{\beta}_{\beta'}\hat{T}^{\alpha'\beta'}\left(x_1,x,x_2\right)\right],$$

where the nonvanishing contributions to $\hat{H^{\mu\nu}_{\alpha\beta}}$ are depicted in 6.6.

In general dimensional analysis allows for even higher twist contributions as shown in 6.7. Nevertheless only the first three of them (the ones we discussed) correspond to non-vanishing contributions. In particular the fourth and fifth vanish because of a common factor $\gamma\cdot\eta\left(i\gamma_{\alpha}\right)\gamma\cdot\eta = 0$. Factors $\gamma\cdot\eta$ arise from special quark propagators and $i\gamma_{\alpha}$ from the quark gluon vertex. Moreover the three last

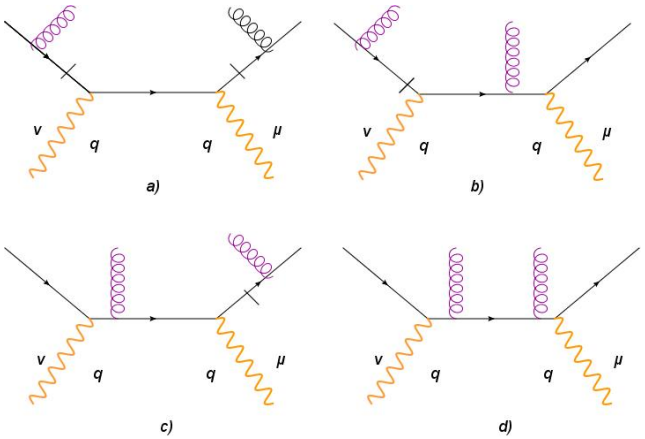

Figure 6.6: Non vanishing "hard" contributions to DIS in $\frac{1}{Q^2}$

ones that arise from [7] a special gluon propagator vanish because of common factor $\gamma \cdot \eta \gamma \cdot \eta = 0$. Here one $\gamma \cdot \eta$ is from a special quark propagator and the other from a special gluon propagator or a cut of a quark line.

6.7.3 A full justification for the final form of the higher twist contribution :

Working more the collinear limit of $\widehat{H}^{\mu\nu}$ replacing the virtual photon momentum $q = -xp + \frac{Q^2}{2x_B}$ becomes apparent that $H^{\mu\nu}$ is proportional to $\gamma^\mu (\gamma \cdot \eta) \gamma^\nu$.

$$
\begin{aligned}
&\widehat{H}^{\mu\nu}(xp) = \gamma^\mu (x \not{p} + \not{q}) \gamma^\nu \times \delta_+((x \not{p} + q)^2) = \\
&= \gamma^\mu (x \not{p} + \not{q}) \gamma^\nu \times (2\pi)\delta\left(-Q^2 + 2xp^+ \frac{Q^2}{2x_B p^+}\right) = \\
&= \gamma^\mu (x \not{p} + \not{q}) \gamma^\nu \times (2\pi)\delta\left(\frac{Q^2}{x_B}(x - x_B)\right) = \\
&= \gamma^\mu (x \not{p} + \not{q}) \gamma^\nu (2\pi) \frac{x_B}{Q^2} \delta(x - x_B) = \\
&= (2\pi)\gamma^\mu (\frac{\gamma \cdot \eta}{2}) \gamma^\nu \delta(x - x_B)
\end{aligned}
$$

The indices μ and ν can be expressed as a combination of [24]:

$$\hat{p}^\mu \hat{p}^\nu, \hat{p}^\mu \eta^\nu, \eta^\mu \hat{p}^\nu, \eta^\mu \eta^\nu,$$

$$d^{\mu\nu} = \hat{p}^\mu n^\nu + n^\mu \hat{p}^\nu - g^{\mu\nu},$$

[4] and

$$\hat{p} = \frac{p^\mu}{p \cdot \eta}.$$

We now limit the possible cases using $\eta^2 = 0$

- A hard part is proportional to $\gamma \cdot n$ when the indices μ and v are transverse.
- A hard part is proportional to $\gamma \cdot p$ when the indices are both equal to - (e.g., $\gamma^\mu = \gamma^- = \gamma \cdot \hat{p}$).

[4] ttransverse vector defined in following chapter

Thus, from figure 6.5 we observe $\gamma \cdot p$ contracting two loop propagators, pulling two special propagators and equal vertices from the matrix element, placing them in the hard part where they belong. The special propagator proportionality to $\gamma \cdot \eta$ and the property $(\gamma \cdot \eta)^2 = 0$ lead towards a twist-4 correction form as the one we found previously with the hard part calculated from the first Feynman diagram of figure 6.7.

$$W^{\mu v'}_{\text{twist}-4} = \int \mathrm{d}x_1 \, \mathrm{d}x \, \mathrm{d}x_2 \, \mathrm{Tr}\left[\hat{H}^{\mu l'}_{\alpha\beta}\left(x_1 p, xp, x_2 p\right) \omega^{\alpha}_{\alpha'} \omega^{\beta}_{\beta'} \hat{T}^{\alpha'\beta'}\left(x_1, x, x_2\right)\right]$$

Even simpler is to pick higher twist contributions from

$$W^{\mu\nu}_{\beta} = \frac{1}{4\pi} \int \mathrm{d}x_1 \, \mathrm{d}x_2 \, \mathrm{Tr}\left[\hat{H}^{\mu\nu}_{\alpha}\left(x_1 p, x_2 p\right) \omega^{\alpha}_{\alpha'} \hat{T}^{\alpha'}\left(x_1, x_2\right)\right]$$

as the γ_μ in the hard part can have only transverse componen :

- We cannot have $\gamma \cdot \hat{p}$ due to contraction with the projector as we proved already
- We cannot have $\gamma \cdot \eta$ due to $(\gamma \cdot \eta)^2 = 0$.

This implies $W^{\mu\nu}_{\beta}$ having only a higher twist contribution and no remainder term as the one W_α has.

Choosing a special propagator as usual and as illustrated in the second and third cases of figure 6.7 we obtain the higher power contribution in a same form but with a different hard part obtained from the second and third diagrams of figure 6.6.

$$W^{\mu v'}_{\text{twist}-4} = \int \mathrm{d}x_1 \, \mathrm{d}x \, \mathrm{d}x_2 \, \mathrm{Tr}\left[\hat{H}^{\mu l'}_{\alpha\beta}\left(x_1 p, xp, x_2 p\right) \omega^{\alpha}_{\alpha'} \omega^{\beta}_{\beta'} \hat{T}^{\alpha'\beta'}\left(x_1, x, x_2\right)\right]$$

Finally we consider power contributions $\frac{1}{Q^2}$ and as we elaborated this leaves no room for the special propagator methodology to be applied in the third part of the hadronic tensor corrections.

$$W^{\mu\nu}_{\mathsf{c}} = \frac{1}{4\pi} \int \mathrm{d}x_1 \, \mathrm{d}x \, \mathrm{d}x_2 \, \mathrm{Tr}\left[\hat{H}^{\mu\nu}_{\alpha\beta}\left(x_1 p, xp, x_2 p\right) \omega^{\alpha}_{\alpha'} \omega^{\beta}_{\beta'} \hat{T}^{\alpha'\beta'}\left(x_1, x, x_2\right)\right]$$

This is directly a twist-4 contribution in usual form, with the hard parts picked from the fourth Feynman diagram of Figure 9.

One could very strictly separate the name of the contributions from the first two expansion components as higher twist and the third one as kinematic $\frac{\Lambda^2}{Q^2}$ contribution. This, even if technically correct, except from providing intuition for the origin of the power corrections does not offer anything more in our procedure. Thus, and as in most of relevant literature, we contain all the $\frac{\Lambda^2}{Q^2}$ contributions in a single term labeled as twist-4. Therefore replacing what we found, in our expansion, we are led to a leading twist contribution from the $\gamma \cdot \eta$ part of the first term of the expansion, accompanied by a twist-4 contribution shaped as:

$$W^{\mu v'}_{\text{twist}-4} = \int \mathrm{d}x_1 \, \mathrm{d}x \, \mathrm{d}x_2 \, \mathrm{Tr}\left[\hat{H}^{\mu l'}_{\alpha\beta}\left(x_1 p, xp, x_2 p\right) \omega^{\alpha}_{\alpha'} \omega^{\beta}_{\beta'} \hat{T}^{\alpha'\beta'}\left(x_1, x, x_2\right)\right]$$

with the hard part being composed of all four diagrams of Figure 6.6.

A different but intuitive approach to prove this and the following can be found in [44] by J. Qiu and G. Sterman.

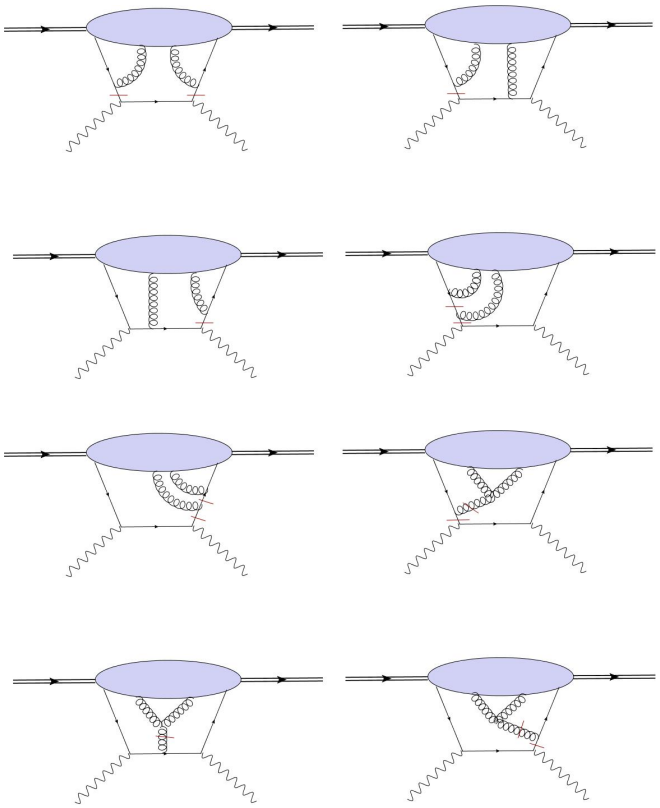

Figure 6.7: All dimensionally possible two-quark — two-gluon Feynman diagrams with special propagators and a higher twist contribution.

6.8 Decoupling of the spinor Trace

The final step of this $W^{\mu\nu}$ treatment is decoupling the hard short-distance part from the long-distance matrix elements in the spinor trace. As in [25][43], we decompose the matrix elements in the standard basis of gamma matrices $(1, \gamma_5, \gamma^\mu, \gamma^\mu\gamma_5, \sigma^{\mu\nu})$:

For massless quarks:

$$\widehat{M} = \gamma_\sigma \widehat{M}^\sigma + \gamma_\sigma\gamma_5 \widehat{\widehat{M}}^\sigma$$

Technically, we Fierz decompose the trace:

$$\begin{aligned}
&\mathrm{Tr}\Big[\widehat{H}^{\mu\nu}_{\alpha\beta}(x_2 p, xp, x_1 p)\widehat{M}^{\alpha\beta}(x_2, x, x_1)\Big] \\
&\quad = \frac{1}{4}\,\mathrm{Tr}\Big[\widehat{H}^{\mu\nu}_{\alpha\beta}(x_2 p, xp, x_1 p)\gamma_\sigma\Big]\,\mathrm{Tr}\Big[\gamma^\sigma \widehat{M}^{\alpha\beta}(x_2, x, x_1)\Big] \\
&\qquad + \frac{1}{4}\,\mathrm{Tr}\Big[\widehat{H}^{\mu\nu}_{\alpha\beta}(x_2 p, xp, x_1 p)\gamma_5\gamma_\sigma\Big]\,\mathrm{Tr}\Big[\gamma^\sigma\gamma_5 \widehat{M}^{\alpha\beta}(x_2, x, x_1)\Big]
\end{aligned}$$

Applying the decomposition to our higher-twist contribution, we now have:

$$
\begin{aligned}
&W^{\mu\nu}|_{\text{twist 4}} = \\
&\int dx_2\, dx\, dx_1 \left\{ H^{\mu\nu}_{\alpha\beta\sigma}\left(x_2 p, xp, x_1 p\right) \omega^{\alpha}_{\alpha'} \omega^{\beta}_{\beta} C^{\sigma\alpha'\beta}\left(x_2, x, x_1\right) \right. \\
&\left. + \widetilde{H}^{\mu\nu}_{\alpha\beta\sigma}\left(x_2 p, xp, x_1 p\right) \omega^{\alpha}_{\alpha'} \omega^{\beta}_{\beta} \widetilde{C}^{\sigma\alpha'\beta'}\left(x_2, x, x_1\right) \right\}_{\text{twist 4}}
\end{aligned}
$$

where,

$$
\begin{aligned}
H^{\mu\nu}_{\alpha\beta\sigma}\left(x_2 p, xp, x_1 p\right) &= \operatorname{Tr}\left[\widehat{H}^{\mu\nu}_{\alpha\beta}\left(x_2 p, xp, x_1 p\right) \gamma_\sigma \right], \\
C^{\sigma\alpha\beta}\left(x_2, x, x_1\right) &= \frac{1}{4} \operatorname{Tr}\left[\gamma^\sigma \widehat{M}^{\alpha\beta}\left(x_2, x, x_1\right) \right], \\
\widetilde{H}^{\mu\nu}_{\alpha\beta\sigma}\left(x_2 p, xp, x_1 p\right) &= \operatorname{Tr}\left[\widehat{H}^{\mu\nu}_{\alpha\beta}\left(x_2 p, xp, x_1 p\right) \gamma_5 \gamma_\sigma \right], \\
\widetilde{C}^{\sigma\alpha\beta}\left(x_2, x, x_1\right) &= \frac{1}{4} \operatorname{Tr}\left[\gamma^\sigma \gamma_5 \widehat{M}^{\alpha\beta}\left(x_2, x, x_1\right) \right].
\end{aligned}
$$

Note: Tilde notation will be associated with γ_5 here. We can also see the decoupling of the spinor traces.

6.8.1 Decomposition of matrix elements in vector combinations

The final step towards factorization involves decoupling of Lorentz indices' sums included in the definition of $W^{\mu\nu}$. As in [24] we decompose the matrix elements:

- $C^{\sigma\alpha\beta}\left(x_2, x, x_1\right)$ to terms proportional to combinations of vectors p η and a symmetric trasverse vector d^{ab}.
- $\widetilde{C}^{\sigma\alpha\beta}\left(x_2, x, x_1\right)$ to terms proportional to combinations of vectors p η and a antisymmetric trasverse vector ϵ^{ab}

- $d^{\alpha\beta} = \hat{p}^\alpha n^\beta + n^\alpha \hat{p}^\beta - g^{\alpha\beta}$
- $\epsilon^{\alpha\beta} = \epsilon^{\alpha\beta\rho\sigma} \hat{p}_\rho n_\sigma$
- $\hat{p} = \frac{p^\mu}{p\cdot\eta}$.

And using[45]:

- Terms with three η vectors vanish when contracted with the hard part.
- Terms proportional to η_σ contribute higher than twist-4 or they vanish.
- Terms with two η vectors but without η_σ being one of them will not contribute
- Terms proportional to p^a or p^b will vanish as they contract with the projection operators. (see page 16)

Therefore we have the decomposition[1]:

$$\begin{aligned}
&C^{\sigma\alpha'\beta'}(y_2^-,y^-,y_1^-) = \\
&\quad C_0(y_2^-,y^-,y_1^-)p^\sigma p^{\alpha'}p^{\beta'} \\
&\quad + C_1(y_2^-,y^-,y_1^-)p^\sigma d^{\alpha'\beta'} + C_2(y_2^-,y^-,y_1^-)p^{\alpha'}d^{\sigma\beta'} \\
&\quad + C_3(y_2^-,y^-,y_1^-)p^{\beta'}d^{\sigma\alpha'} \\
&\quad + C_4(y_2^-,y^-,y_1^-)n^\sigma p^{\alpha'}p^{\beta'} + C_5(y_2^-,y^-,y_1^-)n^{\alpha'}p^\sigma p^{\beta'} \\
&\quad + C_6(y_2^-,y^-,y_1^-)n^{\beta'}p^\sigma p^{\alpha'}
\end{aligned}$$

$$\begin{aligned}
&\widetilde{C}^{\sigma\alpha'\beta'}(y_2^-,y^-,y_1^-) = \\
&\quad i\varepsilon^{\alpha'\beta'}p^\sigma \tilde{C}_1(y_2^-,y^-,y_1^-) \\
&\quad + i\varepsilon^{\sigma\alpha'}p^{\beta'}\tilde{C}_2(y_2^-,y^-,y_1^-) \\
&\quad + i\varepsilon^{\sigma\beta'}p^{\alpha'}\tilde{C}_3(y_2^-,y^-,y_1^-)
\end{aligned}$$

Using the boxed information we realize that only C_1 and $\widetilde{C_1}$ survive.

Decomposing γ_σ :

$$\begin{aligned}
\gamma_\sigma =& \not{p}\,\bar{n}_\sigma + \not{\bar{p}}n_\sigma + \gamma_{\sigma\perp} \\
=& \not{n}\,\frac{p_\sigma}{p^+} + \not{p}\,n_\sigma + \gamma_{\sigma\perp} \\
\approx& \gamma\cdot\eta\frac{p_\sigma}{p^+}
\end{aligned}$$

We also notice that contraction of the projectors with the symmetric tensor gives:

$$\begin{aligned}
\omega^a_{a'}\omega^b_{b'}d^{a'b'} &= \omega^a_{a'}\omega^b_{b'}\left(\hat{p}^{a'}n^{b'} + n^{\alpha'}\hat{p}^{b'} - g^{\alpha'b'}\right) = \\
&= \omega^\alpha_\alpha\left(g^b_{b'} - \bar{n}^b n_{b'}\right)\left(\hat{p}^{\alpha'}n^{b'} + n^{\alpha'}\hat{p}^{b'} - g^{a'b'}\right) = \\
&= \omega^\alpha_{\alpha'}\left(\hat{p}^{\alpha'}n^b + n^{\alpha'}\hat{p}^b - g^{\alpha'b} - \bar{n}^b n^a + \bar{n}^b n^a\right) = \\
&= (g^\alpha_{\alpha'} - \bar{n}^a n_{\alpha'})\left(\hat{p}^{\alpha'}n^b + n^{\alpha'}\hat{p}^b - g^{\alpha'b} - \bar{n}^b n^a + \bar{n}^b n^a\right) = \\
&= \left(\hat{p}^a n^b + n^\alpha\hat{p}^b - g^{\alpha b}\right) = d^{ab}
\end{aligned}$$

If we use the last two results in combination with the vector decomposition for the matrix elements, we see a complete decoupling of the trace and a new form of:

$$\begin{aligned}
C^{\sigma\alpha'\beta'}(y_2^-,y^-,y_1^-) = \omega^a_{a'}\omega^b_{b'}\frac{1}{4}p^\sigma d^{\alpha'\beta'}\,\mathrm{Tr}\Bigg(&\int\frac{p^+\mathrm{d}y_1^-}{2\pi}\frac{p^+\mathrm{d}y_2^-}{2\pi}\frac{p^+\mathrm{d}y^-}{2\pi}\mathrm{e}^{ix_1p^+y_1^-}\mathrm{e}^{i(x-x_1)p^+y^-}\mathrm{e}^{-i(x-x_2)p^+y_2^-} \\
&\times\left\langle p\middle|\mathrm{T}\left\{\bar{\psi}(0)\frac{\gamma\cdot\eta}{p\cdot\eta}D^\alpha(y_2^-)D^\beta(y^-)\psi(y_1^-)\right\}\middle|p\right\rangle\Bigg) \\
= p^\sigma\int&\frac{p^+\mathrm{d}y_1^-}{2\pi}\frac{p^+\mathrm{d}y_2^-}{2\pi}\frac{p^+\mathrm{d}y^-}{2\pi}\mathrm{e}^{ix_1p^+y_1^-}\mathrm{e}^{i(x-x_1)p^+y^-}\mathrm{e}^{-i(x-x_2)p^+y_2^-} \\
&\times\frac{d^{\alpha\beta}}{4p\cdot n}\left\langle p\middle|\mathrm{T}\left\{\bar{\psi}(0)\gamma\cdot\eta D^\alpha(y_2^-)D^\beta(y^-)\psi(y_1^-)\right\}\middle|p\right\rangle
\end{aligned}$$

After the vector decomposition, the hard part is shaped as:

$$\sigma^{\mu\nu}_{\mathrm{qg}}(x_1,x,x_2) = \frac{1}{4\pi}\frac{d^{\beta\alpha}}{2}\,\mathrm{Tr}\left[\hat{H}^{\mu\nu}_{\alpha\beta}(x_1p,xp,x_2p)\,\gamma_\sigma\right]$$

Similarly, using the same decompositions and rules, we find:

$$\widetilde{C}^{\sigma a' b'}\left(x_1, x, x_2\right) = p^{\sigma} \int \frac{p^{+}\mathrm{d}y_1^{-}}{2\pi} \frac{p^{+}\mathrm{d}y_2^{-}}{2\pi} \frac{p^{+}\mathrm{d}y^{-}}{2\pi} \mathrm{e}^{ix_1 p^{+} y_1^{-}} \mathrm{e}^{i(x-x_1)p^{+}y^{-}} \mathrm{e}^{-i(x-x_2)p^{+}y_2^{-}} \times \frac{i\epsilon^{\alpha\beta}}{2p\cdot n} \left\langle p \middle| \mathrm{T}\left\{\bar{\psi}(0)\gamma_5\gamma\cdot n D_{\alpha}(y_2^{-}) D_{\beta}(y^{-})\psi(y_1^{-})\right\} \middle| p \right\rangle$$

and

$$\tilde{\sigma}_{\mathrm{qg}}^{\mu\nu}\left(x_1, x, x_2\right) = \frac{1}{4\pi} \frac{i\epsilon^{\beta\alpha}}{2} \mathrm{Tr}\left[\hat{H}_{\alpha\beta}^{\mu\nu}\left(x_1 p, xp, x_2 p\right)\gamma_{\sigma}\gamma_5\right]$$

Final results

We obtain the following gauge invariant, well separated energy wise and dimensionally proper, power coreections to $W^{\mu\nu}$, subtituting all the individual constituents we derived in the hadronic tensor [44].

$$\begin{aligned} W^{\mu\nu} = & \int \mathrm{d}x \sigma_2^{\mu\nu}(x) q(x) \\ & + \int \mathrm{d}x_1\, \mathrm{d}x\, \mathrm{d}x_2 \Bigg\{ \sigma_{\mathrm{qg}}^{\mu\nu}\left(x_1, x, x_2\right) T_{\mathrm{qg}}\left(x_1, x, x_2\right) \\ & + \tilde{\sigma}_{\mathrm{qg}}^{\mu\nu}\left(x_1, x, x_2\right) \tilde{T}_{\mathrm{qg}}\left(x_1, x, x_2\right) \Bigg\} \end{aligned}$$

- $q(x) = \dfrac{1}{2p\cdot n} \displaystyle\int \frac{p^{+}\mathrm{d}y^{-}}{2\pi} \mathrm{e}^{ixp^{+}y^{-}} \left\langle p \middle| \mathrm{T}\left\{\bar{\psi}(0)\gamma^{+}\psi\left(y^{-}\right)\right\} \middle| p \right\rangle$
- $\Lambda^2 T_{\mathrm{qg}}\left(x_1, x, x_2\right) = \displaystyle\int \frac{p^{+}\mathrm{d}y_1^{-}}{2\pi} \frac{p^{+}\mathrm{d}y_2^{-}}{2\pi} \frac{p^{+}\mathrm{d}y^{-}}{2\pi} \mathrm{e}^{ix_1 p^{+} y_1^{-}} \mathrm{e}^{i(x-x_1)p^{+}y^{-}} \mathrm{e}^{-i(x-x_2)p^{+}y_2^{-}} \times \dfrac{d^{\alpha\beta}}{2p\cdot n} \left\langle p \middle| \mathrm{T}\left\{\bar{\psi}(0)\gamma\cdot n D_{\alpha}\left(y_2^{-}\right) D_{\beta}\left(y^{-}\right)\psi\left(y_1^{-}\right)\right\} \middle| p \right\rangle$
- $\Lambda^2 \tilde{T}_{\mathrm{qg}}\left(x_1, x, x_2\right) = \displaystyle\int \frac{p^{+}\mathrm{d}y_1^{-}}{2\pi} \frac{p^{+}\mathrm{d}y_2^{-}}{2\pi} \frac{p^{+}\mathrm{d}y^{-}}{2\pi} \mathrm{e}^{ix_1 p^{+} y_1^{-}} \mathrm{e}^{i(x-x_1)p^{+}y^{-}} \mathrm{e}^{-i(x-x_2)p^{+}y_2^{-}} \times \dfrac{i\epsilon^{\alpha\beta}}{2p\cdot n} \left\langle p \middle| \mathrm{T}\left\{\bar{\psi}(0)\gamma_5\gamma\cdot n D_{\alpha}\left(y_2^{-}\right) D_{\beta}\left(y^{-}\right)\psi\left(y_1^{-}\right)\right\} \middle| p \right\rangle$

- $\sigma_2^{\mu\nu}(x) = \dfrac{1}{4\pi}\dfrac{1}{2}\mathrm{Tr}\left[\hat{H}^{\mu\nu}(xp)\gamma\cdot p\right]$,
- $\sigma_{\mathrm{qg}}^{\mu\nu}\left(x_1, x, x_2\right) = \Lambda^2 \dfrac{1}{4\pi}\dfrac{d^{\beta\alpha}}{4}\mathrm{Tr}\left[\hat{H}_{\alpha\beta}^{\mu\nu}\left(x_1 p, xp, x_2 p\right)\gamma\cdot p\right]$,
- $\tilde{\sigma}_{\mathrm{qg}}^{\mu\nu}\left(x_1, x, x_2\right) = \Lambda^2 \dfrac{1}{4\pi}\dfrac{i\epsilon^{\beta\alpha}}{4}\mathrm{Tr}\left[\hat{H}_{\alpha\beta}^{\mu\nu}\left(x_1 p, xp, x_2 p\right)\gamma\cdot p\gamma_5\right]$,

Some comments on the results

- The main goal of factorization is achieved as the matrix elements are well separated from the hard parts.
- There is a clear manifestation of color and electromagnetic gauge invariance.
- The hard parts relevant to the final equations are easily extracted from figure 9.
- Matrix elements include line integrals of A^+, quark field operators, and transverse covariant derivatives.
- All external partonic momenta are collinear. .

Part III

”Electromagnetic Gauge Invariance revisited: QED and a special propagator’s perspective”

7 Ward Identities

After examining the factorization theorems within both partonic and hadronic contexts, and analyzing power suppressions beyond the leading power in each case, it is now appropriate to explore whether the so-called higher twist contributions and specific propagation have any interpretation at the partonic level. Initially, I will demonstrate that employing a special propagator in the QED vertex function not only replicates the findings of [34] but also establishes the necessity of a special propagator for maintaining gauge invariance.

> The concept of higher twist procedure can be simply phrased as follows: We can face the problematic situation in which the numerator trace of the hadronic tensor including the convolution of the Matrix Elements and the Hard Part was not manifestly gauge invariant and also the hard part was not decoupled from the matrix element. Applying a usual Fierz decomposition can handle the decoupling part but still gauge invariance is not secured. This procedure handles the issue dimensionally and is based on the observation that the matrix element contains a short distance contribution. Then we use the special propagator to pick this contribution and place it in the Hard Part. This fixes the dimensionality, leads to covariant derivatives and Ward Identities are manifested.

A Ward identities related discussion can start if we consider the special propagators. In general a QFT is made in such a way that gauge invariance is manifest. This is under dispute when we introduce contact terms, or as we call them ”special propagators” which do not propagate in the lightcone direction in the place of quark propagators. We check the consistency of Ward identities in the context of QED vertex function not only to prove that there is no problem with the Ward Identities and QED but on the contrary there are signs that this is how they are secured.

7.1 Ward Identities: QED soft radiation

We consider the simple case of Figure 7.1: A vertex with gauge bosons and quarks including special propagators.

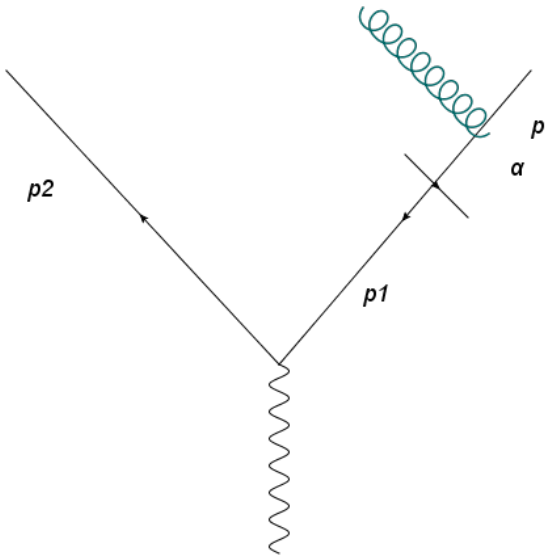

Figure 7.1: *Sample model to check the consistency of Ward Identities.*

Ward Identity

$$(p_2 - p_1)_\mu [S(p_2)\Gamma^\mu(p_2, p_1)S(p_1)] = -[S(p_2) - S(p_1)],$$

- $S(p)$: quark propagator
- $\Gamma^\mu(p_2, p_1)$: vertex function

Left Hand Side:

$$(p_2 - p_1)_\mu \left(\frac{\gamma \cdot p_2}{p_2^2} \gamma^\mu \frac{\gamma \cdot n}{2p_1 \cdot n} \right)$$
$$= -\left(\frac{\gamma \cdot p_2}{p_2^2} \frac{\gamma \cdot p_1 \gamma \cdot n}{2p_1 \cdot n} - \frac{\gamma \cdot n}{2p_1 \cdot n} \right)$$

Right Hand Side:

$$-\left(\frac{\gamma \cdot p_2}{p_2^2} - \frac{\gamma \cdot n}{2p_1 \cdot n} \right)$$

In order for the Ward identities to work, the relation $\gamma \cdot p_1 \gamma \cdot n = 2p_1 \cdot n$ must hold. We have demonstrated in Chapter 6.8 that this is indeed the case. Calculating the full amplitude in Figure 7.1, we observe an additional term arising from the on-shell part of the propagator:

$$\frac{\gamma \cdot p_1 \gamma \cdot n}{2p_1 \cdot n} \cdot \gamma_\sigma \gamma \cdot p_1$$

In a similar vertex [42], Jianwei Qiu proves that $\frac{\gamma \cdot p_1 \gamma \cdot n}{2p_1 \cdot n}$ effectively acts as unity, confirming that the choice of special propagator does not compromise gauge invariance. In [34] but with gluon radiation, I will first use the Clifford Algebra $\{\gamma^\mu, \gamma^\nu\} = 2g^{\mu\nu}$ to rewrite the left-hand side of the required equation as:

$$\gamma \cdot p_1 \gamma \cdot n = -\gamma \cdot \eta \gamma \cdot p_1 + 2p_1 \cdot n$$

Thus, I will now demonstrate the equivalent condition $\gamma \cdot \eta \gamma \cdot p_1$ effectively acting as zero.

Using the Sudakov decomposition:

$$\begin{aligned}\gamma_\sigma =& \not{n}\,\bar{n}_\sigma + \not{\bar{n}} n_\sigma + \gamma_{\sigma\perp} \\ =& \not{n}\,\frac{p_\sigma}{p^+} + \not{\bar{n}} n_\sigma + \gamma_{\sigma\perp} \\ \approx& \gamma\cdot\eta\frac{p_\sigma}{p^+}\end{aligned}$$

and substituting this into the amplitude, we derive from the term we need to show that effectively acts as zero in our context:

$$\approx \frac{\gamma\cdot p_1\gamma\cdot n}{2p_1\cdot n}\gamma\cdot\eta\cdot p_1$$

Therefore, knowing that $(\gamma\cdot\eta)^2 = 0$, we arrive at the equivalent condition, and we emphasize that the special propagator has no detrimental effect on gauge invariance.

On the opposite we see that the terms appearing in $\sqrt{NLP}$ and NLP Jets can afford a higher twist interpretation.

7.2 More Ward Identities

As in part 2 and motivated by the discussion in [42], we remind ourselves upon a collinear expansion:

- Longitudinal momentum dependence (xp^μ) remains in the hard part
- $(n\cdot A)$ components of extra gluons contribute to ordered exponentials in Feynman gauge

Hereafter, as discussed thoroughly in earlier chapters, we will perform a Fierz decomposition of the trace aimed at separating Lorentz indices. Sadly, this step by itself does not ensure gauge invariance, necessitating the use of a special propagator. We use the following slightly altered definitions of the special propagator as introduced in [42] to illustrate the physical process more clearly.

We apply Qiu's [42] notation $(\omega k)^\mu \equiv \omega^\mu_{\mu'}k^{\mu'}$ and as usual rephrase the quark propagators as:

- $\frac{i}{\gamma\cdot k} = \frac{i\gamma\cdot n}{2k\cdot n}\left(1 + i\gamma\cdot(\omega k)\frac{i}{\gamma\cdot k}\right) - \frac{1}{2}(i\gamma\cdot\bar{n})(i\gamma\cdot n)\frac{i}{\gamma\cdot k}$
- $\frac{i}{\gamma\cdot k'} = \frac{i\gamma\cdot n}{2k'\cdot n}\left(\frac{i}{\gamma\cdot k'}i\gamma\cdot(\omega k') + 1\right) - \frac{1}{2}\frac{i}{\gamma\cdot k'}(i\gamma\cdot n)(i\gamma\cdot\bar{n})$

The special propagator secures the em gauge invariance and intrinsically applies all relevant Ward identities, with an indirect normalization of the dimensions of the factorized components. In particular the special propagator identifies and picks a short distance part from the Matrix Element and moves this contribution to the hard part increasing its dimensionality.

For this discussion, we can restrict ourselves to a hard part with "vector" Dirac structure same as in [42],

$$H(k,k') = (\gamma\cdot n)H_n(k,k') + (\gamma\cdot\bar{n})H_{\bar{n}}(k,k') + \gamma_\perp\cdot\boldsymbol{H}_\perp(k,k')$$

Next as we discussed with contract the adjacent quark propagators from left and right and we use the redefinitions we made:

$$\frac{i}{\gamma\cdot k'}H(k',k)\frac{i}{\gamma\cdot k}$$

Expanding each term separately, we obtain [42]:

$$
\begin{aligned}
&\left(\frac{i\gamma\cdot n}{2k\cdot n}\left(1+i\gamma\cdot(\omega k)\frac{i}{\gamma\cdot k}\right)-\frac{1}{2}(i\gamma\cdot\bar{n})(i\gamma\cdot n)\frac{i}{\gamma\cdot k}\right)\cdot\\
&(\gamma\cdot n)H_n\left(k,k'\right)+(\gamma\cdot\bar{n})H_{\bar{n}}\left(k,k'\right)+\gamma_\perp\cdot\boldsymbol{H}_\perp\left(k,k'\right))\cdot\\
&\left(\frac{i\gamma\cdot n}{2k'\cdot n}\left(\frac{i}{\gamma\cdot k'}i\gamma\cdot(\omega k')+1\right)-\frac{1}{2}\frac{i}{\gamma\cdot k'}(i\gamma\cdot n)(i\gamma\cdot\bar{n})\right)=\\
&=\frac{i}{\gamma\cdot k'}(\gamma\cdot n)H_n+\frac{i}{\gamma\cdot k'}i\gamma\cdot(\omega k')(\gamma\cdot n)H_n\frac{i}{\gamma\cdot k}+\\
&+(\gamma\cdot n)H_n i\gamma\cdot(\omega k)\frac{i}{\gamma\cdot k'}+i\gamma\cdot(\omega k')(\gamma\cdot n)H_n i\gamma\cdot(\omega k)\frac{i}{\gamma\cdot k'}\frac{i}{\gamma\cdot k}+\\
&+\frac{i}{\gamma\cdot k'}(\gamma_\perp\cdot\boldsymbol{H}_\perp)+\frac{i}{\gamma\cdot k'}i\gamma\cdot(\omega k')(\gamma_\perp\cdot\boldsymbol{H}_\perp)\frac{i}{\gamma\cdot k}+\\
&+(\gamma_\perp\cdot\boldsymbol{H}_\perp)i\gamma\cdot(\omega k)\frac{i}{\gamma\cdot k'}+i\gamma\cdot(\omega k')(\gamma_\perp\cdot\boldsymbol{H}_\perp)i\gamma\cdot(\omega k)\frac{i}{\gamma\cdot k'}\frac{i}{\gamma\cdot k}
\end{aligned}
$$

Simplification

Based on the relations $\eta^2=\overline{\eta}^2=0$ and $\eta\overline{\eta}=1$:

$$
\begin{aligned}
&\frac{i}{\gamma\cdot k'}H\left(k',k\right)\frac{i}{\gamma\cdot k}=\\
&=\frac{i}{\gamma\cdot k'}\gamma\cdot nH_n\left(k',k\right)\frac{i}{\gamma\cdot k}\\
&+\left(\frac{i}{\gamma\cdot k'}i\gamma\cdot(\omega k')+1\right)\frac{i\gamma\cdot n}{2k'\cdot n}\gamma\cdot\bar{n}H_{\bar{n}}\left(k',k\right)\frac{i\gamma\cdot n}{2k\cdot n}\left(1+i\gamma\cdot(\omega k)\frac{i}{\gamma\cdot k}\right)\\
&+\left(\frac{i}{\gamma\cdot k'}i\gamma\cdot(\omega k')+1\right)\frac{i\gamma\cdot n}{2k'\cdot n}\gamma^{\mathrm{T}}\cdot H_{\mathrm{T}}\left(k',k\right)\frac{i}{\gamma\cdot k}\\
&+\frac{i}{\gamma\cdot k'}\gamma^{\mathrm{T}}\cdot H_{\mathrm{T}}\left(k',k\right)\frac{i\gamma\cdot n}{2k\cdot n}\left(1+i\gamma\cdot(\omega k)\frac{i}{\gamma\cdot k}\right)
\end{aligned}
$$

We also define the special propagator[42]:

Special Propagator $S(k)$  $=\frac{i\gamma\eta}{2k\eta}$

The special propagator is utilized to extract the short-distance components present in the matrix elements and transfer them to the hard part, as previously mentioned. This can be demonstrated mathematically by employing the provided decomposition, contracting the hard part with quark propagators on both sides, and then examining the overall scenario by observing how the matrix element behaves when contracted with these terms.

We can use the above to showcase how this also works in different processes:

Showcase of the action of the special propagator

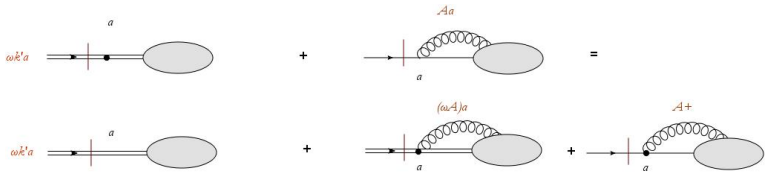

Figure 7.2: Special propagator in action

In Figure 8.4 we see an example of how this works depicting the following in two terms:

$$M\left(p',p\right)\left(\frac{i}{\gamma\cdot p'}i\gamma\cdot\left(\omega p'\right)+1\right)i\frac{\gamma\cdot n}{2p'\cdot n}=M\left(p',p\right)\left(\frac{i}{\gamma\cdot p'}i\gamma_{\alpha}\left(p-\hat{p}\right)^{\alpha}+1\right)i\frac{\gamma\cdot n}{2p'\cdot n}$$

- The first term from the left has the special propagator adjacent to the result of the action of a transpose derivative $(\omega\partial\ )$.
- The other term is a free term, flowing unidisturbed in the matrix element. It picks out the connecting quark gluon vertex as shown in Figure 8.4

Then we can collinearly expand the extracted gluon field as we did before[43]

$$\begin{aligned}A^{\alpha}&=w_{\alpha'}^{\alpha}A^{\alpha'}+\frac{p^{\alpha}}{p\cdot n}\cdot\left(n\cdot A\right)=\\&=w_{\alpha'}^{\alpha}A^{\alpha'}+\frac{p^{\alpha}}{p^{+}}\cdot A^{+}\end{aligned}$$

and split the first line of Figure 8.4 in the second where we now have:

- The first and the second term from the left has the special propagator adjacent to the result of the action of a transpose **covariant** derivative.
- The other term includes the special propagator adjacent to the collinear part A^{+} which contributes to higher order and secures colour gauge invariance as a component of the gauge links.

Each special propagator is associated with an extra action of ωD in the hard part. This gives a suppression of one power of the large momentum in the hard part, paired with an operator ωD in the corresponding matrix element for each such ω

We see now, the manifestation of gauge invariance in the hard-scattering diagram in Figure 7.3 emerging from a tree level Ward identity. The hard part is evaluated also in the collinear limit where $p' = \hat{p}$.

$$\gamma \cdot \bar{n} \frac{i\gamma \cdot n}{2p' \cdot n} (-i\gamma \cdot q) \frac{i}{\gamma \cdot (p'-q)} = \gamma \cdot \bar{n} \left[\frac{i}{\gamma \cdot (p'-q)} - \frac{i\gamma \cdot n}{2p' \cdot n} \right]$$

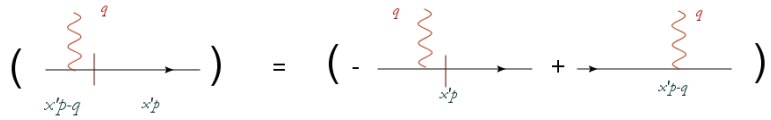

Figure 7.3: Ward Identity

Application: Decoupling of the unphysical polarizations

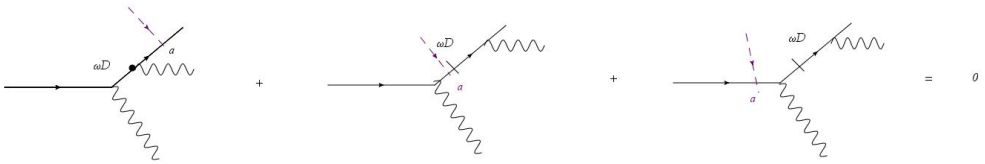

- The unphysical photon would not decouple if there was no special propagator as in [42].
- Unphysical gluons decouple samely.

8 QED

8.1 Power corrections to QED form factor: An alternative approach

The final part of my thesis is commenced with an analysis of QED power corrections mirroring the thesis' first part . Aspiring to check how a special propagator formalism similar with[43] would work in a framework like the one in[34], I will first attempt to bring the factorization formula for QED Jet production in a form as similar as possible to [16], [45],[43]. It will be of particular interest if the result of this effort would be comparable with the work of [34] which was the reference point of Part 1.

Many obstacles arise before we even grab a pen since the work of [45] refers to hadronic collisions and $\frac{\Lambda_{QCD}}{Q}$ power corrections. Nevertheless I stand to believe that the physical way of this approach can be applied after modifications to any factorization quest. What is more, the special propagator applied in this framework is definitely an attractive interplay which can shed light in symmetry properties of the factorized matrix elements. In the following, I will work, neglecting the result of the Sterman-Libby power counting[51] presented in [34] and will try to produce the same result using factorization principles[15]. I shall work only in one loop, and therefore overlook any other factorization possibility except from a photon connection among the hard part and a jet, staying on the safe waters of Hard-Collinear factorization away for turbulence caused by soft pinch surfaces. I will organize the contributions starting from a separation between contributions arising depending on the number of photon connections between the hard part and the matrix elements, which would collectively include every non short-distance and perturbatively calculable contribution.

My strategy is as simple as it gets: I will try to make the hard part, depending only on momenta which are hard scaled, and then try to organize the result based on symmetry constraints. This final part, is more observational and its goal is to find similarities. As a result in some points it lacks strict mathematical coordination as I mainly thrive to find similarities and room for further investigation.

Diagram 1

The first diagram, aiming to collectively represent all the diagrams which can factorize in short and long distance contributions which are connected only by a fermion and an antifermion.

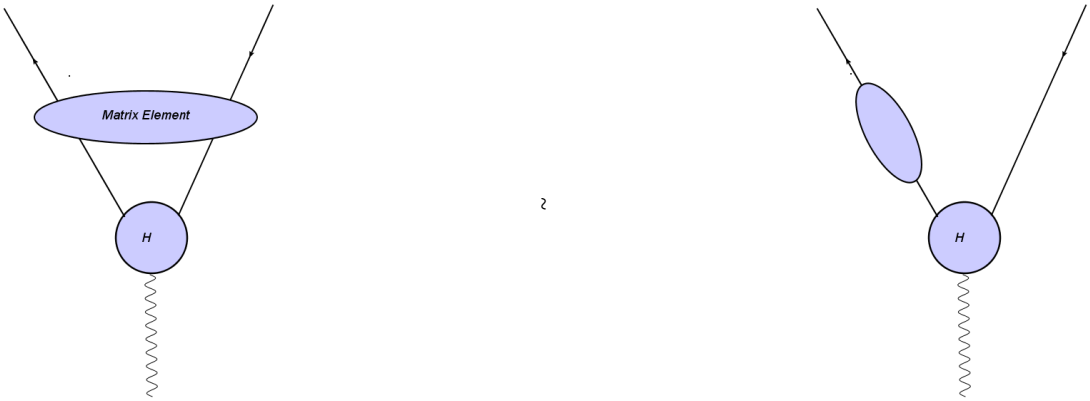

Figure 8.1: **Left**: Reduced diagram collectively depicting factorizable Feynman diagrams of all orders with no extra connections apart the fermion among the factorized areas. **Right**: Working separately with collinear substructure: Implication of complete disentaglement with soft.

Relevant kinematics

Momenta p of outgoing particles

$$p^\mu = (p, 0, 0, p)\,, \qquad p'^\mu = (p, 0, 0, -p)$$

Virtual Photon:

$$q^\mu = (q^+, 0, q^-)$$

Hard Part:

$$\widehat{H}^{\mu\nu}(p, -p', k) = \widehat{H}^{\mu\nu}(p, p, k)$$

Matrix Element:

$$\widehat{M}(p, p') = \int d^4y e^{ipy} < p|\overline{\Psi}(0)\Psi(y)|p' >$$

Naively considering the ”upper” diagram as the long distance non-perturbative part, crudely separating its contribution from the ”lower” hard part, is an one-way alley towards conceptual mistakes underlying a failing theory. In the following the focus will be targeted in separating completely the hard scattering part from the matrix elements. Such a distenglamenent necessitates a separation of any potential index convolution appearing in numerators of Feynman diagrams generated by the reduced diagrams of **??** Furthermore, the dimensions of both the short-range hard and long-range matrix elements need to be fixed. It is hoped that by addressing the issue with a fundamentally sound approach, we can naturally ensure gauge invariance.

Diagram 2

Relevant kinematics

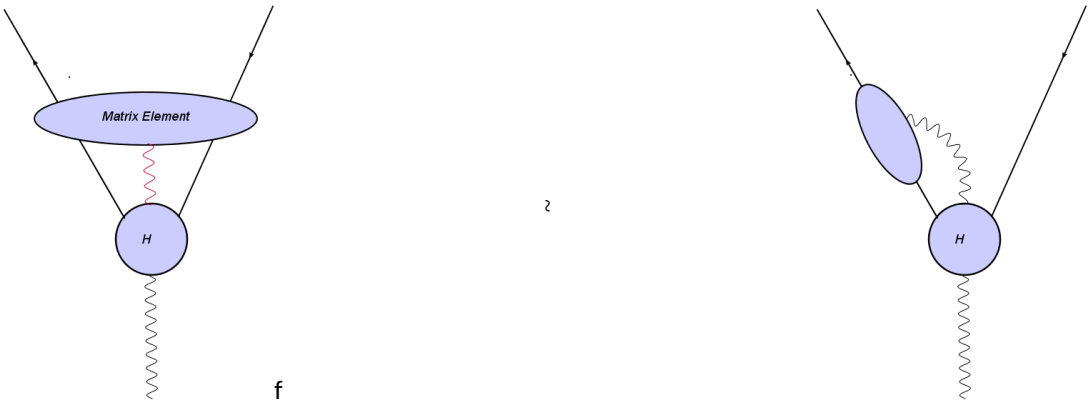

Figure 8.2: Corresponding diagrams with 1 photonic correction more than those in 8.4

Momenta p of outgoing particles

$$\tilde{p}^{\mu} = p^{\mu} - l^{\mu} = (p^{+} - l^{+}, -l^{\perp}, p^{-} - l^{-}), \qquad p'^{\mu} = (p, 0, 0, -p)$$

Connecting line Photon:

$$l^{\mu} = (l^{+}, l_{\perp}, l^{-})$$

Hard Part:

$$\widehat{H}^{\mu\nu}(\tilde{p}, p, k)$$

Matrix Element:

$$M_a(\tilde{p}, p) = \int d^4y_1 d^4y e^{i\tilde{p}y_1 + ip(y-y_1)} \langle p|\overline{\Psi}(0) e A_a(y_1)\Psi(y)|p'\rangle$$

Expressions

Diagram 1:

$$K^{\mu\nu} = \frac{1}{4\pi}\int d^4p H^{\mu\nu}(p) \int d^4y e^{ipy} < p|\overline{\Psi}(0)\Psi(y)|p' >$$

Diagram 2:

$$\Lambda_a^{\mu\nu} = \frac{1}{4\pi}\int d^4p d^4\tilde{p} H_a^{\mu\nu}(p, \tilde{p}) \int d^4y d^4y_1 e^{i\tilde{p}y_1 + ip(y-y_1)} \langle p|\overline{\Psi}(0) e A_a(y_1)\Psi(y)|p' >$$

8.1.1 Expansion around plus component

Projection operator

In analogy with [43] we define $\boxed{\omega^a_{a'} = g^a_{a'} - n^a \overline{n}_{a'}}$, a projection operator, which upon acting on any four vector defined in a lightcone frame, strips off its plus component. $p^+, \tilde{p^+}$.

In our case :

$$(g^a_{a'} - n^a \overline{n}_{a'})\, p^{a'} = (p - p^+)^a$$

and

$$(g^a_{a'} - n^a \overline{n}_{a'})\, \tilde{p}^{a'} = \left(\tilde{p} - \tilde{p^+}\right)^a$$

Then and in order to have hard elements depending only on + components which are the dominant ones and also make the subleading contributions' effect manifested and factorized we expand around the dominant plus momenta:

$$\begin{aligned}\hat{H}^{\mu\nu}(p) =& \hat{H}^{\mu\nu}(p^+) + \frac{\partial \hat{H}^{\mu\nu}(p^+)}{\partial p^\alpha}(p - p^+)^\alpha \\ =& \hat{H}^{\mu\nu}(p^+) + \frac{\partial \hat{H}^{\mu\nu}(p^+)}{\partial p^\alpha}\omega^a_{a'} p^{a'}\end{aligned}$$

$$\widehat{H}^{\mu\nu}_a(p,\tilde{p}) = \widehat{H}^{\mu\nu}_a(p^+,\tilde{p}^+) + \frac{\partial \widehat{H}^{\mu\nu}(p^+,\tilde{p}^+)}{\partial (p-l)^\beta} w^\beta_{\beta'} (p-l)^{\beta'} + \frac{\partial \widehat{H}^{\mu\nu}(p^+,\tilde{p}^+)}{\partial p^\beta} \times$$

$$\times w^\beta_{\beta'} p^{\beta'}$$

The relevant with [34] part is:

$$w^\beta_{\beta'} (p-l)^{\beta'} \frac{\partial \widehat{H}^{\mu\nu}(\hat{p} - \hat{l}, \hat{l})}{\partial (p-l)^\beta} + w^\beta_{\beta'} p^{\beta'} \frac{\partial \widehat{H}^{\mu\nu}(\hat{p} - \hat{l}, \hat{p})}{\partial p^\beta} = l_\perp \frac{\partial \widehat{H}^{\mu\nu}(\hat{p} - \hat{l}, \hat{p})}{\partial l_\perp}$$

To arrive in the convenient result which is identical with the expansion worked in [34], we neglected the derivatives respectful to the $-$ component as they would come with a l^- and a $(p-l)^-$ respectively, which both scale as λ^2 and combined with the Jet contribution they exceed the NLP area. The $+$ derivatives are also absent but those are cancelled due to the application of the projection on the $+$ momentum components.

Once more we use the Ward Identities introduced in Part 2 to reform the expansion in terms only of Hard parts and not their derivatives.

$$\frac{\partial \widehat{H}_{\mu\nu}(p^+)}{\partial p_a} = -H^a_{\mu\nu}(p^+, p^+)$$

Using the Ward identities we have the Taylor expansions expressed as:

- $\widehat{H}^{\mu\nu}(p) = \widehat{H}^{\mu\nu}(p^+) - \widehat{H}^{\mu\nu}_\alpha(p^+, p^+) w^\alpha_{\alpha'} p'^{\alpha'}$
- $\widehat{H}^{\mu\nu}_\alpha(p,\tilde{p}) = \widehat{H}^{\mu\nu}_\alpha(p^+,\tilde{p}^+) - \widehat{H}^{\mu\nu}_{\alpha\beta}(p^+,\tilde{p}^+,\tilde{p}^+) w^\beta_{\beta'} \tilde{p}^{\beta'} - \widehat{H}^{\mu\nu}_{\beta\alpha}(p^+,p^+,\tilde{p}^+) w^\beta_{\beta'} p^{\beta'}$

I define dimensionless variables:

- $x = \frac{l^+}{p^+}$
- $x_1 = \frac{l^+}{\tilde{p^+}}$
- $\zeta = \frac{p^+}{l^+}$
- $\zeta_1 = \frac{\tilde{p^+}}{l^+}$

Subsequently I will plug everything in the factorized relationship derived before, following these rules:

- Introduce $1 = \int d\zeta \delta\left(\zeta - \frac{p^+}{l^+}\right)$ and use the fact that the hard function is now **independent of the transverse partonic momenta**. We can now reduce the $\int d^4p$ dimension-four momentum integral to a single-dimensional integral over the momentum fraction ζ.
- To perform this reduction we also will need the aid of the identity

$$\int \frac{\mathrm{d}^4 l}{(2\pi)^4} \mathrm{e}^{ily} \delta(\zeta - \frac{p^+}{l^+}) = \int \frac{l^+ \mathrm{d}y^-}{2\pi} \mathrm{e}^{i(\zeta l^+)y^-} \delta^4(y - y^-)$$

- Replace Hard parts with the Taylor expansions around the plus component as we expressed using the projection operators and the Ward Identities.
- We replace $p^{\alpha'}$ with $\left(-i\partial^{\alpha'}\right)$

Using the above we now have the following relationships for our factorization formulas:

Diagram 1 contribution

$$\begin{aligned}
K^{\mu\nu} &= \int d^4p d\zeta \delta\left(\zeta - \frac{p^+}{l^+}\right)\left[H^{\mu\nu}\left(p^+\right) + H_a^{\mu\nu}\left(p^+, p^+\right)\omega_{a'}^a\left(i\partial^{a'}\left(y\right)\right)\right] \\
&\times \int d^4y e^{ipy} < p|\overline{\Psi}(0)\Psi(y)|p' > \\
&= \int d\zeta\left(\hat{H}^{\mu v}(p^+)\cdot\int \frac{l^+dy^-}{2\pi} e^{i(\zeta l^+)y^-}\left\langle p\left|\bar{\psi}(0)\psi(y^-)\right|p\right\rangle\right) \\
&+ \int d\zeta\left(\hat{H}_\alpha^{\mu\nu}\left(p^+, p^+\right)\cdot w_{\alpha'}^\alpha \int \frac{l^+dy^-}{2\pi} e^{i(\zeta l^+ y^-)}\left\langle p\left|\bar{\psi}(0) i\partial^{\alpha'}(y)\psi(y^-)\right|p'\right\rangle\right)
\end{aligned}$$

Diagram 2 contribution

$$\begin{aligned}
\Lambda_\alpha^{\mu\nu} &= \int d^4p d^4\tilde{p}\left[\widehat{H}_\alpha^{\mu\nu}(p^+, \tilde{p}^+) - \widehat{H}_{\alpha\beta}^{\mu\nu}(p^+, \tilde{p}^+, \tilde{p}^+) w_{\beta'}^\beta \tilde{p}^{\beta'} - \widehat{H}_{\beta\alpha}^{\mu\nu}(p^+, p^+, \tilde{p}^+) w_{\beta'}^\beta p^{\beta'}\right] \times \\
&\times \int d^4y_1 d^4y e^{i\tilde{p}y_1 + ip(y-y_1)} \langle p|\overline{\Psi}(0) e A_a(y_1)\Psi(y)|p'\rangle = \\
&= \int d\zeta_1 d\zeta\left[\widehat{H}_\alpha^{\mu\nu}(p^+, \tilde{p}^+) - \widehat{H}_{\alpha\beta}^{\mu\nu}(p^+, \tilde{p}^+, \tilde{p}^+) w_{\beta'}^\beta \tilde{p}^{\beta'} - \widehat{H}_{\beta\alpha}^{\mu\nu}(p^+, p^+, \tilde{p}^+) w_{\beta'}^\beta p^{\beta'}\right] \times \\
&\times \int d^4y_1 d^4y d^4p d^4\tilde{p} \delta(\zeta_1 - \frac{\tilde{p}^+}{l^+}) \delta(\zeta - \frac{p^+}{l^+})) e^{i\tilde{p}y_1 + ip(y-y_1)} \langle p|\overline{\Psi}(0) e A_a(y_1)\Psi(y)|p'\rangle = \\
&= \frac{1}{4\pi} \int d\zeta_1 d\zeta H_\alpha^{\mu\nu}\left(\zeta l^+, \zeta_1 l^+\right) \cdot \int \frac{l^+dy_1}{2\pi} \frac{l^+dy^-}{2\pi} e^{i(\zeta_1 l^+)y_1^-} e^{i(\zeta l^+)(y^- - y_1^-)} \times \\
&\times e\langle p|\bar{\psi}(0) A^\alpha(y_1^-)\psi(y^-)|p\rangle +
\end{aligned}$$

$$+\frac{1}{4\pi}\int d\zeta_1 d\zeta H^{\mu\nu}_{\alpha\beta}(\zeta l^+,\zeta_1 l^+,\zeta_1 l^+)\,\omega^{\beta}_{\beta'}\int\frac{l^+dy_1^-}{2\pi}\frac{l^+dy^-}{2\pi}e^{i(\zeta_1 l^+)y_1^-}e^{i(\zeta l^+)(y^- - y_1^-)}\times$$
$$\times e\langle p|\bar\psi(0)\left(i\partial^{b'}(y_1{}^-)\right)A^{\alpha}(y_1^-)\psi(y^-)|p'\rangle+$$
$$+\frac{1}{4\pi}\int d\zeta_1 d\zeta H^{\mu\nu}_{\beta\alpha}(\zeta l^+,\zeta l^+,\zeta_1 l^+)\,\omega^{\beta}_{\beta'}\int\frac{l^+dy_1^-}{2\pi}\frac{l^+dy^-}{2\pi}e^{i(\zeta_1 l^+)y_1^-}e^{i(\zeta_2 l^+)(y^- - y_1^-)}\times$$
$$\times e\langle p|\bar\psi(0)A^{\alpha}(y_1^-)\left(i\partial^{b'}(y^-)\right)\psi(y^-)|p'\rangle$$

Collinear limit of Hard parts

As in part 2, here as well estimating the hard parts in the collinear limit will be of significance. One of the primary assumptions we made in the beggining and one we still follow so as to proceed in this work is that the leading contributions arise from the momenta which enter the hard part in a direction collinear to the + direction and which are on shell. Therefore calculating the hard parts in this limit will be necessary for further advancements as well as will provide room for commentary.

As hard we define the part of the diagram whose lines carry the hard momentum of the virtual photon. The parts of the diagram which do not constitute the so called matrix elements as they have the chance to be dressed with a scale higher than the hard one.

Constraining the virtual momentum q to have a dominant plus component and squared to give $-Q^2$, I will make the following parametrization of its momenta which also produce the expansion parameter used in [34] $\lambda = \frac{p\cdot q}{Q^2}$:

$$q^\mu = \left(\frac{-Q^2}{p\cdot q}\cdot p^+, 0, \frac{p\cdot q}{p^+}\right) \equiv \left(\lambda^{-2}, 0, 1\right)$$

Therefore, we see that the dominant component is in what is defined in [34] as Leading Power and the other components are contributing in subleading powers.

I define

$$\zeta_N = \zeta\cdot\frac{-Q^2}{p\cdot q}$$

mainly for convienence as I express the momenta as functions of l^+. This way the momentum of the virtual photon is expressed as

$$q^\mu = \left(-\zeta_N\cdot l^+, 0, \frac{q^2}{\zeta_N\cdot l^+}\right)$$

An extra advantage of defining ζ_N is that its value is invariant no matter which combination of (momentum, ζ) we choose. In particular it is easy to see $\zeta_{1N} = \zeta_N$.

Based on all the above, and expressing all the momenta in terms of the plus component of the connection we extract the following relationships.

"Lower Contribution Hard Diagram - Collinear limit"

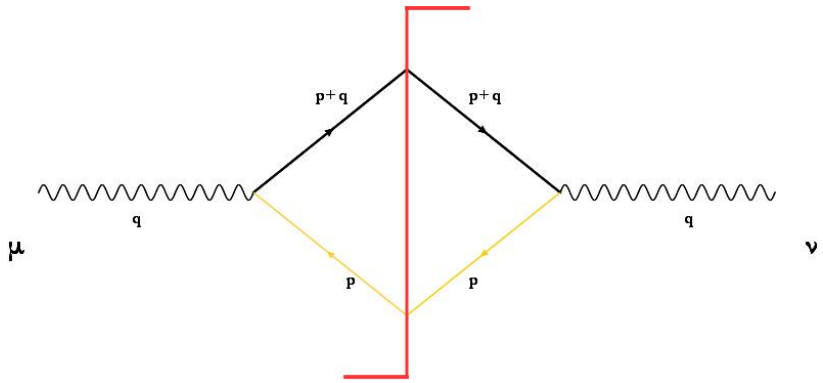

Figure 8.3: Tree Level Cut diagram of the hadronic tensor: Orange lines: Irrelevant to the hard part.

$$
\begin{aligned}
\widehat{H}^{\mu\nu}(\zeta l^+) &= \gamma^\mu \left(\zeta \not{l}^+ + \not{q}\right) \gamma^\nu \times \delta_+((\zeta \not{l}^+ + q)^2) = \\
&= \gamma^\mu \left(\zeta \not{l}^+ + \not{q}\right) \gamma^\nu \times (2\pi)\delta\left(-Q^2 + 2\zeta l^+ \frac{Q^2}{2\zeta_N l^+}\right) = \\
&= \gamma^\mu \left(\zeta \not{l}^+ + \not{q}\right) \gamma^\nu \times (2\pi)\delta\left(\frac{Q^2}{\zeta_N}(\zeta - \zeta_N)\right) = \\
&= \gamma^\mu (\zeta \not{l}^+ + \not{q}) \gamma^\nu (2\pi) \frac{\zeta_N}{Q^2} \delta(\zeta - \zeta_N)
\end{aligned}
$$

"Subleading Contribution Hard Diagram - Collinear limit"

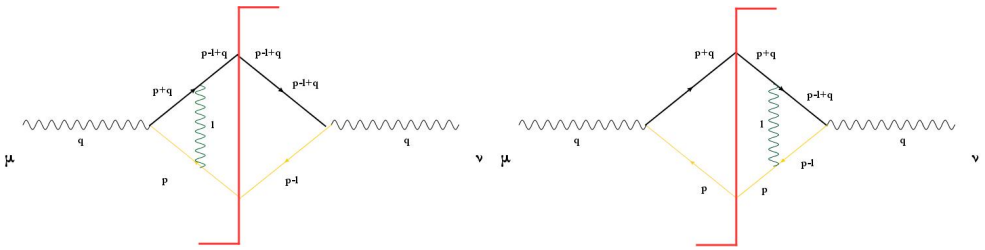

Figure 8.4: Cut diagrams relevant to the virtual correction

$$
\begin{aligned}
\widehat{H}^a_{\mu\nu}(\zeta_1 l^+, \zeta l^+, q) &= \gamma_\mu (\zeta_1 \not{l}^+ + \not{q}) \gamma^\alpha \frac{\zeta \not{l}^+ + \not{q}}{(\zeta l^+ + q)^2 - i\epsilon} \gamma_\nu (2\pi)\delta_+\left((\zeta_1 l^+ + q)^2\right) + \\
&+ \gamma_\mu (\zeta_1 \not{l}^+ + \not{q}) \gamma^\alpha \frac{\zeta \not{l}^+ + \not{q}}{(\zeta_1 l^+ + q)^2 + i\epsilon} \gamma_\nu (2\pi)\delta_+\left((\zeta l^+ + q)^2\right) = \\
&= \gamma_\mu (\zeta_1 \not{l}^+ + \not{q}) \gamma^\alpha \frac{\zeta \not{l}^+ + \not{q}}{(\zeta l^+ + q)^2 - i\epsilon} \gamma_\nu (2\pi) \frac{\zeta_N}{Q^2} \delta(\zeta_1 - \zeta_N) + \\
&+ \gamma_\mu (\zeta_1 \not{l}^+ + \not{q}) \gamma^\alpha \frac{\zeta \not{l}^+ + \not{q}}{(\zeta_1 l^+ + q)^2 + i\epsilon} \gamma_\nu (2\pi) \frac{\zeta_N}{Q^2} \delta(\zeta - \zeta_N)
\end{aligned}
$$

8.1.2 Collinear expansion of the gauge field

,

$$A^{\alpha} = \omega^{\alpha}_{\alpha'} A^{\alpha'} + \frac{l^{\alpha}}{l\cdot\overline{n}} \cdot (\overline{n} \cdot A)$$
$$= \omega^{\alpha}_{\alpha'} A^{\alpha'} + \frac{l^{\alpha}}{l^{+}} \cdot A^{+}$$

With a photon field successfully separated in a "transverse" and a longitudinal component we further rearrange the integrals. The "transverse" part $\omega^{\alpha}_{\alpha'} A^{\alpha'}$ can be combined with terms $\omega^{\alpha}_{\alpha'} \partial^{\alpha'}$ and form "transverse" covariant derivatives, of the form $\omega^{\alpha}_{\alpha'} D(y) = \left(i\partial^{\alpha'}(y) - g A^{\alpha'}(y) \right)$, while the p^{α} momentum in the longitudinal part of the A field can contract with and via the aforementioned generalized Ward identities lower the order of Hard diagrams. We will also use the following extensively as previously:

$$p_{\alpha} \omega^{\alpha}_{\alpha'} = 0$$

Physically now we have decomposed the photon in two components. The scalar component is in the direction of the collinear jet in discussion as well as collinear to the hard momenta as modified when we expand.

Employing the expansion in the second diagram's contribution will further reorganize our terms depending on more specific criteria making them more flexible upon combination.

$$\begin{aligned}
\Lambda^{\mu\nu}_{\alpha} = {} & \frac{1}{4\pi} \int d\zeta_1 d\zeta H^{\mu\nu}_{\alpha}(\zeta l^{+}, \zeta_1 l^{+}) \cdot \int \frac{l^{+} dy_1}{2\pi} \frac{l^{+} dy^{-}}{2\pi} e^{i(\zeta_1 l^{+}) y_1^{-}} e^{i(\zeta l^{+})(y^{-} - y_1^{-})} \times \\
& \times e \langle p | \bar{\psi}(0) \left(\omega^{\alpha}_{\alpha'} A^{\alpha'}(y_1^{-}) - l^{\alpha} \frac{A^{+}(y_1^{-})}{l^{+}} \right) \psi(y^{-}) | p' \rangle + \\
& + \frac{1}{4\pi} \int d\zeta_1 d\zeta H^{\mu\nu}_{\alpha\beta}(\zeta l^{+}, \zeta_1 l^{+}, \zeta_1 l^{+}) \omega^{\beta}_{\beta'} \int \frac{l^{+} dy_1^{-}}{2\pi} \frac{l^{+} dy^{-}}{2\pi} e^{i(\zeta_1 l^{+}) y_1^{-}} e^{i(\zeta l^{+})(y^{-} - y_1^{-})} \times \\
& \times e \langle p | \bar{\psi}(0) \left(i\partial^{b'}(y_1{}^{-}) \right) \left(\omega^{\alpha}_{\alpha'} A^{\alpha'}(y_1^{-}) - l^{\alpha} \frac{A^{+}(y_1^{-})}{l^{+}} \right) \psi(y^{-}) | p' \rangle + \\
& + \frac{1}{4\pi} \int d\zeta_1 d\zeta H^{\mu\nu}_{\beta\alpha}(\zeta l^{+}, \zeta l^{+}, \zeta_1 l^{+}) \omega^{\beta}_{\beta'} \int \frac{l^{+} dy_1^{-}}{2\pi} \frac{l^{+} dy^{-}}{2\pi} e^{i(\zeta_1 l^{+}) y_1^{-}} e^{i(\zeta_2 l^{+})(y^{-} - y_1^{-})} \times \\
& \times e \langle p | \bar{\psi}(0) \left(\omega^{\alpha}_{\alpha'} A^{\alpha'}(y_1^{-}) - l^{\alpha} \frac{A^{+}(y_1^{-})}{l^{+}} \right) \left(i\partial^{b'}(y^{-}) \right) \psi(y^{-}) | p' \rangle = \\
= {} & \frac{1}{4\pi} \int d\zeta_1 d\zeta H^{\mu\nu}_{\alpha}(\zeta l^{+}, \zeta_1 l^{+}) \cdot \int \frac{l^{+} dy_1}{2\pi} \frac{l^{+} dy^{-}}{2\pi} e^{i(\zeta_1 l^{+}) y_1^{-}} e^{i(\zeta l^{+})(y^{-} - y_1^{-})} \times \\
& \times \langle p | \bar{\psi}(0) \left(\omega^{\alpha}_{\alpha'} A^{\alpha'}(y_1^{-}) \right) \psi(y^{-}) | p' \rangle + \\
& + \frac{1}{4\pi} \int d\zeta_1 d\zeta H^{\mu\nu}_{\alpha\beta}(\zeta l^{+}, \zeta_1 l^{+}, \zeta_1 l^{+}) \omega^{\beta}_{\beta'} \int \frac{l^{+} dy_1^{-}}{2\pi} \frac{l^{+} dy^{-}}{2\pi} e^{i(\zeta_1 l^{+}) y_1^{-}} e^{i(\zeta l^{+})(y^{-} - y_1^{-})} \times \\
& \times \langle p | \bar{\psi}(0) e \left(\omega^{\alpha}_{\alpha'} \left(i\partial^{b'}(y_1{}^{-}) \right) A^{\alpha'}(y_1^{-}) \right) \psi(y^{-}) | p' \rangle + \\
& + \frac{1}{4\pi} \int d\zeta_1 d\zeta H^{\mu\nu}_{\beta\alpha}(\zeta l^{+}, \zeta l^{+}, \zeta_1 l^{+}) \omega^{\beta}_{\beta'} \int \frac{l^{+} dy_1^{-}}{2\pi} \frac{l^{+} dy^{-}}{2\pi} e^{i(\zeta_1 l^{+}) y_1^{-}} e^{i(\zeta_2 l^{+})(y^{-} - y_1^{-})} \times \\
& \times \langle p | \bar{\psi}(0) e \left(\omega^{\alpha}_{\alpha'} A^{\alpha'}(y_1^{-}) \right) \left(i\partial^{b'}(y^{-}) \right) \psi(y^{-}) | p' \rangle + \\
& + \frac{1}{4\pi} \int d\zeta_1 d\zeta H^{\mu\nu}_{\alpha}(\zeta l^{+}, \zeta_1 l^{+}) \cdot \int \frac{l^{+} dy_1}{2\pi} \frac{l^{+} dy^{-}}{2\pi} e^{i(\zeta_1 l^{+}) y_1^{-}} e^{i(\zeta l^{+})(y^{-} - y_1^{-})} \times \\
& \times e \langle p | \bar{\psi}(0) \left(-l^{\alpha} \frac{A^{+}(y_1^{-})}{l^{+}} \right) \psi(y^{-}) | p' \rangle +
\end{aligned}$$

$$+\frac{1}{4\pi}\int d\zeta_1 d\zeta H^{\mu\nu}_{\alpha\beta}(\zeta l^+,\zeta_1 l^+,\zeta_1 l^+)\,\omega^{\beta}_{\beta'}\int\frac{l^+dy_1^-}{2\pi}\frac{l^+dy^-}{2\pi}e^{i(\zeta_1 l^+)y_1^-}e^{i(\zeta l^+)(y^- - y_1^-)}\times$$
$$\times\langle p|\bar\psi(0)e\left(\left(i\partial^{b'}(y_1{}^-)\right)(-l^\alpha)\frac{A^+(y_1^-)}{l^+}\right)\psi(y^-)|p'\rangle+$$
$$+\frac{1}{4\pi}\int d\zeta_1 d\zeta H^{\mu\nu}_{\beta\alpha}(\zeta l^+,\zeta l^+,\zeta_1 l^+)\,\omega^{\beta}_{\beta'}\int\frac{l^+dy_1^-}{2\pi}\frac{l^+dy^-}{2\pi}e^{i(\zeta_1 l^+)y_1^-}e^{i(\zeta_2 l^+)(y^- - y_1^-)}\times$$
$$\times\langle p|\bar\psi(0)e\left(-l^\alpha\frac{A^+(y_1^-)}{l^+}\right)\left(i\partial^{b'}(y^-)\right)\psi(y^-)|p'\rangle$$

8.2 Emergence of Wilson Lines

Manipulation after manipulation, we have brought our formulas in a form which can allow us to combine some terms which on first look, appear similar to an expanded Wilson line. Thereafter and respecting the number of photons attached to the Hard part we will try to combine those terms and see how practically we combine the Wilson lines.

To do this in an organized way I will separate here the two contributions from diagram 1 and the six arising from the second one and I will assign a number to each of them.

Diagram 1

$$M_1{}^{\mu\nu}=\int d\zeta\left(\hat H^{\mu v}(p^+)\cdot\int\frac{l^+dy^-}{2\pi}e^{i(\zeta l^+)y^-}\left\langle p\left|\bar\psi(0)\psi(y^-)\right|p'\right\rangle\right)$$
$$M_2{}^{\mu\nu}\int d\zeta\left(\hat H^{\mu\nu}_{\alpha}(p^+,p^+)\cdot w^{\alpha}_{\alpha'}\int\frac{l^+dy^-}{2\pi}e^{i(\zeta l^+ y^-)}\left\langle p\left|\bar\psi(0)i\partial^{\alpha'}(y)\psi(y^-)\right|p'\right\rangle\right)$$

Diagram 2

$$\Lambda_4{}^{\mu\nu}=\frac{1}{4\pi}\int d\zeta_1 d\zeta H^{\mu\nu}_{\alpha}(\zeta l^+,\zeta_1 l^+)\cdot\int\frac{l^+dy_1}{2\pi}\frac{l^+dy^-}{2\pi}e^{i(\zeta_1 l^+)y_1^-}e^{i(\zeta l^+)(y^- - y_1^-)}\times$$
$$\times e\langle p|\bar\psi(0)\left(-l^\alpha\tfrac{A^+(y_1^-)}{l^+}\right)\psi(y^-)|p'\rangle$$

8.2.1 Leading Power contribution

I will now incorporate the contributions $M_1{}^{\mu nu}$ and $\Lambda^{\mu nu}_{4\alpha}$, resulting in the appearance of the Wilson line. Some preliminary redefinitions of the second contribution are necessary to ensure a smooth combination.

Final form of $\Lambda^{\mu\nu}_a$

Using the Ward identity

$$l_\alpha\widehat H^{\alpha}_{\mu\nu}(\zeta l^+,\zeta_1 l^+)=-\frac{H_{\mu\nu}(\zeta_1 l^+)}{\zeta-\zeta_N-i\varepsilon}-\frac{H_{\mu\nu}(\zeta l^+)}{\zeta_1-\zeta_N+i\varepsilon}$$

I proved previously when I also defined

$$\zeta_N = \zeta \cdot \frac{Q^2}{p \cdot q}$$

and renaming $\xi_i = y_i l^+$ I begin :

$$\Lambda^{\mu\nu}_{(4\alpha)} = \frac{1}{4\pi}\int d\zeta_1 d\zeta \int \frac{d\xi_1}{2\pi}\frac{d\xi}{2\pi}\frac{1}{l^+}\left(H^{\mu\nu}(\zeta_1 l^+)\frac{1}{\zeta - \zeta_N - i\varepsilon}\right) e^{i\xi_1\zeta_1} e^{i(\zeta-\zeta_1)\xi} < p\left|\bar{\psi}(0) eA^+(\xi_1^-)\psi(\xi^-)\right|p' > + \frac{1}{4\pi}\int d\zeta_1 d\zeta \int \frac{d\xi_1}{2\pi}\frac{d\xi}{2\pi}\frac{1}{l^+}\left(H^{\mu\nu}(\zeta l^+)\frac{1}{\zeta_1 - \zeta_N + i\varepsilon}\right) e^{i\zeta_1\xi_1} e^{i(\xi-\xi_1)\zeta} < p\left|\bar{\psi}(0) eA^+(\xi_1^-)\psi(\xi^-)\right|p' >$$

In this point I will make use of the collinear limit of the hard function estimated before to make use of the delta function included and its properties. Using:

$$H_{\mu v}(\zeta l^+) = \gamma_\mu(\zeta \not{l} + \not{q})\gamma_v(2\pi)\frac{\zeta_N}{Q^2}\delta(\zeta - \zeta_N)$$

I obtain:

$$\begin{aligned}\Lambda^{\mu\nu}_{(4\alpha)} = \frac{1}{4\pi}\int d\zeta_1 d\zeta \int \frac{d\xi_1}{2\pi}\frac{d\xi}{2\pi}\frac{1}{l^+}\left(\gamma_\mu(\zeta_1 \not{p} + \not{q})\gamma_\nu(2\pi)\frac{\zeta_N}{Q^2}\delta(\zeta_1 - \zeta_N)\frac{1}{\zeta - \zeta_N - i\varepsilon}\right)\times \\ \times e^{i\xi_1\zeta_1} e^{i(\xi-\xi_1)\zeta}\left\langle p\left|\bar{\psi}(0) eA^+(\xi_1^-)\psi(\xi^-)\right|p'\right\rangle + \\ + \frac{1}{4\pi}\int d\zeta_1 d\zeta \int \frac{d\xi_1}{2\pi}\frac{d\xi}{2\pi}\frac{1}{l^+}\left(\gamma_\mu(\zeta \not{p} + \not{q})\gamma_\nu(2\pi)\frac{\zeta_N}{Q^2}\delta(\zeta - \zeta_N)\frac{1}{\zeta_1 - \zeta_N - i\varepsilon}\right)\times \\ \times e^{i\xi_1\zeta_1} e^{i(\xi-\xi_1)\zeta}\left\langle p\left|\bar{\psi}(0) eA^+(\xi_1^-)\psi(\xi^-)\right|p'\right\rangle\end{aligned}$$

From the definition of the θ function I will combine the unwanted denominators with the equally not helpful exponentials acquiring nicely a path ordering for our integrations which are necessary for building Wilson lines:

$$\theta(\mp\xi) = \mp\int \frac{d\zeta}{2\pi i}\frac{e^{i\xi\zeta}}{\zeta \pm i\varepsilon} = \pm\int \frac{d\zeta}{2\pi i}\frac{e^{-i\xi\zeta}}{\xi \mp i\varepsilon}$$

Using the definition I deduce:

$$\theta(\xi_1) = -\frac{1}{2\pi i}\int d\zeta_1 \frac{e^{i\xi_1(\zeta_1-\zeta_N)}}{\zeta_1 - \zeta_N + i\varepsilon} \Leftrightarrow$$
$$\int d\zeta_1 \frac{e^{i\xi_1\zeta_1}}{\zeta_1 - \zeta_N + i\varepsilon} = -2\pi i\theta(\xi_1) e^{i\xi_1\zeta_N}$$

and

$$\theta(\xi-\xi_1)=\int\frac{d\zeta}{2\pi i}\frac{e^{i(\zeta-\zeta_N)(\xi-\xi_1)}}{\zeta-\zeta_N-i\varepsilon}\Leftrightarrow$$
$$\int d\zeta\frac{e^{i\zeta(\xi-\xi_1)}}{\zeta-\zeta_N-i\varepsilon}=2\pi i\cdot\theta(\xi-\xi_1)\,e^{i\zeta_N(\xi-\xi_1)}$$

$$\begin{aligned}
\Lambda^{\mu\nu}_{4\alpha}&=\frac{1}{4\pi}\int d\zeta_1 d\zeta\int\frac{d\xi_1}{2\pi}\frac{d\xi}{2\pi}\frac{1}{l^+}\left(\gamma_\mu(\zeta_1\not{p}+\not{q})\gamma_\nu(2\pi)\frac{\zeta_N}{Q^2}\delta(\zeta_1-\zeta_N)\frac{1}{\zeta-\zeta_N-i\varepsilon}\right)\times\\
&\times e^{i\xi_1\zeta_1}e^{i(\xi-\xi_1)\zeta}\left\langle p\left|\bar\psi(0)eA^+(\xi_1^-)\psi(\xi^-)\right|p'\right\rangle+\\
&+\frac{1}{4\pi}\int d\zeta_1 d\zeta\int\frac{d\xi_1}{2\pi}\frac{d\xi}{2\pi}\frac{1}{l^+}\left(\gamma_\mu(\zeta\not{p}+\not{q})\gamma_\nu(2\pi)\frac{\zeta_N}{Q^2}\delta(\zeta-\zeta_N)\frac{1}{\zeta_1-\zeta_N-i\varepsilon}\right)\times\\
&\times e^{i\xi_1\zeta_1}e^{i(\xi-\xi_1)\zeta}\left\langle p\left|\bar\psi(0)eA^+(\xi_1^-)\psi(\xi^-)\right|p'\right\rangle\\
&=\frac{1}{4\pi}\int d\zeta_1\int\frac{d\xi_1}{2\pi}\frac{d\xi}{2\pi}\frac{1}{l^+}\gamma_\mu(\zeta_1\not{p}+\not{q})\gamma_\nu(2\pi)\frac{\zeta_N}{Q^2}\delta(\zeta_1-\zeta_N)\,e^{i\xi_1\zeta_1}e^{i(\xi-\xi_1)\zeta_N}(2\pi)\theta(\xi-\xi_1)\times\\
&\times\left\langle p\left|\bar\psi(0)ieA^+(\xi_1^-)\psi(\xi^-)\right|p\right\rangle-\\
&-\frac{1}{4\pi}\int d\zeta\int\frac{d\xi_1}{2\pi}\frac{d\xi}{2\pi}\frac{1}{l^+}\gamma_\mu(\zeta\not{p}+\not{q})\gamma_\nu(2\pi)\frac{\zeta_N}{Q^2}\delta(\zeta-\zeta_N)\,e^{i\xi_1\zeta_N}e^{i(\xi-\xi_1)\zeta}(2\pi)\theta(\xi_1)\times\\
&\times\left\langle p\left|\bar\psi(0)ieA^+(\xi_1^-)\psi(\xi^-)\right|p'\right\rangle\\
&=\frac{1}{4\pi}\int\frac{d\xi}{2\pi}\frac{1}{l^+}\gamma_\mu(\zeta_N\not{p}+\not{q})\gamma_\nu(2\pi)\frac{\zeta_N}{Q^2}e^{i\xi_1\zeta_N}\left\langle p\left|\bar\psi(0)\int d\xi_1 ie\theta(\xi-\xi_1)A^+(\xi_1^-)\psi(\xi^-)\right|p\right\rangle-\\
&-\frac{1}{4\pi}\int\frac{d\xi}{2\pi}\frac{1}{l^+}\gamma_\mu(\zeta_N\not{p}+\not{q})\gamma_\nu(2\pi)\frac{\zeta_N}{Q^2}e^{i\xi_1\zeta_N}\left\langle p\left|\bar\psi(0)\int d\xi_1 ie\theta(\xi_1)A^+(\xi_1^-)\psi(\xi^-)\right|p\right\rangle\\
&=\frac{1}{4\pi}\int\frac{d\xi}{2\pi}\frac{1}{l^+}\gamma_\mu(\zeta_N\not{p}+\not{q})\gamma_\nu(2\pi)\frac{\zeta_N}{Q^2}e^{i\xi_1\zeta_N}\times\\
&\times\left\langle p\left|\bar\psi(0)\int_{-\infty}^{\infty}d\xi_1 ie\left(\theta(\xi-\xi_1)-\theta(\xi_1)\right)A^+(\xi_1^-)\psi(\xi^-)\right|p'\right\rangle\\
&=\frac{1}{4\pi}\int\frac{d\xi}{2\pi}\frac{1}{l^+}\gamma_\mu(\zeta_N\not{p}+\not{q})\gamma_\nu(2\pi)\frac{\zeta_N}{Q^2}e^{i\xi_1\zeta_N}\left\langle p\left|\bar\psi(0)\int_0^{\xi}d\xi_1 ieA^+(\xi_1^-)\psi(\xi^-)\right|p'\right\rangle
\end{aligned}$$

Finally I use

$$1=\int d\zeta\delta(\zeta-\zeta_N)$$

and restore the original form of the hard function, which includes the dirac delta. The exponentials are also fixed and after we restore

$$\xi=yi\cdot l^+$$

and invert the integration boundaries, a perfect form for this contributions has emerged:

$$\Lambda^{\mu\nu}_{4\alpha}=\frac{1}{4\pi}\int d\zeta\left(\widehat{H}^{\mu\nu}(\zeta l^+)\cdot\int\frac{l^+dy^-}{2\pi}e^{i(\zeta l^+)y^-}\langle p|\overline{\psi}(0)\mathrm{P}\left[-ie\int_{y^-}^0\mathrm{d}y'^-A^+(y'^-)\right]\psi(y^-)|p'\rangle\right)$$

Adding to the lower order contribution now I have:

$$\begin{aligned}
\widetilde{M_{a1+b4}}^{\mu\nu}&=\frac{1}{4\pi}\int d\zeta\widehat{H}^{\mu\nu}(\zeta l^+)\int\frac{l^+dy^-}{2\pi}e^{i(\zeta l^+)y^-}\langle p|\overline{\psi}(0)\left(1-\mathrm{P}\left[-ie\int_{y^-}^0\mathrm{d}y'^-A^+(y'^-)\right]\right)\psi(y^-)|p'\rangle=\\
&=\frac{1}{4\pi}\int d\zeta\widehat{H}^{\mu\nu}(\zeta l^+)\int\frac{l^+dy^-}{2\pi}e^{i(\zeta l^+)y^-}\langle p|\overline{\psi}(0)\mathrm{P}e^{\left[-ie\int_{y^-}^0\mathrm{d}y'^-A^+(y'^-)\right]}\psi(y^-)|p'\rangle
\end{aligned}$$

$$\widetilde{M_{a1+b4}}^{\mu\nu} = \frac{1}{4\pi}\int d\zeta \widehat{H}^{\mu\nu}(\zeta l^+)\int \frac{l^+ dy^-}{2\pi} e^{i(\zeta l^+)y^-}\langle p|\overline{\psi}(0)\mathrm{P}e^{\left[-ie\int_{y^-}^{0}\mathrm{d}y'^- A^+(y'^-)\right]}\psi(y^-)|p'\rangle$$

Finally, we will show the existence of similar (almost identical) non-perturbative objects as the Jets in [35] by observing our Matrix Element. Specifically, using the following expressions from [34]:

- $$J_{(f)}(p) = \left\langle p\left|\bar{\psi}(0)\Phi_{\bar{n}}(0,\infty)\right|0\right\rangle$$
- $$\Phi_{\bar{n}}(0,\infty) = \exp\left[-ie\int_{\infty}^{0} d\lambda\, \bar{n}\cdot A(\lambda\bar{n})\right]$$
- $$J^{(0)}_{(f)} = \bar{u}(p)$$
- $$\left\langle p\left|\bar{\psi}(x)\right.\right. = \left\langle 0\left|\bar{u}(p)e^{ipx}\right.\right.$$

We combine those and very roughly we obtain the following ”object”:

$$\begin{aligned} J^{(0)}_{(f)}J_{(f)}(p) &= \left\langle p\left|\bar{\psi}(0)\Phi_{\bar{n}}(0,\infty)\right|0\right\rangle u(p') \\ &= \left\langle p\left|\bar{\psi}(0)\exp\left[-ie\int_{\infty}^{0} d\lambda\, \bar{n}\cdot A(\lambda\bar{n})\right]\right|0\right\rangle u(p) \\ &= e^{i(\zeta l^+)y^-}\left\langle p\left|\overline{\psi}(0)\mathrm{P}\exp\left[-ie\int_{y^\infty}^{0}\mathrm{d}y'^- A^+(y'^-)\right]\psi(y^-)\right|p'\right\rangle \end{aligned}$$

- We note that this is a very rough parallelism and not a bold statement as the initial configuration and constraints are my constructions, manipulated so as to allow for comparisons.
- Nevertheless the resemblance is striking and it is worth the effort to do conduct further investigation.
- The l^+ missing here is because it would cancel in [34] because of different integration measure.
- The difference in the gauge link boundaries can be possibly traced in the cross section definition including the squaring of the matrix element.
- In any case the result is expected if one considers the universality of the non-perturbative matrix elements.

Conclusion

A collinear expansion like the one made in [43] would lead at least to leading power to similar matrix elements as the ones which would create the Jet functions in [34]. This if true opens a discussion triggered by many possible extensions or interpretations:

- What would happen if we apply a special propagator or an OPE oriented technique to those matrix elements?
- What would be the interpretation of a higher twist in a non hadronic context? Would we expect the soft functions to acquire a new role?
- In inclusive DIS there is no $\sqrt{NLP}$ contribution at the end, after the special propagator rearrange the terms. What about our case?

9 Conclusion

In this thesis, we began by illustrating the significance of the factorization scheme proposed by [34]. Extensions to QCD corrections in processes of high interest in modern collider physics like Drell-Yan or Gluon fusion have been done showing the applicability of the method. Later after a detailed study on higher-twist contributions [45] we observed that those can be of use in the interpretation of non-perturbative matrix elements as well as in their construction. Thus, there is potential for future research in the latter, given that the initial findings are encouraging and a more comprehensive study as a complete extension to NLP needs to be conducted.

Bibliography

[1] Henso Abreu et al. “First Direct Observation of Collider Neutrinos with FASER at the LHC.” In: *Physical Review Letters* 131.031801 (2023). DOI: 10.1103/PhysRevLett.131.031801.

[2] Neelima Agarwal, Lorenzo Magnea, Chiara Signorile-Signorile, and Anurag Tripathi. *The Infrared Structure of Perturbative Gauge Theories*. 2021. arXiv: 2112.07099 [hep-ph].

[3] A. Idilbi et al. “Factorization and resummation for Higgs boson differential distributions in soft-collinear effective theory.” In: *Journal of High Energy Physics* 12 (2006), p. 061. URL: https://arxiv.org/abs/hep-ph/0601156.

[4] R. Contino et al. “Effective field theory analysis of double Higgs boson production via gluon fusion.” In: *Journal of High Energy Physics* 10 (2012), p. 012. URL: https://arxiv.org/abs/1210.8111.

[5] R. Balsach, A. Kulesza, and D. Bonocore. “The emission of soft-photons and the LBK theorem, revisited.” In: *arXiv preprint arXiv:2401.01820* (2024). URL: https://arxiv.org/abs/2401.01820.

[6] Avanish Prashan Basdew-Sharma. “On QCD Corrections to Jet Functions and Deep Inelastic Scattering.” PhD thesis. University Name, June 2023.

[7] Melissa Van Beekveld. “PhD thesis.” PhD thesis. URL: https://hdl.handle.net/2066/221857.

[8] Carola F. Berger. *Soft Gluon Exponentiation and Resummation*. 2003. arXiv: hep-ph/0305076 [hep-ph].

[9] D. Binosi, J. Collins, C. Kaufhold, and L. Theussl. “JaxoDraw: A graphical user interface for drawing Feynman diagrams. Version 2.0 release notes.” In: *Computer Physics Communications* 180.9 (Sept. 2009), pp. 1709–1715. ISSN: 0010-4655. DOI: 10.1016/j.cpc.2009.02.020. URL: http://dx.doi.org/10.1016/j.cpc.2009.02.020.

[10] Domenico Bonocore. “Next-to-Soft Factorization and Unitarity in Drell-Yan Processes.” PhD thesis. Amsterdam U., 2016.

[11] CERN. “Upgraded LHC begins epic run to search for new physics.” In: *Nature* 607 (2022), pp. 219–220. DOI: 10.1038/d41586-022-01859-w. URL: https://www.nature.com/articles/d41586-022-01859-w.

[12] Sidney Richard Coleman and Richard E. Norton. “Singularities in the physical region.” In: *Il Nuovo Cimento (1955-1965)* 38 (1965), pp. 438–442. URL: https://api.semanticscholar.org/CorpusID:122581639.

[13] ATLAS Collaboration. “Observation of a new particle in the search for the Standard Model Higgs boson with the ATLAS detector at the LHC.” In: *Physics Letters B* 716.1 (2012), pp. 1–29.

[14] John Collins. *Foundations of Perturbative QCD*. Cambridge Monographs on Particle Physics, Nuclear Physics and Cosmology. Cambridge University Press, 2023.

[15] John C. Collins, Davison E. Soper, and George Sterman. *Factorization of Hard Processes in QCD*. 2004. arXiv: hep-ph/0409313 [hep-ph].

[16] R. E. Cutkosky. “Singularities and Discontinuities of Feynman Amplitudes.” In: *Journal of Mathematical Physics* 1.5 (Sept. 1960), pp. 429–433. ISSN: 0022-2488. DOI: 10.1063/1.1703676. eprint: https://pubs.aip.org/aip/jmp/article-pdf/1/5/429/19167756/429_1_online.pdf. URL: https://doi.org/10.1063/1.1703676.

[17] S. Dawson, L. H. Orr, L. Reina, and D. Wackeroth. “Associated top quark-Higgs boson production at the LHC.” In: *Physical Review D* 58.1 (1998), p. 013005.

[18] B. DE WIT and J. SMITH. “9 - Asymptotic behaviour.” In: *Field Theory in Particle Physics*. Ed. by B. DE WIT and J. SMITH. Amsterdam: Elsevier, 1986, pp. 367–410. ISBN: 978-0-444-86996-8. DOI: https://doi.org/10.1016/B978-0-444-86999-9.50101-6. URL: https://www.sciencedirect.com/science/article/pii/B9780444869999501016.

[19] S. et al. Dittmaier. “Handbook of LHC Higgs Cross Sections: 1. Inclusive Observables.” In: *CERN Report* CERN-2011-002 (2011).

[20] A. Djouadi. “The Anatomy of Electro-Weak Symmetry Breaking. I: The Higgs boson in the Standard Model.” In: *Physics Reports* 457.1-2 (2008), pp. 1–216.

[21] Jun Du, Sicen Lu, and Tianyi Yang. “Cauchy Integral Theorem and its Applications.” In: *Journal of Physics: Conference Series* 2386 (Dec. 2022), p. 012017. DOI: 10.1088/1742-6596/2386/1/012017.

[22] R. K. Ellis, W. J. Stirling, and B. R. Webber. *QCD and Collider Physics*. Cambridge University Press, 1996. ISBN: 978-0521545891.

[23] R.K. Ellis, W. Furmanski, and R. Petronzio. “Power corrections to the parton model in QCD.” In: *Nuclear Physics B* 207.1 (1982), pp. 1–14. DOI: 10.1016/0550-3213(82)90132-8.

[24] R.K. Ellis, W. Furmanski, and R. Petronzio. “Unravelling higher twists.” In: *Nuclear Physics B* 212.1 (1983), pp. 29–98. ISSN: 0550-3213. DOI: https://doi.org/10.1016/0550-3213(83)90597-7. URL: https://www.sciencedirect.com/science/article/pii/0550321383905977.

[25] R.K. Ellis, W. Furmanski, and R. Petronzio. “Unravelling higher twists.” In: *Nuclear Physics B* 212.1 (1983), pp. 29–92. DOI: 10.1016/0550-3213(83)90597-7.

[26] Ilya Feige and Matthew D. Schwartz. “Hard-soft-collinear factorization to all orders.” In: *Phys. Rev. D* 90 (10 Nov. 2014), p. 105020. DOI: 10.1103/PhysRevD.90.105020. URL: https://link.aps.org/doi/10.1103/PhysRevD.90.105020.

[27] H. Georgi, S. L. Glashow, M. Machacek, and D. V. Nanopoulos. “Higgs bosons from two-gluon annihilation in proton-proton collisions.” In: *Physical Review Letters* 40.11 (1978), pp. 692–694.

[28] T. Han and S. Willenbrock. “QCD correction to the pp → WH and ZH total cross sections.” In: *Physics Letters B* 273.1-2 (1991), pp. 167–172.

[29] R. V. Harlander and W. B. Kilgore. “Next-to-Next-to-Leading Order Higgs Production at Hadron Colliders.” In: *Physical Review Letters* 88.20 (2002), p. 201801.

[30] S. et al. Heinemeyer. “Handbook of LHC Higgs Cross Sections: 3. Higgs Properties.” In: *CERN Report* CERN-2013-004 (2013).

[31] U-Rae Kim, Sungwoong Cho, and Jungil Lee. “The art of Schwinger and Feynman parametrizations.” In: *Journal of the Korean Physical Society* 82 (Mar. 2023). DOI: 10.1007/s40042-023-00764-3.

[32] Brookhaven National Laboratory. “The Electron-Ion Collider: A precision tool for studying the ’glue’ that binds visible matter.” In: *Phys.org* (2023). URL: https://phys.org/news/2023-08-neutrinos-cern-large-hadron-collider.html.

[33] E. Laenen, L. Magnea, G. Stavenga, and C.D. White. “On next-to-eikonal exponentiation.” In: *Nuclear Physics B - Proceedings Supplements* 205–206 (Aug. 2010), pp. 260–265. ISSN: 0920-5632. DOI: 10.1016/j.nuclphysbps.2010.09.003. URL: http://dx.doi.org/10.1016/j.nuclphysbps.2010.09.003.

[34] E. Laenen, J. Sinninghe Damsté, L. Vernazza, W. Waalewijn, and L. Zoppi. “Towards all-order factorization of QED amplitudes at next-to-leading power.” In: *Physical Review D* 103.3 (Feb. 2021). ISSN: 2470-0029. DOI: 10.1103/physrevd.103.034022. URL: http://dx.doi.org/10.1103/PhysRevD.103.034022.

[35] Eric Laenen, Lorenzo Magnea, Gerben Stavenga, and Chris D. White. “Next-to-eikonal corrections to soft gluon radiation: a diagrammatic approach.” In: *Journal of High Energy Physics* 2011.1 (Jan. 2011). ISSN: 1029-8479. DOI: 10.1007/jhep01(2011)141. URL: http://dx.doi.org/10.1007/JHEP01(2011)141.

[36] L.D. Landau. “On analytic properties of vertex parts in quantum field theory.” In: *Nuclear Physics* 13.1 (1959), pp. 181–192. ISSN: 0029-5582. DOI: https://doi.org/10.1016/0029-5582(59)90154-3. URL: https://www.sciencedirect.com/science/article/pii/0029558259901543.

[37] P.J. Mulders and R.D. Tangerman. “The complete tree-level result up to order 1/Q for polarized deep-inelastic lepton production.” In: *Nuclear Physics B* 461 (1996), pp. 197–237. DOI: 10.1016/0550-3213(95)00632-X.

[38] Roger G. Newton. “Optical theorem and beyond.” In: *American Journal of Physics* 44.7 (July 1976), pp. 639–642. ISSN: 0002-9505. DOI: 10.1119/1.10324. eprint: https://pubs.aip.org/aapt/ajp/article-pdf/44/7/639/11948216/639_1_online.pdf. URL: https://doi.org/10.1119/1.10324.

[39] V. Peraro. “The LBK theorem to all orders.” In: *Journal of High Energy Physics* (2023). URL: https://arxiv.org/abs/2304.11689.

[40] Michael E Peskin and Daniel V Schroeder. *An Introduction to Quantum Field Theory*. Addison-Wesley, 1995.

[41] Michael E. Peskin and Daniel V. Schroeder. *An Introduction to Quantum Field Theory*. Addison-Wesley, 1995. ISBN: 978-0201503975.

[42] Jianwei Qiu. “Twist-four contributions to the parton structure functions.” In: *Physical Review D* 42.1 (1990), pp. 30–50. DOI: 10.1103/PhysRevD.42.30.

[43] Jianwei Qiu and George Sterman. “Power corrections in hadronic scattering (I). Leading 1/Q2 corrections to the Drell-Yan cross section.” In: *Nuclear Physics B* 353.1 (1991), pp. 105–136. ISSN: 0550-3213. DOI: https://doi.org/10.1016/0550-3213(91)90503-P. URL: https://www.sciencedirect.com/science/article/pii/055032139190503P.

[44] Jianwei Qiu and George Sterman. “Single transverse spin asymmetries in direct photon production.” In: *Nuclear Physics B* 378.1-2 (1992), pp. 52–78. DOI: 10.1016/0550-3213(92)90003-T.

[45] Jianwei Qiu and George Sterman. “Single transverse spin asymmetries in direct photon production.” In: *Nuclear Physics B* 378.1 (1992), pp. 52–78. ISSN: 0550-3213. DOI: https://doi.org/10.1016/0550-3213(92)90003-T. URL: https://www.sciencedirect.com/science/article/pii/055032139290003T.

[46] D. Rainwater and D. Zeppenfeld. “Observing H → W$^{(*)}W^{(*)}ep_T^m issinweakbosonfusionwithdualforwardjettaggin$ In: *Physical Review D* 60.11 (1999), p. 113004.

[47] Matthew D. Schwartz. *Quantum Field Theory and the Standard Model*. Cambridge University Press, 2014. ISBN: 978-1107034730.

[48] G. Sterman. *An Introduction to Quantum Field Theory*. Cambridge: Cambridge University Press, 1995.

[49] George Sterman. *An Introduction to Quantum Field Theory*. Cambridge University Press, 1993. ISBN: 978-0521311328.

[50] George Sterman. “Partons, Factorization and Resummation.” In: *TASI 95: QCD and Beyond*. World Scientific, 1995.

[51] George Sterman. *Partons, Factorization and Resummation, TASI95*. 1996. arXiv: hep-ph/9606312 [hep-ph].

[52] O. V. Teryaev. “Ph.D. thesis.” PhD thesis. Moscow University, 1984.

[53] Steven Weinberg. *The Quantum Theory of Fields*. Vol. 1. Cambridge University Press, 1995. ISBN: 978-0521670531.